Fall 12-2016

MIX DESIGN AND MECHANICAL CHARACTERIZATION OF STABILIZED COMPRESSED EARTH BLOCKS AND ASSEMBLIES FOR THE JEMEZ PUEBLO IN NEW MEXICO

Nicole B. Trujillo
University of New Mexico

Nicole Bernadette Trujillo

Candidate

Civil Engineering

Department

This thesis is approved, and it is acceptable in quality and form for publication:

Approved by the Thesis Committee:

Dr. Mahmoud Reda Taha , Chairperson

Dr. John Stormont

Tom Bowen

MIX DESIGN AND MECHANICAL CHARACTERIZATION OF STABILIZED COMPRESSED EARTH BLOCKS AND ASSEMBLIES FOR THE JEMEZ PUEBLO IN NEW MEXICO

by

NICOLE BERNADETTE TRUJILLO

B.A.E, ARCHITECTURAL ENGINEERING, THE PENNSYLVANIA STATE UNIVERSITY, 2012

M.S., CIVIL ENGINEERING, UNIVERSITY OF NEW MEXICO, 2016

THESIS

Submitted in Partial Fulfillment of the

Requirements for the Degree of

Master of Science

Civil Engineering

The University of New Mexico

Albuquerque, New Mexico

December, 2016

ACKNOWLEDGEMENTS

I wish to thank my advisor and committee chair Dr. Mahmoud Taha for his guidance on this research and time spent reviewing my thesis. Thank you for offering me the opportunity to work on this project. I would also like to extend my gratitude to my committee members, Dr. John Stormont and Tom Bowen. Thank you both for your guidance and involvement in this research.

I would like to thank my loving husband, Humberto for his patience and support. Even though we were hundreds of miles away, you were always there when I needed you. You encouraged me to complete my graduate degree and pushed me to achieve my goal.

Thank you to my parents for their unfailing support and continuous encouragement throughout my years of study. I would especially like to thank them for the time spent supporting me on this project. Mom, for your constant love, immeasurable sacrifices, and faith in me. Dad, for teaching me to stay focused and to strive to reach my potential. To my sister, brother, grandparents and godparents, thanks for your support and unconditional love. Thank you to all my family and friends.

I would like to thank Dr. Eric Peterson at the Department of Earth and Planetary Sciences for conducting the XRD testing and his assistance in providing the mineralogy presented in this thesis. I would also like to thank Dr. Adrian Brearley, Professor at the Department of Earth and Planetary Sciences, for providing me with the SEM data presented in this thesis. I express my gratitude to Mr. Francisco Uvina, Lecturer in the School of Architecture and Planning for sharing his knowledge about adobe and compressed earth block construction.

I would like to express my gratitude to the many people who helped me in the UNM Structural Lab. Kenny Martinez for training me how to use laboratory equipment, assisting me in obtaining materials for various tests, and helping me set up experiments in the laboratory. I would like to thank Dr. Mehmet Emiroglu for all of his advice, guidance, and assistance in the lab, especially with the wall testing. I am grateful for all the assistance from Nicholas Martinez, Sumanth Doddikindi, Mohamad Hallal, and Conner Rusch who helped in performing various testing in the lab. I would also like to thank Jason Church from the Mechanical Engineering Machine Shop for machining many apparatuses for use in my experiments.

I would like to thank George Shendo, Production Manager and David Chinana, Assistant Production Manager from the Jemez Community Development Corporation for delivering SCEBs to UNM and for building the SCEB wall panels. I am grateful for the financial support provided by the Jemez Community Development Corporation towards this project.

MIX DESIGN AND MECHANICAL CHARACTERIZATION OF STABILIZED COMPRESSED EARTH BLOCKS AND ASSEMBLIES FOR THE JEMEZ PUEBLO IN NEW MEXICO

by Nicole Trujillo

B.A.E., Architectural Engineering, The Pennsylvania State University, 2012

M.S., Civil Engineering, University of New Mexico, 2016

ABSTRACT

Earthen structures have a long architectural and cultural heritage in New Mexico. Similar structures are evident around the world. With the current depletion of natural resources and high cost of materials, compressed earth block construction offers a sustainable building material alternative. Stabilized compressed earth blocks (SCEB) are compressed earth blocks with additives such as, hydrated lime or Portland cement to protect the earth block from absorbing water. SCEBs are being produced using native soils for residential construction on the Jemez Pueblo in New Mexico.

The primary goal of this research is to enable production of SCEBs with native soils from the Jemez Pueblo. The objectives of this research are to identify suitable local soils to be used to develop a compressed earth block mix design, compare the mechanical characteristics of SCEB to commercial adobe blocks, and investigate the mechanical behavior of SCEB prism and wall assemblies.

Close to 50 native soil locations at the Jemez reservation in New Mexico were investigated. These soils were classified according to the Unified Soil Classification System (USCS) considering their grain size distribution, plasticity limit and swelling potential. A method for down selection of the soils suitable for compressed earth block

production was developed. In addition, the clay mineralogy of the suitable soils and soil mix designs were determined using X-ray Diffraction (XRD) and Scanning electron microscopy (SEM).

SCEB mix design included two selected native soils, two sands and either Type S hydrated lime or Type II Portland cement. These materials were mixed to fabricate SCEBs of nine different SCEB mix designs. Compressive and flexural strength tests of the SCEBs were performed and compared to commercial adobe blocks. Tests to determine water absorption characteristics in SCEBs including initial rate of absorption, total absorption and sorptivity were also carried out. The mechanical and absorption characteristics of SCEBs were correlated to the mix design and the native soil classification. The ratio of clay and sand in the compressed earth block mix has a significant correlation with the mechanical and absorption characteristics of SCEBs. The results from all the testing showed that an optimum mix design was found for the nine blocks evaluated.

SCEB assemblies, including prisms and wall panels were produced with standard type S mortar. Prisms made of SCEB units were tested to determine the compressive strength, bond strength, and shear strength. The time-dependent creep of the SCEB prism at 56 days of age was also evaluated. These measurements showed that creep displacement has a significant effect on the total displacement of the prism assembly. The approximately 570 mm x 570 mm (22 in. x 22 in.) SCEB wall panels made of the optimum SCEB were tested under in-plane shear using a diagonal compression test. The results of the diagonal compression test show that the SCEB wall assembly obtained a lateral strength comparable to rammed earth.

The results showed that some SCEBs have higher compressive and flexural strengths than commercial stabilized adobe. SCEBs provide a resilient, sustainable building material and are suitable for use in residential construction for the Jemez Pueblo in New Mexico.

TABLE OF CONTENTS

LIST OF FIGURES

LIST OF TABLES

CHAPTER 1: INTRODUCTION

1.1 Background

Earthen construction is a form of sustainable architecture. It can be said that one of the first homes man lived in after he came out of a cave was made of earth (*Wolfskill et al. 1980*). Primitive man did little more than stick mud on poles woven closely together. But even with this, he found shelter that would be wherever he wanted, having an advantage to move around. Today, there are earth dwellings in many parts of the world that have endured centuries.

Climate is an important factor when deciding where to build an earth dwelling. They have a better performance in arid regions, where there is no more than 64-76 cm (25-30 in.) of rainfall a year (*Wolfskill et. al. 1980*).

There are various forms of earth-building materials, such as: adobe bricks, compressed (pressed) earth blocks, and others. Adobe blocks are the most popular and oldest form of earthen construction. Adobes are made from a mud composed of water, sand and finer material (clay and silt) (*Smith and Austin, 1996*). The mud is placed in wooden molding forms and allowed to cure for about one month in the sun (*Wolfskill et al. 1980*).

CEBs are a mixture by weight of angular sand aggregate, clayey soil, and water (*Allen, 2012*). Stabilized compressed earth blocks (SCEBs) are CEBs with additives such as, hydrated lime or Portland cement. The stabilizer aims to reduce the soil plasticity, improve its workability and provide resistance to erosion (*Pacheco-Torgal and Jalali, 2012*). CEBs are manufactured using a hand-operated CINVA-Ram or a hydraulically operated, gasoline or diesel-powered machine that produces one block at a time.

1.2 Motivation

This research on SCEBs through the University of New Mexico was based on the Soil and Stabilized Compressed Earth Block (SCEB) project for the Jemez Community Development Corporation. This project aimed to explore SCEB technology as a sustainable high performance adobe (HPA) solution in order to satisfy the employment and housing needs of the Jemez Pueblo in New Mexico.

The research is intended to improve our understanding of the structural performance of SCEBs and walls using SCEBs. By improving the understanding of the soil mechanics, the mechanical characteristics of the SCEBs, and block-mortar interaction, the structural performance of SCEBs can be improved dramatically abling their use in a larger range of climates and seismic prone areas.

The quality of the masonry depends on the quality of the CEB, the mortar, and bonding pattern. It is a function of the compatibility between the block and mortar. It is well established that direct exposure to moisture is an important factor in the performance of earthen construction materials. Excessive moisture from rainfall, high relative humidity, and snow affect the performance of an earthen structure. Therefore, it will be necessary to measure the water transport through the SCEBs and determine the mechanical properties of the saturated block. The mechanical performance of SCEBs and systems can be known in understanding the suitable composition of soils and SCEB mixture.

1.3 Research Objectives

There are three main objectives of this thesis. The primary objective is to study the effect of varying clay to sand ratios and various soil types for the SCEBs on block compressive and flexural strength. This will lead to the development of a systematic engineering method to select the clay source and the optimum mix proportions for SCEB.

The secondary objective is to compare the performance of SCEB to traditional commercially available Adobe bricks. The third objective is to evaluate the behavior of SCEB assemblies under stress built using standard mortar. This includes compression, shear, bond and creep behavior of SCEB prisms and the shear strength of SCEB wall panels.

1.4 Summary of Work

Over 50 soil samples were tested for particle size analysis, plasticity limit, and swelling potential in order to classify the soils. These soils were classified according to the Unified Soil Classification System (USCS). A method for down selection of the soils suitable for compressed earth block production was developed.

Two selected native soils were mixed with sand making various clay-to-sand ratios to make 9 different mix ratios which were used to fabricate SCEBs. Dry and saturated compressive strength and dry and saturated flexural strength tests of the SCEBs were performed under ambient conditions. Tests to characterize water transport in SCEBs including initial rate of absorption, total absorption and sorptivity were also carried out. The mechanical and absorption characteristics of SCEBs are correlated to the mix design and the native soil classification. The SCEB mechanical characteristics are compared to the commercial stabilized adobe brick.

SCEB assemblies, including prisms and wall panels were produced with standard type S mortar. The 7-day and 28-day mortar compressive strengths and flowability were determined. The compressive strength, bond strength, and shear strength of prisms made of SCEB units and selected mortar were produced and tested. In addition the time-dependent creep of the SCEB prism at 56 days of age was also evaluated. Finally, 570 mm

x 570 mm (22 in. x 22 in.) SCEB wall panels made of the optimum SCEB mixture were tested under in-plane shear using a diagonal compression test.

1.5 Outline

Chapter 2 is the literature review. Chapter 3 defines the experimental methods used for soils testing, block testing, prism testing, and wall testing. Chapter 4 describes the results and provides a discussion on soils testing and describes mix ratios chosen for SCEBs. In Chapter 4, the results from testing performed to determine the mechanical properties of the SCEBs, SCEB prisms, and SCEB walls are also analyzed and discussed. Chapter 5 concludes the research and provides a list of recommendations for future research.

CHAPTER 2: LITERATURE REVIEW

2.1 Introduction

In the construction industry, there has been a persistent need to turn to more sustainable construction solutions. Engineering professionals recognize that the construction industry accounts for about 40% of the world's energy use *(Jenkins Swan et. al 2012).* Not only the use of energy, but the amount of carbon dioxide (CO_2) emitted by building materials needs to be reduced. The construction industry accounts for 30% of CO_2 emissions. In addition, the construction industry throughout the world consumes more raw materials than any other industry. With an expected increase in the world population of more than 2 billion people by 2030, there will be a demand for buildings and other infrastructure to accommodate the increase in population (*Pacheco-Torgal and Jalali, 2012*). This would cause a further increase in the consumption of non-renewable materials and waste production. According to the Kyoto Agreement in 1997, countries have agreed to reduce the amount of production of cement until the year 2050 *(Fahmy, 2007).*

As a result, many designers and engineers of the built environment are looking to locally resourced materials for construction in order to reduce energy consumption. Earthen materials have been suggested as one alternative to offer a sustainable construction material (*Pacheco-Torgal and Jalali, 2012*).

2.2 History of Earthen Structures

There are various forms of earthen-building materials, such as: adobe bricks, compressed (pressed) earth blocks, rammed earth, cob, and wattle and daub. Adobe bricks are the most popular and oldest form of earthen construction. Adobes are made from a wet "mud" composed of 55-85% sand, 15-45% finer material (more silt than clay), and usually containing caliche. Caliche is formed in the soil calcium carbonate *(Smith and Austin,*

1996). The wet "mud" is placed in wooden molding forms and allowed to dry (cure) for about one month in the sun *(Wolfskill et al. 1980).*

Compressed earth blocks (CEBs) are formed one at a time using a hand-operated CINVA-Ram or a hydraulically operated, gasoline or diesel-powered machine. The first machine used to make CEB was the CINVA-Ram created by Raul Ramirez of the International American Housing Centre (CINVA) in Bogota, Columbia, in 1952 (*Pacheco-Torgal and Jalali, 2012*). CEBs are a mixture by weight of angular sand aggregate (40-70%), clayey soil (30-60%), and water (8-12%) *(Allen, 2012).* Stabilized compressed earth blocks (SCEBs) are CEBs with additives/binders such as, Type S hydrated lime or Type II Portland cement to protect the earth block from water intrusion.

Rammed earth construction consists of continuous walls which are constructed by ramming moist soil between two wooden forms *(Wolfskill et al. 1980).* The use of rammed earth walls are built in more humid climates than adobe blocks *(Niroumand et al. 2013).* The next earth building material, cob consists of molding stiff mud to create walls. The mud is stiffer than the adobe brick due to the high straw content. The mud is shaped on a trowel and placed directly on the structure and let to harden before more mud is applied on top (*Wolfskill et al. 1980*). This is the simplest of earthen building materials. Finally, the wattle and daub earthen structures consist of two parts. First, using materials such as, reeds, bamboo, branches and twigs to create the wattle, these materials are woven together to create a stiff frame. Daub or mud is then smeared on to the wattle by hand until the entire surface is covered and let to dry *(Niroumand et al. 2013).* Wattle and daub walls are thin and lack the thermal mass properties provided by all other earth building systems. Despite

this, wattle and daub construction are used in seismic zones throughout the world because the woven structure is earthquake resistant due to its ductility *(Niroumand et al. 2013)*.

Earthen architecture is a vernacular architecture which is used throughout the world *(Niromand et al. 2013)*. It is estimated that 30-40% of the world population currently live or work in earthen structures *(Miccoli et al. 2014)*. The majority of earth construction is located in less developed countries (*Pacheco-Torgal and Jalali, 2012*). Yet, earthen construction is also used in the United States, Germany, France, the United Kingdom, Australia, and New Zealand. Earthen construction is dependent on adequate training for builders and homeowners but also on specific local regulations. (*Pacheco-Torgal and Jalali, 2012*). Several countries already have earthen construction related standards, such as New Zealand, Australia, Germany, Ecuador, India, and Peru (*ASTM E2392, 2010*). The United States has no specific earthen building code, but New Mexico has a state regulation, the 2009 New Mexico Earthen Building Materials Code (*NMAC, 2009*).

Within the United States, New Mexico is the largest producer and user of adobe bricks and compressed earth blocks *(Smith and Austin, 1996)*. Earthen structures have a long architectural and cultural heritage in New Mexico. The traditional earthen construction method (adobe blocks) has been altered by using stabilizers such as hydrated lime or Portland cement to enhance the durability performance in order to make an improved construction material for low-cost, sustainable buildings (compressed earth blocks). However, there are advantages and disadvantages to using compressed earth blocks.

2.3 Advantages and Disadvantages of Stabilized Compressed Earth Block

Several advantages and disadvantages to using earthen building materials were found in literature. The most significant ones are described below.

2.3.1 Advantages

The most significant advantages of using earthen building materials are the environmental benefits associated with it. Several publications have compared the energy consumption and environmental impacts of earthen materials to more traditional building materials.

Jenkins Swan et al. *(2012)* compared two sustainable structural wall assemblies, wood-frame and compressed earth block (CEB). The two wall assemblies were compared in a full life cycle analysis and an economic analysis on an existing earthen residence in Summerland, British Colombia. The adverse environmental impacts were categorized into 4 different areas: human health, ecosystem quality, global warming, and resources. CEB had a greater impact than wood on human health and the ecosystem quality yet, the greater use of resources and the global warming impacts by the wood frame assembly surpass these CEB results when considering the total impact of the assemblies. The overall impact from CEB are 70% that of the wood-frame *(Jenkins Swan et. al 2012).* Therefore, the advantage to use CEB is that it lowers the overall environmental impact. The environmental advantage will decrease when cement is used as a stabilizer for SCEB blocks.

Morel et al. (*2001*) also performed an environmental assessment on the energy consumption for three different residential construction materials: stone masonry, concrete, and rammed earth homes built in the South of France. The results showed that the concrete home consumed 248% more energy than the stone masonry home and 270% more energy than the rammed earth home.

In addition to decreased carbon dioxide emissions, Pacheco-Torgal and Jalali *(2012)* discussed the other advantages such as the economic benefits, low waste generation,

and improved indoor air quality by using earthen building materials. According to Pacheco-Torgal and Jalali *(2012)*, the replacement of 5% of concrete blocks used in the UK with unstabilized earthen masonry led to a reduction in CO_2 emissions of approximately 100,000 tons (112,000 US ton). Rammed earth walls stabilized with cement cause the amount of carbon to increase from 26 to 70 kg (0.029 to 0.077 US ton) CO_2 thus, increasing its environmental impact. Nonetheless, stabilized compressed earth blocks are more sustainable than clay fired bricks. SCEB production consumes 15 times less energy and pollutes 8 times less than clay fired bricks (*Pacheco-Torgal and Jalali, 2012)*.

The economic benefits of earthen construction depends on several aspects, such as: construction technique, labor costs, amount of stabilization, and repair needs (*Pacheco-Torgal and Jalali, 2012)*. For example in a country, such as the US in which skilled labor is expensive as opposed to less developed countries in which skilled labor is available for a very low cost. This is an important factor because the production and construction costs of earthen structures represent the most important part because earth construction is labor intensive. Yet, earthen construction is still a very cost-effective construction technique compared with traditional construction materials.

Earthen construction materials are composed of soil located in the vicinity of the building site causing reduced emissions of greenhouse gases associated to its transportation compared to other building materials. Also, earthen construction wastes can be deposited at the boring location without any environmental impact. The boring location is where the soil is obtained for use in the earthen material production. If the soil is stabilized with cement or lime, it can be reused. Therefore, earthen construction materials generates little waste (*Pacheco-Torgal and Jalali, 2012).*

Indoor air quality is important to consider when comparing construction materials for residential construction. Residential buildings contain high amounts of chemicals and heavy metals, which contaminate indoor air, thus causing several health related problems such as: asthma or skin irritations. Earthen construction does not emit indoor air volatile organic compounds (VOCs) leading to better indoor air quality (*Pacheco-Torgal and Jalali, 2012).* Another advantage of the indoor air quality of earthen construction relates to its ability to control the relative humidity. Earthen structures equalize the relative humidity of the external environment with that of the pores within the walls (*Pacheco-Torgal and Jalali, 2012).* It is important to note that water can cause the deterioration of earthen construction materials, but stabilized earth masonry has the ability to provide good performance to water transport. Pacheco-Torgal and Jalali *(2012)* discussed a study conducted in the UK where it was determined that earthen construction was capable of maintaining the relative humidity of indoor air between 40% and 60%, this range being the most appropriate for human health purposes (*Pacheco-Torgal and Jalali, 2012).*

According to Morel et al. (*2001*), another advantage of earthen building materials was that thermal insulation of residential building was naturally obtained by the thick walls 400 to 600 mm (16 to 24 in.). In the Mediterranean climate, the thermal mass of the thick walls warm the house during the winter evenings because the walls release the heat absorbed during the day (*Morel et al. 2001*). Natural cooling of earthen structures in hot climates has been reported by many architects.

2.3.2 Disadvantages

Despite all the many advantages to use earthen construction materials, there are some disadvantages.

Typical earthen structures, such as adobe require high maintenance as they are prone to durability issues such as erosion under rainfall (*Miccoli et al. 2014*). Therefore, stabilization is sometimes used for CEBs in order to improve the long-term performance. Otherwise, the use of CEBs is limited to arid climates due to moisture effects. Earthen materials are dependent upon moisture content and are sensitive toward different moisture contents than any other porous mineral construction material. CEBs show a higher compressive strength in the dry state than the saturated state (*Miccoli et al. 2014*).

According to Pacheco-Torgal and Jalali *(2012)*, there are some limitations for the use of earth construction. There is a lack of skilled craftsmanship and also an absence of earth related courses to educate laborers.

There are also some disadvantages in using earthen construction, such as it is less durable in the long term as a construction material compared to conventional building materials, and it requires maintenance. Earthen construction is labor intensive and requires skilled laborers. Earthen construction has structural limitations because certain construction techniques cannot extend more than 1 story. In addition, earthen construction needs to be designed with a larger wall thickness to withstand the seismic loads (*Pacheco-Torgal and Jalali, 2012).*

2.4 Soil Classification for Compressed Earth Block

Understanding the characteristics of native soils is important in identifying suitable soils to produce compressed earth block. These soils are usually classified according to the Unified Soil Classification System (USCS) or other classifications in the literature, considering their grain size distribution, plasticity limit, swelling potential, and clay mineralogy.

"The principal soil grain properties are the size and shape of the grains and, in clay soils, the mineralogical character of the smallest grains" (*Terzaghi and Peck, 1948*). Sand and gravel are cohesionless aggregates of rounded subangular or angular fragments of more or less unaltered rocks or minerals (*Terzaghi and Peck, 1948*). Particles with a diameter size up to 0.3 cm (1/8 in.) are referred to as sand, and those with a size from 0.3 cm to 20 cm (1/8 in. to 8 in.) are gravel. Quartz and feldspars are major constituents of rock and sand *(Smith and Austin, 1996).* The clay-size, which is less than <2 μm (0.000008 in.) fraction of soil is made up of different minerals in varying proportions *(Smith and Austin, 1996).* Kaolinite, illite, smectite (montmorillinite), vermiculite, and mixed-layer illite/smecite (I/S) are the principal clay-mineral groups (*Smith and Austin, 1996).* Nonclay minerals such as quartz, feldspar, and calcite may also be present in the clay-size fraction of soil. Smectite and (I/S) are expandable clays and will swell in the presence of water. While, kaolinite and illite are nonexpandable clays and will only expand slightly in the presence of water *(Smith and Austin, 1996).*

The primary method for identifying and analyzing clay minerals is X-ray diffraction (*Moore and Reynolds, 1997*). There are different layer types of the individual clay minerals. In 1:1 type (e.g. Kaolinite), there is no or very small layer change (*Moore and Reynolds, 1997*). Each layer is composed of one tetrahedral and one octahedral sheet as shown in Figure 2.1. In the 2:1 layer type with z < 1, minerals such as, illite, smecitite (montmorillonite), vermiculite, and chlorite, each layer is composed of one octahedral sheet sandwiched between two tetrahedral as shown in Figure 2.1.

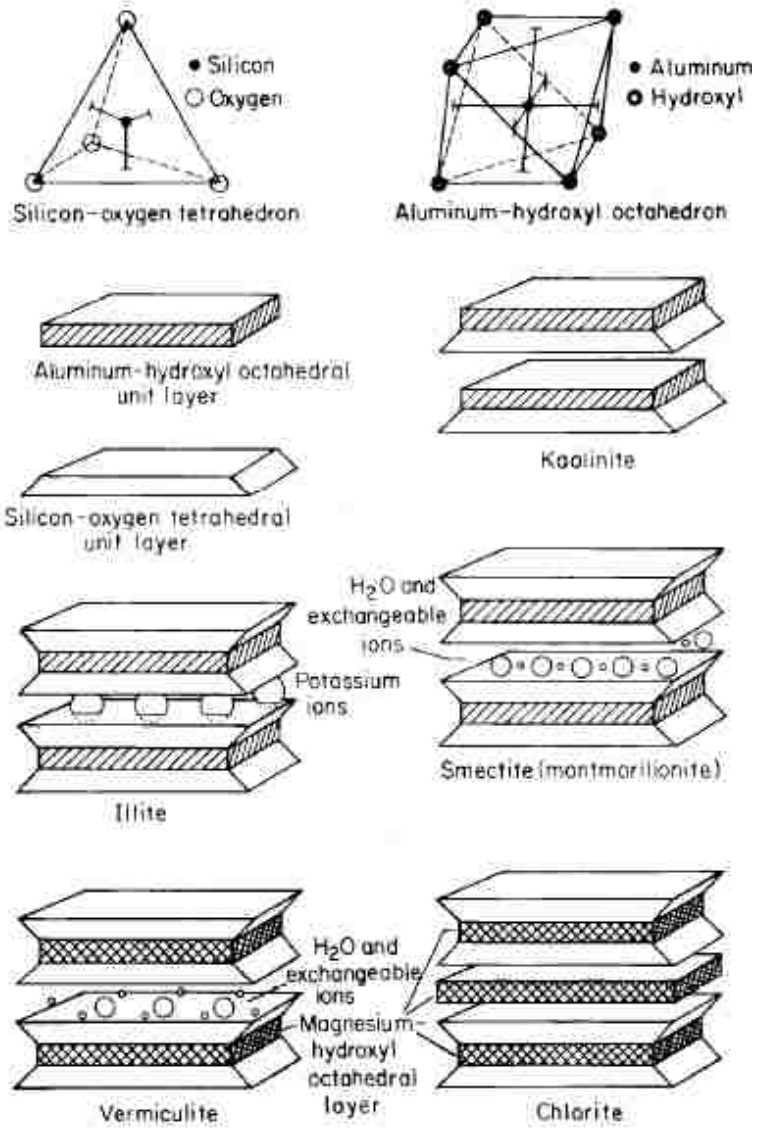

Figure 2. 1. Structure of a silicon-oxygen tetrahedron (upmost left), and an aluminum-hydroxyl octahedron (upmost right). Diagram of major clay-mineral groups. (Smith and Austin, 1996).

Soils suitable for earthen construction are found throughout the world. Houben and Guillaud (*1994*) provided a map of the locations where soil can be used for earthen building (Figure 2.2). It is important to note that if some soils do not have sufficient amounts of clay content, then cement or lime, may be used as a binder (*Morel et al. 2001*).

Figure 2. 2. Location of soil suitable for building (Houben and Guillaud, 1994).

According to Burroughs (*2008*), there is a great importance in selecting a soil suitable for stabilization. Soil stabilization means changing the soil characteristics in order to improve its mechanical or physical behavior. The stabilization process aims at reducing soil plasticity and also increasing its resistance to erosion (*Pacheco-Torgal and Jalali, 2012*). For example, soils unsuitable for stabilization include clean gravels and sands, and highly plastic clays (*Burroughs, 2008*). Burroughs (*2008*) developed a criteria of soil suitability for the use of stabilizers, such as cement and lime for rammed earth construction based on the natural soil properties. Figure 2.3 was taken from Burroughs (*2008*) and shows the recommended procedure for determining suitable soils for stabilization based on the soil properties. The study was performed on 104 soils to determine the soil properties, including plasticity, particle size distribution, and linear shrinkage, then the soils were stabilized with cement and/or lime and/or asphalt making 219 stabilization samples measured for the saturated unconfined compressive strength. A "successful" stabilized soil met the criterion of 2 MPa (290 psi) minimum compressive strength for stabilized rammed earth walls according to the 1997 Uniform Building Code. According to Burroughs (*2008*), the linear shrinkage and plasticity index were the best indicators of soil suitability for

SCEB production. The linear shrinkage was obtained by calculating the difference of the dried specimen height from the mold height (*Jimenez Delgado and Canas Guerrero, 2007*).

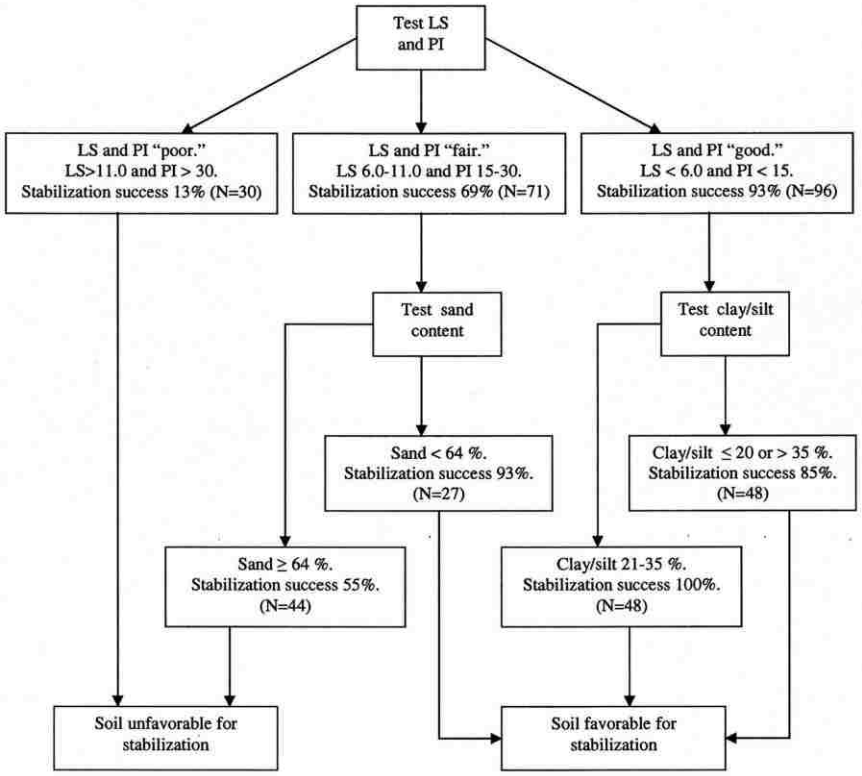

Figure 2. 3. Recommended procedure for determining soil for stabilization based on soil properties: linear Shrinkage (LS), plasticity index (PI), and soil grading. Stabilization success is the percentage of samples with unconfined compressive strength (UCS) ≥ 2 MPa (Burroughs, 2008).

Soil grading and mineralogy of the soil-sand mixture, cement content, and block density are some of the major parameters that influence the mechanical characteristics of earth blocks (Reddy et. al 2007). The particle size analysis is important because it has a high influence on the soil behavior. Reddy et. al (*2007*) performed a study which investigated the impact of soil grading on strength characteristics of earth blocks. The study showed that strength and durability properties of the earth blocks depend upon the clay fraction of the soil mixture. It was found that in general soils containing nonexpansive

clay minerals, sandy and gravely soils are suitable for use in earth block production (Reddy et. al 2007).

2.5 Mechanical Properties of Compressed Earth Blocks (CEB) and CEB Assemblies

The mechanical properties of compressed earth blocks in the literature vary. This is due to factors such as variabilities in soil worldwide, workmanship and weathering, but also due to differences in testing procedures (*Miccoli et al. 2014*). The mechanical properties of compressed earth blocks from nine reviewed documents are presented in Table 2.2 from Smith and Austin (*1996*), Walker (*1999*), Bei and Papayianni (2003), Walker (*2004*), Reddy et al. (2007), Reddy et al. (2007), Lawson et al. (2011), Bharath et al. (2014) and Miccoli et al. (2014). The soil properties of the CEBs are shown in Table 2.1.

Table 2. 1. Soil Characteristics of Compressed Earth Block by the reviewed documents.

Reference	*Smith & Austin, 1996*	*Walker, 1999*	*Bei & Papayianni, 2003*	*Walker, 2004*	*Walker, 2004*	*Walker, 2004*	*Reddy et al. 2007*	*Reddy et al. 2007*	*Reddy et al. 2007*	*Lawson et al. 2011*	*Bharath et al. 2014*	*Miccoli et al. 2014*
Soil ID	**Earth Press II**	**Soil IV**	**C**	**Soil Ia**	**Soil Ib**	**Soil Ic**	**RS1**	**NS1**	**NS2**	**OMC**	**B3**	**Earth block**
Clay to Sand Ratio	-	0.8:0.2	0.7:0.3	0.1:0.9	0.3:0.7	0.4:0.6	5:7	1:0.33	1:1	-	-	-
Grading (by mass)												
Sand (%) (2-0.06 mm)* (4.75-0.075 mm)	69	63	41.86	78*	62*	56*	78.8	68.3	76	69	50.17	43*
Silt (%) (0.06- 0.002mm)* (0.075-0.002 mm)	22	4	35.54	11*	14*	16*	8.5	15.4	13.1	31	28.96	45*
Clay (%) (<0.002 mm)	9	20	22	11*	24*	28*	12.7	16.3	10.9		20.87	12*
Atterberg Limits												
Liquid limit	-	27	32.5	19	22	30	36.3	25.4	24.7	24	37.5	-
Plasticity index	-	7	13.0	7	13	16	16.1	10.5	6.2	8	17.5	-
USCS Classification	-	-	CL	-	-	-	SC	SC	SM	SC	-	-
Predominant clay minerals	Kaolinite	-	Illite	Kaolinite	Kaolinite	Kaolinite	Kaolinite	Kaolinite	Kaolinite	-	-	Smectite

Table 2. 2. Mechanical Characteristics of Compressed Earth Block by the reviewed documents.

Reference	Soil ID	Cement Content (%)	Dry density (kg/m^3)	Dry Compressive Strength (MPa)	Wet Compressive Strength (MPa)	Dry Flexural strength (MPa)	Wet Flexural strength (MPa)	Young's Modulus (MPa)	Poisson Ratio	Water Absorption (%)	IRA (g/min/193.55 cm2)	Shear bond strength (MPa)	Bond Strength (MPa)
Smith & Austin, 1996	Earth Press II	0	-	6.3	-	0.41	-	-	-	1.9	-	-	-
Walker, 1999	IV	10	1520	3.11	1.67	-	0.141	-	-	24.9	-	-	0.05
Bei & Papayianni, 2003	C	-	2100	4.46	-	-	-	-	-	-	-	-	-
Walker, 2004	Ia	5	1851	12.8	3.8	1.05	0.56	-	-	-	-	-	-
Walker, 2004	Ib	5	1980	18.3	6.6	1.79	0.70	-	-	-	-	-	-
Walker, 2004	Ic	0	1933	21.9	6.2	1.37	-	-	-	-	-	-	-
Reddy et al. 2007	RS1	8	1835	-	8.34	-	1.21	-	-	12.02	62.1	0.04	-
Reddy et al. 2007	NS1	4	1814	8.33	3.14	-	0.38	-	0.20	15.7	40.8	0.06	-
Reddy et al. 2007	NS2	4	1772	5.56	2.77	-	0.36	-	0.13	15.25	54.0	0.05	-
Reddy et al. 2007	NS1	8	1814	12.04	5.73	-	0.95	-	0.18	14.97	36.2	0.13	-
Reddy et al. 2007	NS2	8	1785	9.77	4.99	-	0.81	-	0.13	14.84	45.1	0.10	-
Lawson et al. 2011	OMC	0	1876	4.5	-	0.55	-	-	-	-	-	-	-
Bharath et al. 2014	B3	8 3% lime	-	6.08	4.44	-	-	-	-	12.35	14.8	-	-
Miccoli et al. 2014	Earth block	-	-	5.21	-	-	-	2197	0.45	-	-	-	-

The mechanical properties of the blocks measured in the nine reviewed articles in the literature varied. However, the mechanical properties reported for CEBs were dry density, dry and saturated compressive strength, dry and saturated flexural strength, Young's modulus, Poisson's ratio, amount of water absorption, and the initial rate of absorption (IRA) as displayed in Table 2.2.

Walker (*2004*) investigated the influence of block geometry, constituent materials, and moisture content on the compressive strength of CEBs. Earthen materials are dependent upon moisture content and are more sensitive toward different moisture contents than any other porous mineral construction material. During production of SCEBs, there must be sufficient water present to enable the fines to bind the aggregate together and to hydrate any cement used. The moisture content of the SCEB mix prior to compaction shall be within 3% of the optimum moisture content for maximum dry density compaction as defined by the New Zealand Building Code (*NZS, 2000*).

The amount of water contained in a SCEB effects the soil behavior as well as the Portland cement within the block. The natural water content contained in the soils in the bonding agent. Water has positive ions which balances the negative charge of the clay layers making the soil workable and able to be used as a building material (*Prost et. al 1998*) (*Low, 1985*). When Portland cement is mixed with water, a chemical reaction called hydration takes place (*Thomas, 1996*). Portland cement and water are transformed into calcium silicate hydrate compounds as hydration proceeds over time (*Thomas, 1996*). These compounds are the bonding agent that hold the aggregates together. Curing is the process of maintaining moisture levels inside the SCEB so that hydration can continue and the strength, hardness and density of the block can continue to gradually increase (*Thomas,*

1996). Yet, if there is a high amount of water content in the SCEB while it is curing, this can lead to a larger amount of void spaces once the water is evaporated. A large amount of voids within the SCEB will lead to decreased mechanical strength properties.

In addition to the mechanical strength of the CEBs, the mechanical strength of the CEB assemblies was found in the literature. The quality of masonry depends on the interaction of the CEB and the mortar which can be measured by the shear strength and the bond strength. Reddy et al. (*2007*) reported results of shear bond strength testing of CEBs as shown in Table 2.2. Walker (*1999*) reported the bond strength of a CEB prism was 0.05 MPa (7.3 psi). The bond strength of traditional clay fired brick masonry prism was determined by Reda and Shrive (*2000*) to be 0.46 MPa (66.7 psi) for prism that was air cured. This average prism strength was from Group 1. The mortar used for Group 1 prism construction was made of 1 part Portland cement, 1 part Lime, and 6 parts sand.

According to Walker (*1999*), there has been investigations on the bond developed between cement mortars and various masonry units. Bond strength relies on the formation of a layer of ettringite crystals at the unit/mortar interface (*Walker, 1999*). The development of this layer depends on a variety of factors, including unit initial rate of absorption, unit moisture content, water retention properties of the mortar, mortar consistency, mortar composition, fullness of joints, cleanness of bonding surfaces, disturbance of joint after initial construction, quality of work, unit surface characteristics, sand grading, and applied precompression (*Walker, 1999*). These factors also contribute in the bonding between SCEBs and mortars.

Masonry structures are often subjected to large, sustained loads which cause time-dependent effects on the structure, such as creep. Creep of masonry structures is a well-

established effect. Binda et al. (*1992*) discussed the sudden failure of the Civic Tower at Pavia in Italy in 1989 which was attributed to long-term damage accumulation under sustained stresses. Masonry is a composite structure of brick units and mortar. The two materials have different creep rates. When the materials creep at different rates, it causes an increase in the long term deformations as well as an increase in the stress distributions. The stress distributions lead to peak stresses within the masonry element which may unexpectedly cause material cracking and subsequently, failure. The stability of masonry under creep deformations was addressed by Shrive et al. (*1997*), Binda et al. (*2008*), Anzani (*2009*), and Kim et al. (*2012*). The creep coefficient is a dimensionless parameter to predict creep in a material and is obtained for compressed earth block in this investigation. Shrive et al. (*1997*) determined that the creep coefficient for clay brick masonry ranged between 0.7 and 3.33 for dry conditions. Kim et al. (2012) showed that the creep coefficient used for clay brick masonry ranged from 2 to 4.

The shear strength of earthen walls was found in the literature. Miccoli et al. *(2014)* performed diagonal compression tests on a 500 x 500 x 110 mm^3 (20 x 20 x 4 $in.^3$) wall. Specimens for the diagonal compression test were performed following ASTM E519 (ASTM, *2010*). Wallets were rotated by 45° around the middle axis, so that one diagonal of the wallet was perpendicular to loading and the other one was parallel to the loading direction in order to induce shear forces. The load was applied via a loading shoe placed at the top and bottom of each upper and lower corner (See Figure 2.4). Loading was applied at a rate of 130 N/s. Results indicate that the rammed earth wallets reached the highest strength of all three types of earthen materials. The shear strength of: wetted earth block masonry was 0.34 MPa (49.3 psi), earth block masonry was 0.09 MPa (13.1 psi), rammed

earth was 0.71 MPa (102.9 psi), and cob was 0.50 MPa (72.5 psi). Figure 2.4 shows the crack patterns of the three earthen materials under diagonal compression.

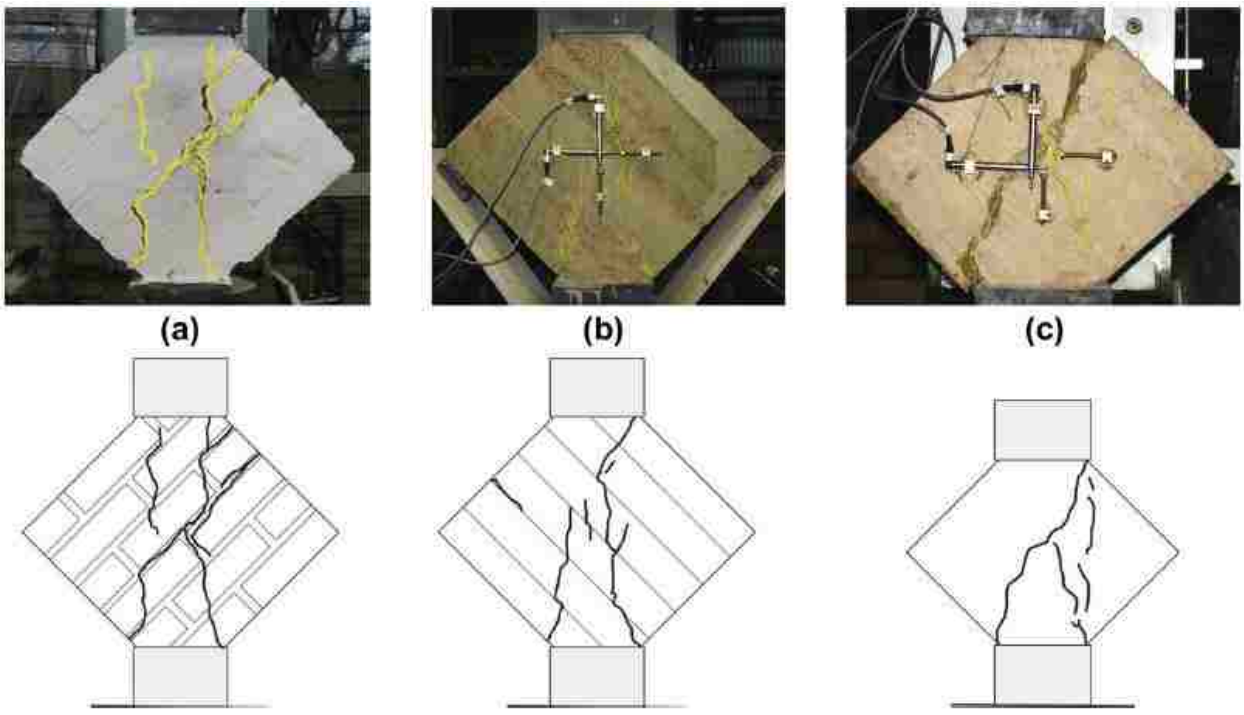

Figure 2. 4. (a) Earth block masonry, (b) rammed earth, and (c) cob specimens under diagonal compression. Crack patterns are marked in yellow lines. (Miccoli et al. 2014).

Varum et al. (*2007*) evaluated the shear strength of traditional adobe masonry walls. Thirteen wallets of dimensions, 170 x 170 x 100 mm^3 (7 x 7 x 4 $in.^3$), were constructed and put under the diagonal compression test. The shear strength obtained from the tests varied between 0.07 to 0.19 MPa (10.2 to 27.6 psi) (*Varum et al. 2007*). Silva et al. (*2013*) measured the shear strength of three geopolymer stabilized rammed earth wallets of 550 x 550 x 200 mm^3 (22 x 22 x 8 $in.^3$) using the diagonal compression tests. The wallets were compacted in 9 layers. A monotonic displacement of 4 μm/min (0.00016 in./min) was used. The vertical and horizontal displacements were measured on both faces using 4 LVDTs.

The rammed earth wallets were stabilized with 2.5% (GSRE_2.5), 5.0% (GRSE_5.0), and 7.5% (GRSE_7.5) fly ash content. The shear strength obtained for GRSE_2.5 was 0.14 MPa, GRSE_5.0 was 0.14 MPa (20.3 psi), and GRSE_7.5 was 0.18 MPa (26.1 psi) (*Silva et al. 2013*).

Other researchers are discussing new areas of research that are improving the flexural strength of SCEBs. Also, researchers are investigating alterative stabilizers to replace the use of cement. Sturm et al. (2015), Qu et al. (2015) and Jayasinghe and Mallawaarachchi (2009) have all begun research to understand the improved flexural strength of interlocking SCEBs. Geopolymers are one solution as an alternative binder. Geopolymers are a synthetic material made by alkaline activation of solid particles rich in silica and alumina. For good activation, it is necessary that these materials are in the amorphous form, as in metakaolin, slag and fly-ash (Marques Timoteo de Sousa et al. 2012). Geopolymers allow the complete elimination of cement in SCEBs without compromising the strength and durability of SCEBs (Venugopal et al. 2015).

CHAPTER 3: EXPERIMENTAL METHODS

3.1 Introduction

This chapter describes the experimental methods for soils testing, block production, the design and fabrication of equipment according to relevant standards and test procedures for block, prism, and wall testing. It also includes data analysis methods used in this research.

3.2 Soil Testing

There were over 50 soil samples tested in order to identify the sites with a suitable quantity of clay for making SCEBs. Excavation was performed by geologists from the Colorado State Division of Energy and Mineral Development. Excavated soils were placed into 5 gallon buckets. These buckets were transported to the University of New Mexico Structural Lab by the Jemez Community Development Corporation (JCDC). The soil testing for soils used in SCEB production occurred in four phases.

In Phase 1, 12 areas within the Jemez Pueblo were identified as suitable for excavation based on exploration and analysis performed by geologists from the Division of Energy and Mineral Development. From the original 12 areas, two sites were identified as appropriate for use in SCEB mix design based on the soil testing and results from Phase 1 as well as, the ease of access to site . These sites were identified as UNM 11 (JEZ 26) and UNM 12 (JEZ 27). In Phase 2, 21 soils excavated from various locations within sites UNM 11 and UNM 12 and at various depths as shown in Figure 3.1 were tested. There were 13 soils tested in Phase 3 also at various locations within sites UNM 11 and UNM 12 and at various depths as shown in Figure 3.1. Phase 4 includes testing of the final soils and SCEB mixes selected for use in SCEB production.

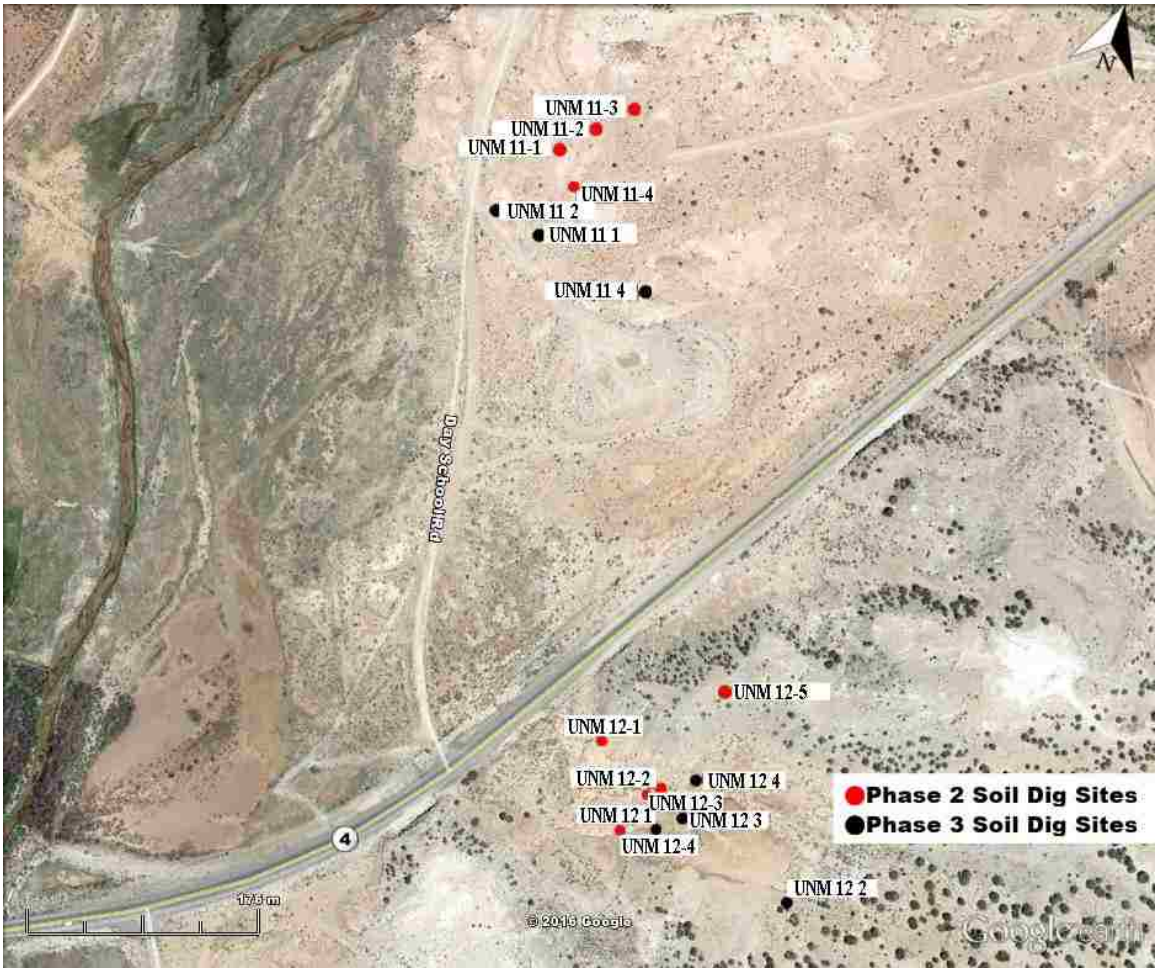

Figure 3. 1. Aerial photograph (from Google Earth) of soil dig sites on Jemez Pueblo .

A summary of the tests performed on the soils and the methodology for down selection are listed in Figure 3.2 for Phases 1 and 2 and in Figure 3.3 for Phases 3 and 4.

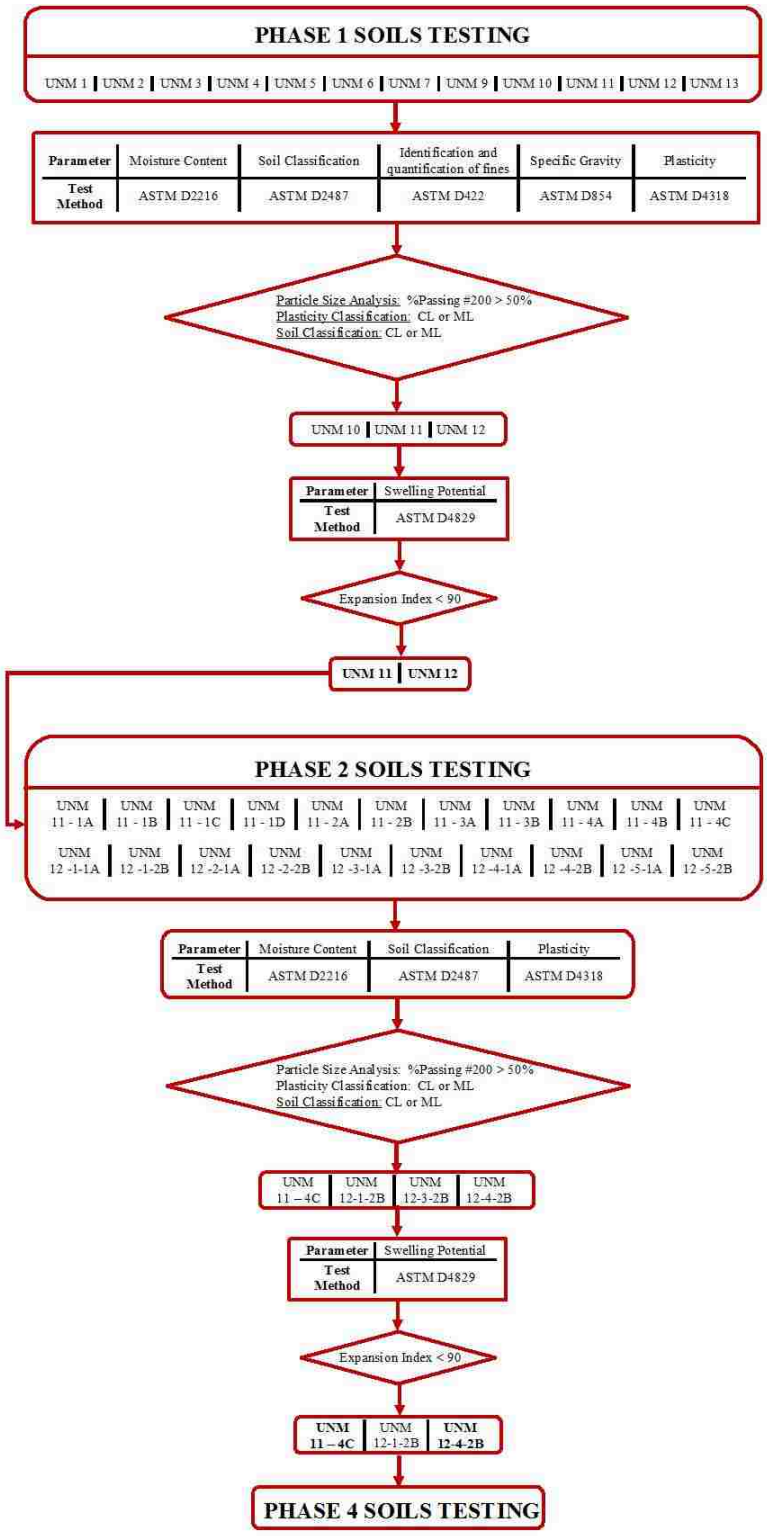

Figure 3. 2. Phase 1 and 2 summary of test methods and method for down selection of the soils suitable for SCEBs.

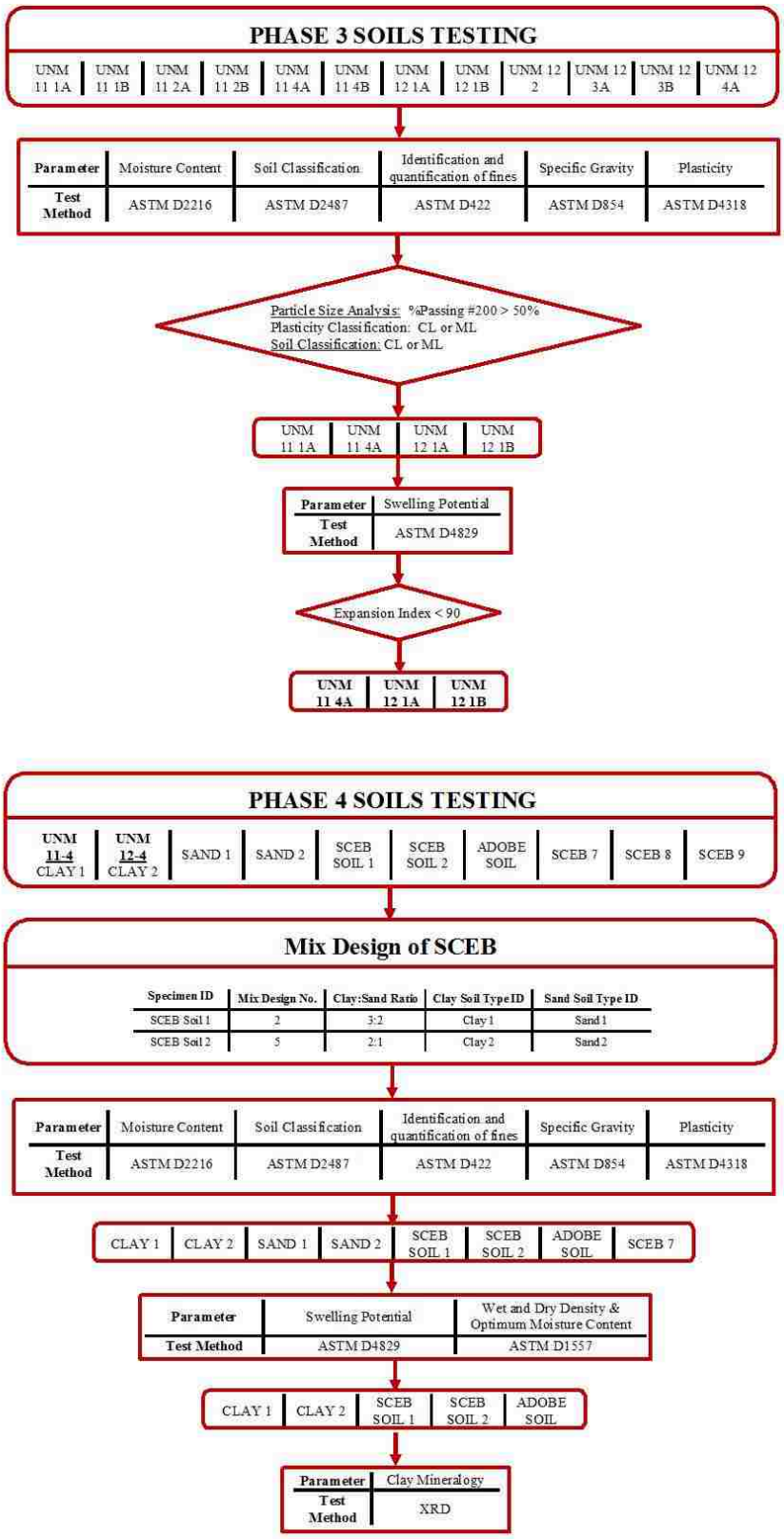

Figure 3. 3. Phase 3 and 4 summary of test methods and method for down selection of the soils suitable for SCEBs.

It was evident that there was variability in the soil's physical properties at each site. There was also variability in the soil within each dig site at varying depths. This required designing a robust mixture design to enable limiting the variation in mechanical properties of stabilized earth blocks with potential variability in soil. The schematic in Figure 3.4 shows the process used for soils testing and determining an optimal mix design for SCEBs. The experimental program was developed by the project team due to experience in the production of compressed earth blocks and knowledge of masonry. The first process shows how to down select a suitable clay(ey) soil as well as a sand for use in the SCEBs. Both the clay(ey) soil and sand are subjected to tests using ASTM test methodology to determine certain soil parameters. The diagram describes the process in determining the soils desirable for use in SCEBs. Process 1 was used to determine the suitable soils for Phases 1, 2, and 3. The clay(ey) soil and sand are then combined at various mix ratios to create the dry mix for a SCEB. The second process describes the methodology in determining if a soil mixture is suitable for SCEB production. The soil mixture is subjected to ASTM standard testing methodology to determine certain soil parameters. The diagram details the soil property criteria for a successful soil mixture for use in SCEBs. Process 2 was used to determine the suitable soil mixture for Phase 4. The "suitable" soil property criteria in Process 1 and 2 was developed in this research by using the soil characteristics of the SCEB that met NM Earthen Building Code minimum strength criteria. The soil property criteria, namely the Plasticity Index (PI) and sand content recommended in this research can be compared to the results published by Burroughs (*2008*) indicating that PI falls within the "fair" range with a 93% stabilization success in the literature.

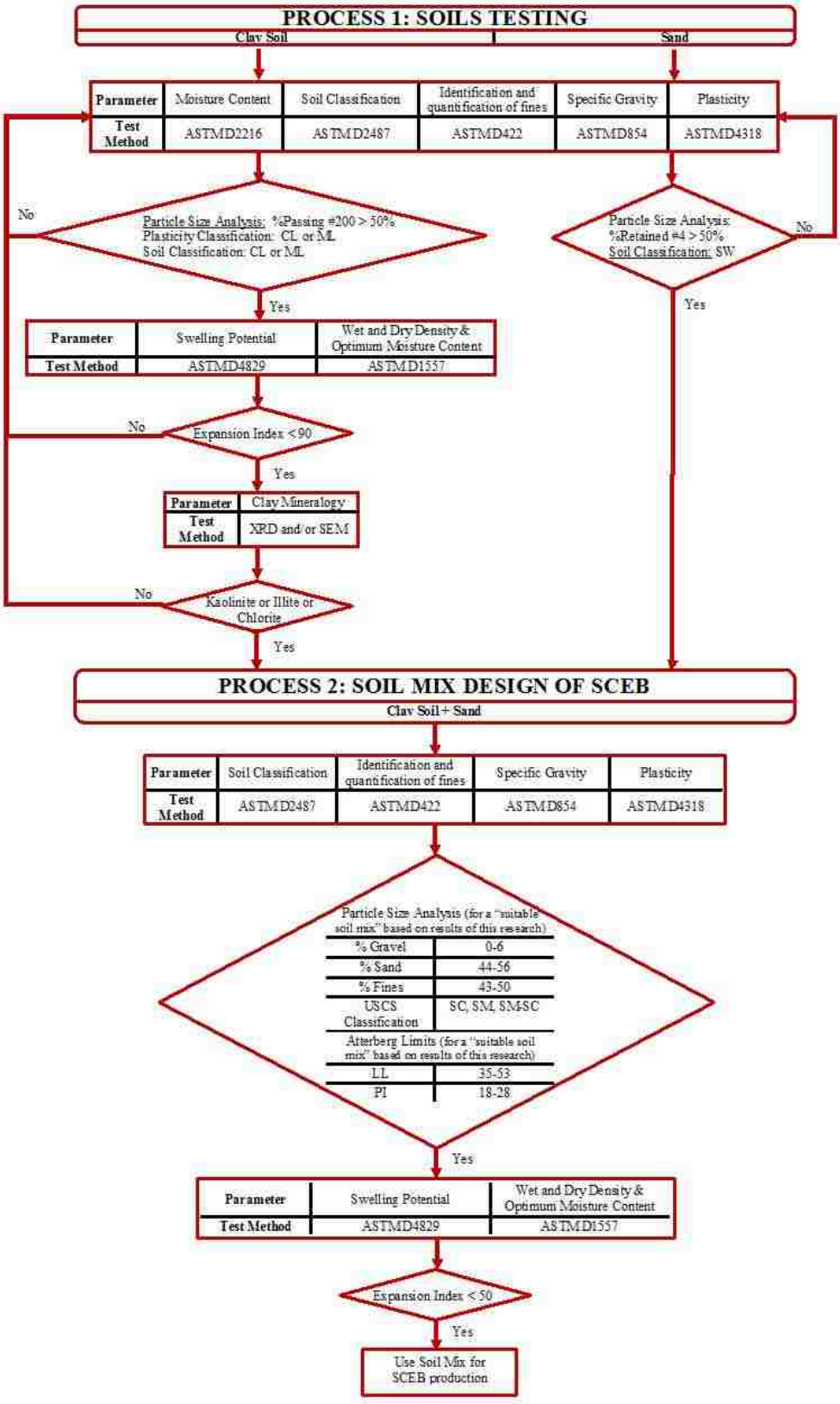

Figure 3. 4. Schematic for determining the suitability of soils for SCEB production.

3.2.1 Soil preparation and moisture content

In order to obtain a representative sample for testing, method B "Quartering" in ASTM C702 (*ASTM, 2011*) was used. In Method B, the sample is shoveled into a conical pile, flattened, and then the pile is quartered as shown in Figure 3.5. Two diagonally opposite quarters are removed from the pile and then the process is repeated until the sample is reduced to the desired size for testing.

(a)

(b)

(c)

Figure 3. 5. (a) Soil sample received from site excavation. (b) Soil sample in a conical pile. (c) Soil sample quartered.

The natural moisture content for the soil specimens as received from the site was measured in general accordance with ASTM D2216 (*ASTM, 2010*). Once the soil sample

was obtained, it was then placed in an oven at 110°C (230°F) for 24 hours as shown in Figure 3.6.

Figure 3. 6. Soil samples determining moisture content in oven at 110°C.

3.2.2 Particle Size Analysis

The grain size distribution of the soil samples was determined in accordance with ASTM D422 (*ASTM, 2007*). Sieve analysis of the portion retained on a No. 10 sieve was performed usinga 500g (17.6 oz.) sample, which has been oven dried at 110°C (230°F), washed on the No. 200 sieve and the remaining sample was placed in an oven at 110°C (230°F) for 24 hours. After 24 hours, the sample was removed from the oven and placed in the following sieve stack: 3/8 inch, No. 4, No. 20, No. 40, No. 60, No. 140, and No. 200 sieve. The stack was placed in a sieve shaker for 10 minutes and then the mass of each fraction was weighed as shown in Figure 3.7. The total percent passing for each sieve was calculated.

(a) (b)

Figure 3. 7. (a) Sieve stack in shaker for sieve analysis of the portion retained on a No. 10 sieve. (b) Weighing the soil retained on each sieve.

3.2.3 Identification and Classification of Fines

Using ASTM D422 (*ASTM, 2007*), the hydrometer and sieve analysis of portion passing the No. 10 sieve was performed to determine the amounts fines in the soil sample. In the hydrometer test, 50 g (1.8 oz.) of the soil sample was used. The soil sample was soaked in a sodium hexametaphosphate solution for 24 hours and further dispersed using a Hamilton Beach stirring apparatus for 1 minute as shown in Figure 3.8(a). Then the soil-water slurry was transferred to a 1000 mL (33.8 US fl. oz.) sedimentation cylinder. The slurry was agitated for 1 minute and then hydrometer readings were taken at 2, 5, 15, 30, 60, 250, and 1440 minutes. The hydrometer test was conducted for 24 hours as shown in Figure 3.8(b). After 24 hours, the soil sample was washed on a No. 200 sieve and placed in the oven at 110°C (230°F) for 24 hours. Then, the sample was removed from the oven

and placed in the following sieve stack: No. 20, No. 40, No. 60, No. 140, and No. 200 sieve. The stack was placed in a sieve shaker for 10 minutes and then the mass of each fraction was weighed. The total percent passing for each sieve was calculated.

(a) (b) (c)

Figure 3. 8. (a) The soil sample is prepared by mixing the specimen for 1 min then placing into a 1000 mL cylinder. (b) Hydrometer tests being performed. (c) Specific Gravity test.

In the hydrometer test, the percentages of soil in suspension was calculated using Equation (3.1) as well as the diameter of the soil particles using Equation (3.2).

$$P = {}^{Ra}/_{W} \times 100 \tag{3.1}$$

where,
P is the percentage of soil remaining in suspension at the level at which the hydrometer measures the density of the suspension, %.
a is correction faction to be applied to the reading of hydrometer 152H from Table 1 ASTM D422.
R is hydrometer reading with composite correction.
W is the oven-dry mass of soil in a total test sample represented by mass of soil dispersed, g.

$$D = K\sqrt{{}^{L}/_{T}} \tag{3.2}$$

where,
D is the diameter of particle, mm.
K is constant depending on the temperature of the suspension and the specific gravity of the soil particles. Use Table 3 in ASTM D422 to determine value.
L is the distance from the surface of the suspension to the level at which the density of the suspension is being measured, cm. The effective depth is determine by Table 2 in ASTM D422 from the hydrometer reading.
T is the time interval from beginning of sedimentation to the taking of reading, min.

In order to determine the K constant in Equation (3.2), the specific gravity was needed for each soil sample. Therefore, the specific gravity for the soil samples was determined in accordance with ASTM D854 (*ASTM, 2014*). Using Method B, about 65 g (2.29 oz.) of the soil sample is placed in a 250 mL (8.5 US fl. oz.) pycnometer. Distilled water is added to a marked water level and the pycnometer is agitated to mix the soil and distilled water to form a slurry. The pycnometer is then connected to a vacuum and the slurry is agitated under the vacuum in order to de-air the soil slurry as shown in Figure 3.8 (c). Then the mass of the pycnometer, soil and water was measured. The specific gravity was calculated using Equation (3.3).

$$G_t = \frac{\rho_s}{\rho_{w,t}} = \frac{M_s}{\left(M_{\rho_{w,t}} - \left(M_{\rho_{ws,t}} - M_s\right)\right)} \tag{3.3}$$

where,
G_t is the specific gravity at the test temperature.
ρ_s is the density of the soil solids, g/cm^3.
$\rho_{w,t}$ is the density of the water at test temperature, g/cm^3. Use Table 2 in ASTM D854.
$M_{\rho w,t}$ is the mass of the pycnometer and water at test temperature, g.
$M_{\rho ws,t}$ is the mass of the pycnometer, water, and soil solids at the test temperature, g.
M_s is the mass of the oven dry solids, g.

3.2.4 Plasticity

When a clay(ey) soil slurry decreases water content, the clay passes from a liquid state to a plastic state, and finally to a solid state (*Terzahi and Peck, 1948*). There is variability in the amount of water content at which different clays pass from one state to another. However, the transition from one state to another does not occur abruptly, it occurs over a range of water contents. Therefore, the water contents at these transitions are used for identification and comparison of different clays at defined boundaries, such as the Atterberg's limits (*Terzahi and Peck, 1948*).

In this research, tests to determine the Atterberg limits were performed in accordance with ASTM D4318 (*ASTM, 2010*). The test method determines the liquid limit, plastic limit, and the plasticity index of the soil.

The liquid limit is the percentage of water content of a soil at the boundary between the semi-liquid and plastic states. Method B was used to determine the liquid limit. The liquid limit was determined by placing the soil specimen in a brass cup, dividing it in two by a grooving tool, and then subjecting the soil specimen to blows caused by repeatedly dropping the cup in a standard mechanical device as shown in Figure 3.9 (a). The number of blows required to close the groove are 20 to 30. Equation (3.4) defines how to calculate the liquid limit using the number of blows.

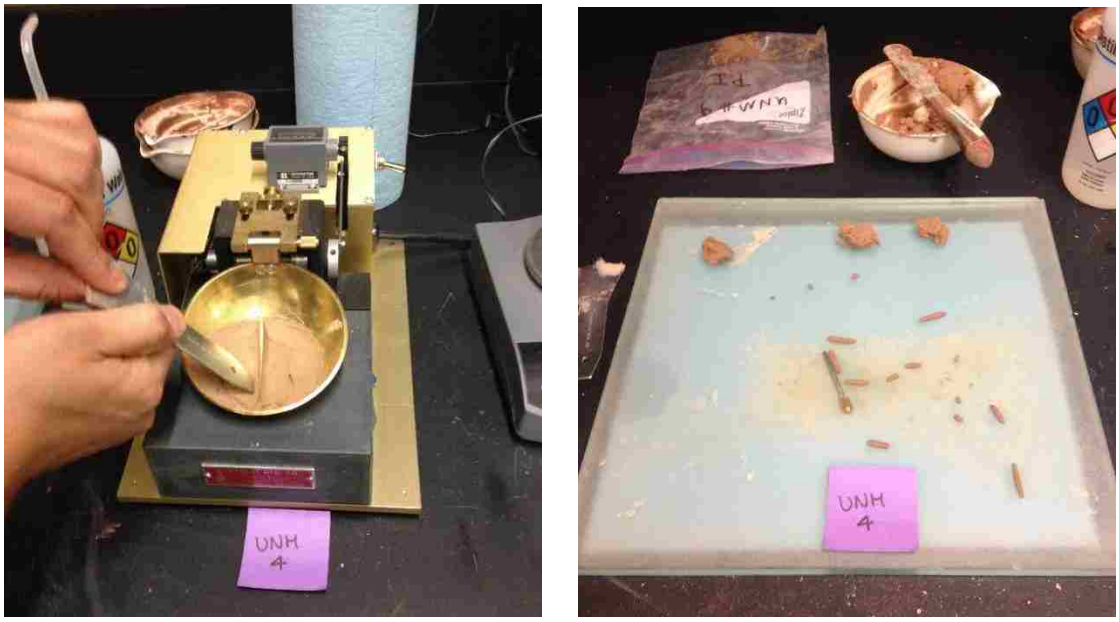

(a) (b)

Figure 3. 9. (a) Liquid Limit. (b) Plastic Limit

$$LL = w\left(N/25\right)^{0.121} \tag{3.4}$$

where,
LL is the liquid limit, %.
w is the water content for given trial, %.
N is the number of blows causing closure of the groove for given trial.

The plastic limit is the percentage of water content of a soil at the boundary between the plastic and semi-solid states. Using the hand method, the plastic limit was determined by pressing and rolling the soil into a 3.2 mm (0.13 in.) diameter thread as shown in Figure 3.9 (b). The plastic limit was reported when the soil is pressed until its water content is reduced to a point at which the thread crumbles and can no longer be pressed together and re-rolled. The portions of crumbled thread are placed in a container until it had at least 6 g (0.2 oz.) of soil and the water content was determined. Another container of at least 6 g (0.2 oz.) of soil was obtained and the average of the two water contents was calculated. The plastic limit was calculated using Equation (3.5).

$$PL = \frac{w_w - w_d}{w_d} \tag{3.5}$$

where,
PL is the plastic limit, %.
w_w is the weight of wet soil, g.
w_d is the weight of dry soil, g.

The plasticity index (PI) was calculated as the difference between the liquid limit and plastic limit in Equation (3.6). It is the range of water content over which a soil behaves plastically.

$$PI = LL - PL \tag{3.6}$$

where,
PI is the plasticity index, %.
LL is the liquid limit, %.
PL is the plastic limit, %.

Plasticity of the clay is important for molding operation. The plasticity is related to the amount of water content required to make the soil workable for block production. The more water required for workability of the soil will lead to the more pores within the block after curing is complete and the water has evaporated from the block. The large amount of voids within a block will lead to a decreased compressive and flexural strength of the block.

Therefore, the plasticity index, which is the range of the water content that the soil behaves plastically should be limited. In other words, a reduced PI is more desirable.

3.2.5 Soil Classification

The soils were classified according to Table 1 in ASTM D2487 (*ASTM, 2011*). The practice defines a system for classifying soils for engineering purposes based on the laboratory determination of soil particle-size, liquid limit, and plasticity index (*ASTM, 2011*).

3.2.6 Swelling Potential

The swelling potential of the soils were determined after being inundated in water using ASTM D4829 (*ASTM, 2011*). A test specimen was prepared by compacting the soil into a 2.54 cm (1 in.) metal ring at a degree of saturation of 50 $\pm$ 2 %.

The degree of saturation of the soil specimen was calculated using the moist density, dry density, water content, and specific gravity of the soil as shown in Equation (3.9). The moist density was calculated using Equation (3.7) and the dry density was calculated using Equation (3.8). If the degree of saturation was less than 50%, then water content should be increased and decreased if the degree of saturation was greater than 50%.

$$\rho_m = k \times \frac{(M_t - M_{md})}{V} \tag{3.7}$$

where,
ρ_m is the moist density of compaction point, g/cm^3.
k is the conversion constant, 1 for g/cm^3.
M_t is the mass of moist soil in ring and ring, g.
M_{md} is the mass of the ring, g.
V is the volume of compaction mold, cm^3.

$$\rho_d = \frac{\rho_m}{1 + \frac{w}{100}} \tag{3.8}$$

where,
ρ_d is the dry density of compaction point, g/cm^3.
ρ_w is the moist density of compaction point, g/cm^3.
w is the water content of compaction point, %.

$$S = \frac{w\, G_s\, \rho_d}{G_s\, \gamma_w - \rho_d} \tag{3.9}$$

where,
S is the degree of saturation, %.
w is the water content of compaction point, %.
G_s is the specific gravity of the soil.
ρ_d is the dry density of compaction point, g/cm^3.
γ_w is the unit weight of water, 9.79 kN/m^3 at 20°C.

Once the degree of saturation was satisfied according to ASTM D4829 (*ASTM, 2011*), the specimen and the ring were then placed in a consolidometer. A vertical confining pressure of 6.9 kPa (1 psi) was then applied to the specimen and the specimen was then inundated with distilled water for 24 hours as shown in Figure 3.10.

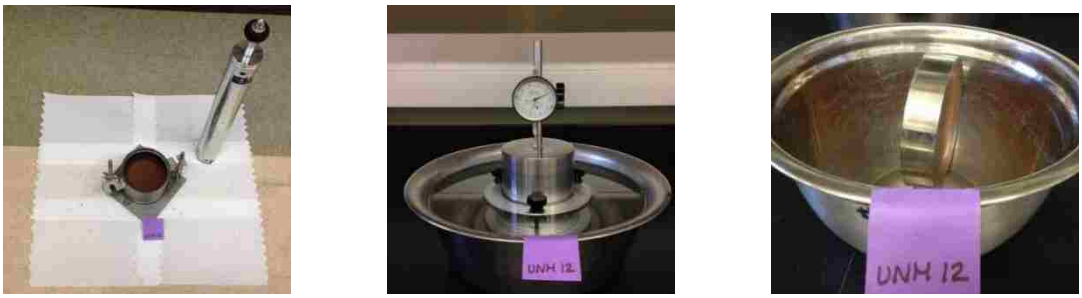

(a) (b) (c)

Figure 3. 10. (a) Soil compacted in 1" ring. (b) soil sample inundated in water. (c) Post 24 hour inundated in distilled water.

The expansion index (EI) was calculated using Equation (3.10). The soils were classified for their potential expansion using the EI according to Table 1 in ASTM D4829 (*ASTM, 2011*).

$$EI = \frac{\Delta H}{H_1}(1000) \quad (3.10)$$

where,
EI is the expansion index.
ΔH is the change in height, mm.
H_1 is the initial height, mm.

3.2.7 Modified Proctor

The test method used to determine the wet and dry density of the soil was performed in accordance with ASTM D1557 (*ASTM, 2012*). Method A from ASTM D1557 was used based on the particle size analysis, since less than 25% by mass of the soil specimen was retained on the No.4 sieve for each soil tested. The soil, at a selected molding water content, was placed in a 101.6 mm (40 in.) diameter mold and compacted into 5 layers by 25 blows per layer with a 44.48 N (10 lb.) rammer dropped from a height of 457.2 mm (180 in.) producing a compactive effort of 2700 kN-m/m^3 (2.7 MPa) (*ASTM, 2012*). The laboratory compaction method was repeated for a sufficient number of molding water contents to show the curvilinear relationship between the molding water content and the dry unit weights of the soil in order to plot the compaction curve. The values of optimum water content, maximum saturated unit weight, and maximum dry unit weight were determined from the compaction curve. The water content corresponding to the maximum dry unit weight is the optimum water content. The dry unit weight was calculated using Equation (3.11). In order to calculate the dry density of the compaction point, Equation (3.8) was used.

While the soil is being compacted, the water acts as a lubricant for the soil particles. At a water content higher than the optimum, the additional water reduces the dry density because the water occupies the space that might have been occupied by the soil and does not allow bonding. At lower water content than optimum, the soil is stiff and offers more

resistance to compaction, which reduces the degree of compaction. The optimum water content is influenced by the reaction of the soil particles to water. For the soils tested that classify as clay, the clay mineralogy effects whether a soil will expand in the presence of water which influences the optimum water content.

$$\gamma_d = K_2 \, \rho_d \tag{3.11}$$

where,
γ_d is the dry unit weight of compacted specimen, kN/m^3.
ρ_d is the dry density of compaction point, g/cm^3.
K_2 is the conversion constant. Use 9.8066 for density in g/cm^3.

3.2.8 Mineralogy

Clay size particles are less than 2 μm (0.00008 in.) in diameter. Silt-size particles are larger than 2 μm (0.00008 in.), but smaller than 0.075 mm (0.003 in.). Sand-size particles are larger than 0.075 mm (0.003 in.), but smaller than 4.75 mm (0.19 in.). Silt and sand-size particles are made up of many different minerals, the most common are quartz (SiO_2) and feldspars (calcium, sodium, and potassium aluminosilicates) (*Smith and Austin, 1996*). Clay minerals include kaolinite, illite, smectite, chlorite, vermiculite, and mixed-layer illite/smectite (I/S) which are the principal clay groups or types. High aluminum kaolinite and high potassium illite are nonexpendable, meaning they will only expand slightly in the presence of water. While calcium or sodium rich smecitite or (I/S) are expandable and will swell in the presence of water (*Smith and Austin, 1996*).

Soils that classify as clay and used in the SCEBs were evaluated using X-ray diffraction (XRD). This test identified the dominant clay minerals in these soils. The UNM Earth & Planetary Sciences X-Ray Diffraction Laboratory was used to obtain these measurements. XRD continuous scan was performed using the Rigaku SmartLab system

as shown in Figure 3.11 with optimization for scattering angles θ of $2^o < \theta < 150^o$ with 0.02^o per step. The scan rate was 6.1^o/min for 40 minutes. Equation (3.12) shows the relation between the d-spacing and the angle of diffraction.

$$\lambda = 2dsin\theta \tag{3.12}$$

where,
λ is the wave length use, nm.
d is the d-spacing, nm.
θ is the diffraction angle, degrees.

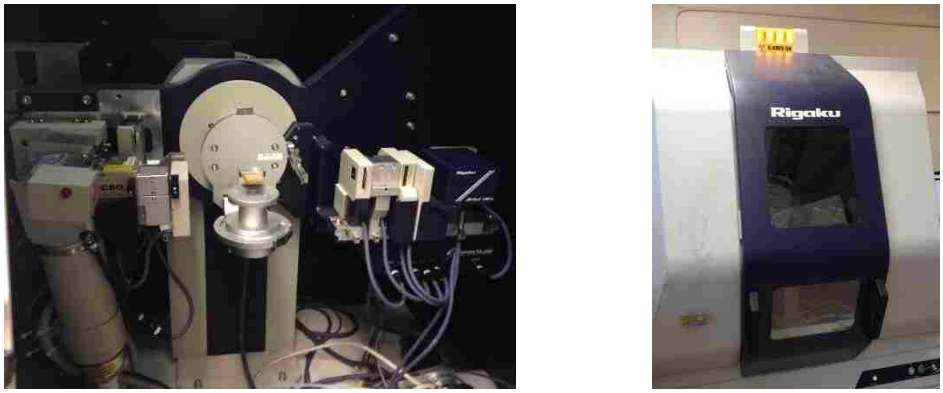

(a) (b)

Figure 3. 11. (a) Soil specimen placed in Rigaku SmartLab system. (b) Rigaku SmartLab system.

In order to identify the clay minerals, there were five XRD scans performed on each soil sample; one scan per each orientation. There were five different orientations and sample preparations used: random orientated mount, oriented mount air dried, oriented mount treated with ethylene glycol, oriented mount heated to 400°C (752°F), and oriented mount heated to 550°C (1022°F). For the random mount sample preparation, the soil sample was placed in a mold by means of side drifting and taping into place as shown in Figure 3.12. The oriented mount sample preparation included placing 1 g (0.04 oz.) of the soil sample with 10 mL (0.34 US fl. oz.) of distilled water in a vial, shaking it, and leaving it to disperse for 24 hours as shown in Figure 3.13 (a). After 24 hours, water was decanted

in order to remove salts and let the clay deflocculate. This process was repeated three times. After 3 to 4 days, the soil sample was placed on a slide with a pipette and allowed to air dry on the slide for 24 hours as shown in Figure 3.13 (b). Then the oriented mount air dried sample was placed in the Rigaku SmartLab system for a XRD scan. The same oriented mount sample was placed in a dissector with ethylene glycol for 48 hours as shown in Figure 3.13 (c). Then the oriented mount treated with ethylene glycol was placed in the Rigaku SmartLab system for a XRD scan. The same oriented mount sample was then placed in an oven at 400°C (752°F) for at least 30 minutes and then placed in the Rigaku SmartLab system for a XRD scan. Finally, the same oriented mount sample was then placed in an oven at 550°C (1022°F) for at least 30 minutes and then placed in the Rigaku SmartLab system for a XRD scan.

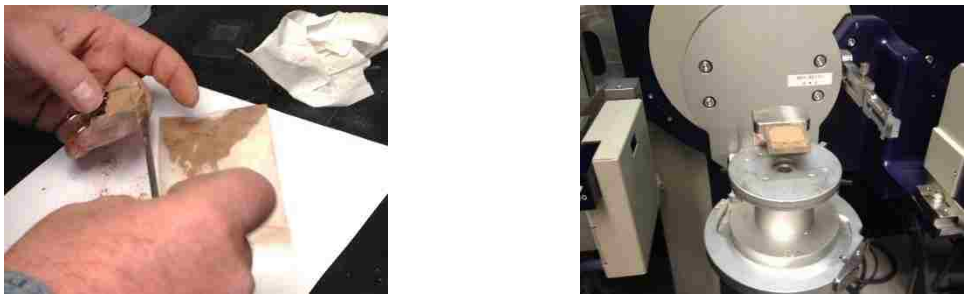

(a) (b)

Figure 3. 12. (a) Preparing random mount sample. (b)Random mount sample placed in Rigaku SmartLab.

(a) (b) (c)

Figure 3. 13. (a) Oriented Mount Sample prepared. (b) Slide with oriented mount sample. (c) Desiccator with Ethylene Glycol.

The clay particle size was also investigated by scanning electron microscope (SEM) using a FEI Quanta 3D Field Emission Gun SEM as shown in Figure 3.14. The sample was dispersed onto carbon sticky tape mounted on an aluminum SEM stub. The sample was imaged, uncoated at 30 kV and a beam current of 4 nA using secondary electron imaging and backscattered electron imaging. Full spectral X-ray maps of the sample were obtained using an EDAX Genesis X-ray analysis system equipped with an Apollo 40 mm^2 solid state detector (SDD) at typical count rates 100-150 K per second with collection dead times of around 50%.

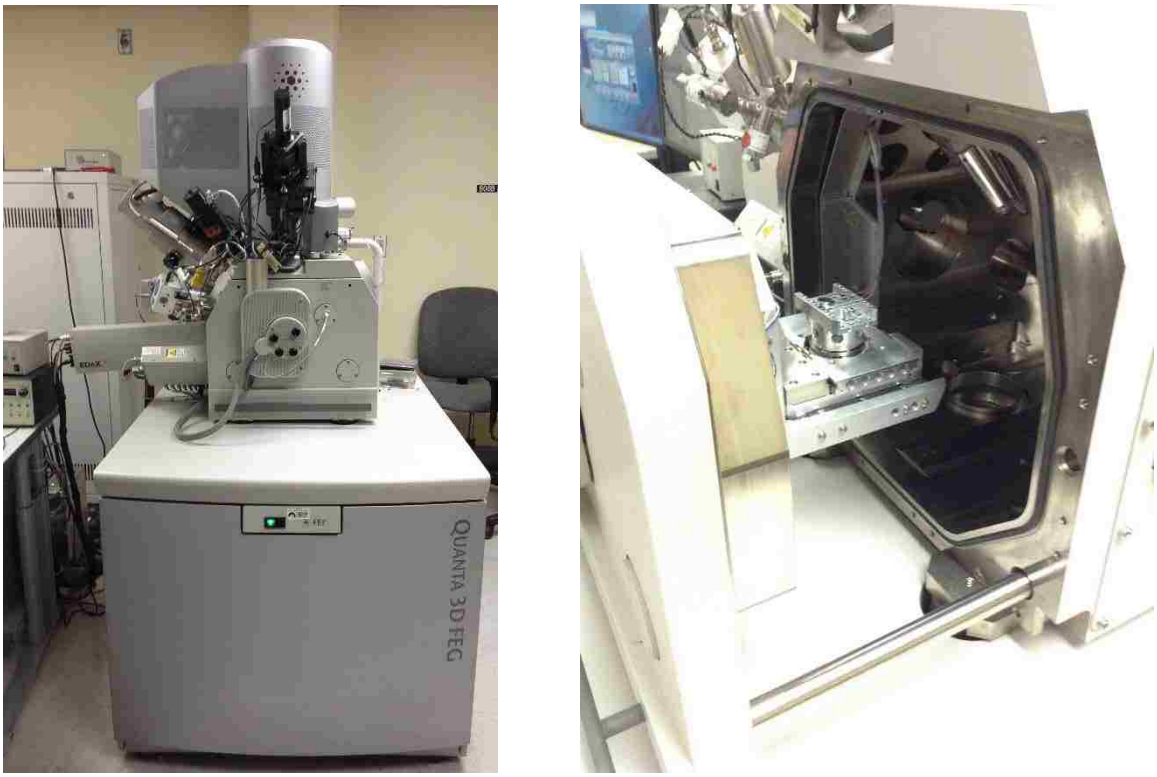

(a) (b)

Figure 3. 14. (a) FEI Quanta 3D Field Emission Gun SEM. (b) Soil sample on a carbon sticky tape mounted on an aluminum SEM stub.

3.3 Stabilized Compressed Earth Block Construction

The device used for SCEB production was a two stage horizontal hydraulic compression machine. The process to produce SCEBs is shown in seven stages.

The first stage was excavating the sand and clay(ey) soil material and transporting to the production site. The sand and clay (ey) soil piles on site are shown in Figure 3.15 (a). The second stage was sieving the clay(ey) soil on a 6.3 mm (0.25 in.) sieve. The sieve is shown in Figure 3.15 (b). The third stage included the dry mixing of sand, clay(ey) sand and adding the cement by a determined mix ratio. The dry mixing was performed with the Bobcat as shown in Figure 3.15 (c). The fourth stage consisted of placing the dry SCEB soil mix in the hopper to be further mixed as shown in Figure 3.15 (d). The fifth stage comprised of the SCEB soil mix fed to the conveyor belt where water was added at a high pressure and was collected in the Bobcat as shown in Figure 3.16 (a). The sixth stage included placing the moist SCEB soil mix into the two stage horizontal hydraulic compression machine as shown in Figure 3.16 (b). The seventh and final stage consisted of molding the SCEB block and placing blocks on a pallet to cure. The SCEB soil mix was gravity fed into a mold which was then compressed horizontally first at a pressure of approximately 13.8 MPa (2000 psi) and then at a pressure of 6.9 MPa (1000 psi), per the manufacturer recommendation. The blocks were produced at a rate of 5 to 6 blocks per minute. The full size SCEB blocks were 35.6 cm x 25.4 cm x 10.2 cm (14 in. x 10 in. x 4in.). Once compressed, the blocks were placed on a wooden pallet, wrapped with shrink wrap, and allowed to cure for 28 days as shown in Figure 3.17 and 3.18. They were transported to the University of New Mexico Structural Lab and stored in a room of 25°C (77°F) and a relative humidity of 20%.

(a)

(b)

(c)

(d)

Figure 3. 15. (a) Left pile is Sand and Right plie is Clay(ey) soil. (b) Clay(ey) soil is sieved on the No. 4 sieve. (c) Dry Mix on Site with Bobcat. (d) Placing dry mix in the hopper to add water.

(a)

(b)

Figure 3. 16. (a) Water added on conveyor belt of hopper. (b) Moist mix is added to Compression machine.

(a) (b)

Figure 3. 17. (a) CEB Machine. (b) CEB being pushed out of the two stage horizontal compression.

Figure 3. 18 Recently compressed SCEBs on pallet to be wrapped in order to cure.

The adobe bricks used to compare the strengths of SCEB were purchased from New Mexico Earth, Inc. located in Albuquerque, New Mexico. New Mexico Earth produces adobe bricks from a mud mixture which was poured in to a wooden mold. When the bricks are dry, the mold was lifted. Then, the adobe bricks are turned on edge to complete the

drying process. Since it was winter when the adobe bricks were purchased for use in this research, the bricks were located in the storage yard as shown in Figure 3.19.

Figure 3. 19. NM Earth Adobe yard with Stabilized Adobe and Formwork shown.

3.4 Block Testing

Stabilized compressed earth blocks (SCEBs) were tested to determine dry and saturated compressive strength, dry and saturated flexural strength, water absorption, the initial rate of absorption, sorptivity, modulus of elasticity, and poisson's ratio.

The SCEBs were provided by Functional Earth Consulting, LLC. Received SCEBs were given a specimen identification as shown in Table 3.1. The soil sample used for earth block production of blocks: SCEB 1, 2, 3, and 4 was soil sample, UNM 11-4 (Clay 1). The soil sample used for earth block production of blocks: SCEB 5, 6, 7, 8, and 9 was soil sample, UNM 12-4 (Clay 2).

In addition, the SCEBs were compared to the results from commercial Adobe blocks purchased from New Mexico Earth Inc. There were two types of adobe tested: unstabilized and stabilized as shown in Table 3.2.

Table 3. 1. SCEB Specimen Identification.

Specimen ID	Clay:Sand Ratio (by Volume)	Stabilizer	Soil Type	Production Date
SCEB 1	1:1	1% Lime	UNM 11 - 4	8-25-15
SCEB 2	3:2	4% Lime	UNM 11 - 4	9-1-15
SCEB 3	3:2	5% Cement	UNM 11 - 4	9-8-15
SCEB 4	3:2	6% Cement	UNM 11 - 4	9-10-15
SCEB 5	2:3	6% Cement	UNM 12 - 4	1-27-16
SCEB 6	1:1	6% Cement	UNM 12 - 4	1-27-16
SCEB 7	2:1	10% Cement	UNM 12 - 4	2-18-16
SCEB 8	2:1	10% Cement	UNM 12 - 4	3-2-16
SCEB 9	2:1	10% Cement	UNM 12 - 4	3-2-16

Table 3. 2. Adobe Specimen Identification.

Specimen ID	Stabilizer	Soil Type
SAB	Asphalt	Adobe Soil
AB	N/A	Adobe Soil w/ straw

A summary of the tests performed on the blocks and the methodology for down selection of optimum blocks are listed in Figure 3.20.

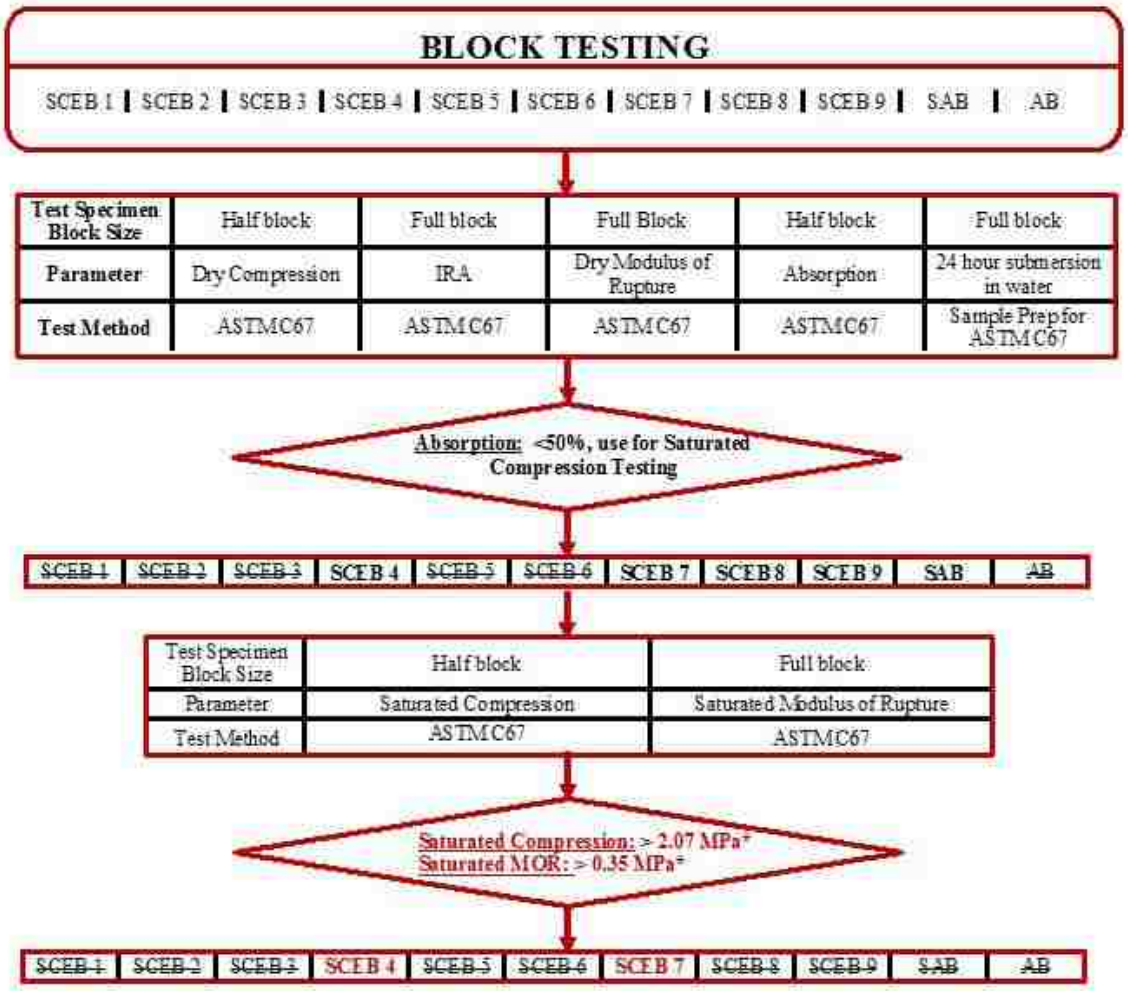

Figure 3. 20. Diagram.showing SCEB and Adobe block testing and methodology for down selection of optimum blocks.

3.4.1 Unconfined Compressive Strength

The unconfined compression test is a laboratory method to determine the compressive strength of the SCEB blocks and compare to that of the Adobes. In order to design a load-bearing masonry wall, the design engineer needs to know the unit compressive strength.

The structural strength of SCEBs are affected by moisture. Therefore, there were two simulated environmental conditions tested on the blocks. First, the dry unconfined

compressive strength was determined and second the saturated unconfined compressive strength. For all testing, the SCEBs were cured for 28 days in a plastic wrapped pallet stored in the UNM Structures Laboratory at a temperature of 25°C and relative humidity of 20%.

For the dry unconfined compression test, full size SCEB blocks, 35.6 cm x 25.4 cm x 10.2 cm (14 in. x 10 in. x 4 in.) were cut with a brick saw into half blocks, 35.6 cm x 12.7 cm x 10.2 cm (14 in. x 5 in. x 4 in.) and used for testing. Five samples of each of the blocks were tested for statistical purposes. Once cut, the samples were placed in an oven at 110°C (230°F) for 24 hours and allowed to cool for at least 4 hours prior to testing.

SCEB 1, 2, 3, and 4 were tested on the 1779 kN (400 kip) capacity Forney Machine, Model No. QC-400-D using a loading rate of 3.4 MPa/min (500 psi/min) as shown in Figure 3.21 (a). The blocks: SCEB 5, 6, 7, 8, 9, SAB and AB were tested using the 1779 kN (400 kip) capacity Tinius Olsen machine, Model No. 139000 using a loading rate of 3.4 MPa/min (500 psi/min) as shown in Figure 3.21 (b). If the loading rate of 3.4 MPa/min (500 psi/min) was deemed to be too fast, the speed of testing as recommended by ASTM C67 (*ASTM, 2012*) was used to guide testing. The SCEBs were tested in the flat position and a 35.6 cm x 12.7 cm x 1.3 cm (14 in. x 5 in. x 1.5 in.) cold rolled steel plate was used between the SCEB and the upper spherical bearing area attached to the upper head of the machine.

The unconfined compressive strength of the SCEBs were determined in general accordance with New Mexico Earthen Building Materials Code, Section J of 14.7.4.23 (*NMAC, 2012*). Equation (3.13) was used to calculate the compressive strength of the SCEBs.

$$UCS = \frac{P_f}{A} \tag{3.13}$$

where,
UCS is the unconfined compressive strength, MPa.
Pf is the force at failure indicated by testing machine, N.
A is the cross-sectional area of the top face of the block, mm^2.

For the saturated unconfined compression test, the same half-block specimens, 35.6 cm x 12.7 cm x 10.2 cm (14 in. x 5 in. x 4 in.), used in the absorption test were used to determine its saturated unconfined compressive strength. Once the full size SCEB units were cured, the blocks were cut using a brick saw to half size, 35.6 cm x 12.7 cm x 10.2 cm (14 in. x 5 in. x 4 in.). Then the half size SCEBs were placed in an oven at 110°C (230°F) for 24 hours and allowed to cool for at least 4 hours prior to absorption testing. Then, the SCEBs and Adobes were placed in a container filled with distilled water and saturated for 24 hours at room temperature. After being saturated for 24 hours, the half size SCEBs were again placed in an oven at 110°C (230°F) for 24 hours and allowed to cool for at least 4 hours prior to compression testing.

SCEB 1, 2, 3, and 4 were tested on the 1779 kN (400 kip) capacity Forney Machine, Model No. QC-400-D using a loading rate of 3.4 MPa/min (500 psi/min) as shown in Figure 3.21 (a). The blocks: SCEB 5, 6, 7, 8, 9, SAB and AB were tested using the 1779 kN (400 kip) capacity Tinius Olsen machine, Model No. 139000 using a loading rate of 3.4 MPa/min (500 psi/min) as shown in Figure 3.21 (b). If the loading rate of 3.4 MPa/min (500 psi/min) was deemed to be too fast, the speed of testing as recommended by ASTM C67 (*ASTM, 2012*) was used to guide testing.

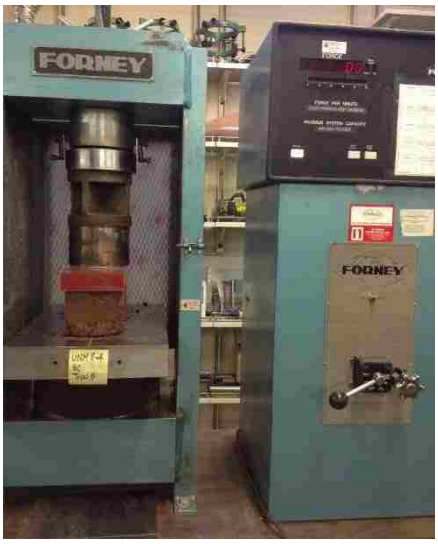

(a) (b)

Figure 3. 21. (a) Dry Compression test on Forney. (b) Dry Compression test on Tinius Olsen.

The saturated unconfined compressive strength of the SCEBs were calculated using Equation (3.13). The compressive strength was compared with the New Mexico Earthen Building Materials Code, Section J of 14.7.4.23 minimum saturated compressive strength of 2.1 MPa (300 psi) (*NMAC, 2012*).

3.4.2 Modulus of Elasticity and Poisson's Ratio

The modulus of elasticity of the block is used to describe a material's tensile elasticity. It is the ratio of the stress applied to the material to the strain (resistance) produced by that material.

The modulus of elasticity was determined using the data obtained from the dry compression testing of the SCEB and Adobe blocks. The Tinius Olsen machine, Model No. 139000 (Figure 3.22 (a)) was used to obtain the force and displacement data points of SCEB 5, 6, 7, 8, 9, SAB, and AB. The stress and strain data points were calculated using the force and displacement data and Equations (3.14) and (3.15). The modulus of elasticity

was calculated using the slope of the elastic portion of the stress vs. strain curve and Equation (3.16).

$$\sigma = \frac{F}{A} \tag{3.14}$$

where,
σ is the stress, MPa.
F is the applied force, N.
A is the cross-sectional area of the top face of the block, mm^2.

$$\varepsilon = \frac{\Delta L}{L} \tag{3.15}$$

where,
ε is the strain, mm/mm.
ΔL is the change in length, mm.
L is the original length, mm.

$$E = \frac{\Delta \sigma}{\Delta \varepsilon} \tag{3.16}$$

where,
E is the modulus of elasticity, MPa.
Δσ is the change in stress before the elastic limit, MPa.
Δε is the change in strain before the elastic limit, mm/mm.

Figure 3. 22. (a) 400 kip capacity Tinius Olsen machine, Model No. 139000 (b) SCEB dry compression test to determine Poisson's Ratio on 120 kip capacity Instron machine, Model No.AW2568-3.

Poisson's ratio is a material property and is the ratio of transverse (vertical) strain to longitudinal (horizontal) strain along the vertical direction. Tensile deformation is considered positive and compressive deformation is considered negative.

Poisson's ratio was determined only for SCEB 7 using an unconfined dry compression test on the 120 kip capacity Instron, Model No. AW2568-3. A loading rate of 3.4 MPa/min (500 psi/min) was used. Two x-y planar rosettes, 10 mm grid, 120 Ω, 3-leads, 3 m long, were placed on the SCEB to measure the change vertical and horizontal displacement as shown in Figure 3.22 (b). Equation (3.17) was used to determine the Poisson's ratio.

$$\nu = -\frac{\varepsilon_{trans}}{\varepsilon_{axial}} \tag{3.17}$$

where,
ν is Poisson's ratio.
ε_{trans} is the transverse strain, mm/mm.
ε_{axial} is the axial strain, mm/mm.

3.4.3 Modulus of Rupture

The modulus of rupture (MOR) quantifies a SCEB or Adobe blocks ability to resist flexural stress. Also when designing a load-bearing masonry wall, the design engineer needs to know the flexural strength of the unit.

The structural strength of SCEBs are affected by moisture as previously stated. Therefore, the dry and saturated modulus of rupture were determined. For all testing, the SCEBs were cured for 28 days in a plastic wrapped pallet and stored in the UNM Structures Laboratory at a temperature of 25°C (77°F) and relative humidity of 20%.

For the dry modulus of rupture (three point bending) test, the full size SCEBs, 35.6 cm x 25.4 cm x 10.2 cm (14 in. x 10 in. x 4 in.) were used. Five samples of each of the blocks were tested for statistical purposes. After curing, specimens were placed in an oven at 110°C for 24 hours and allowed to cool for at least 4 hours prior to testing.

SCEB 1, 2, 3, and 4 were tested on the 1779 kN (400 kip) capacity Forney Machine, Model No. QC-400-D using a loading rate of 3.4 MPa/min (500 psi/min) as shown in Figure 3.23 (a). The blocks: SCEB 5, 6, 7, 8, 9, SAB and AB were tested using the 1779 kN (400 kip) capacity Tinius Olsen machine, Model No. 139000 using a loading rate of 3.4 MPa/min (500 psi/min) as shown in Figure 3.23 (b). If the loading rate of 3.4 MPa/min (500 psi/min) was deemed to be too fast, the speed of testing as recommended by ASTM C67 (*ASTM, 2012*) was used to guide testing. The SCEBs were tested in the flat position. The SCEB was placed upon two - 5.1 cm (2 in.) diameter cold rolled steel cylindrical supports which were spaced 5.1 cm (2 in.) from each end of the block. The span between supports was 25.4 cm (10 in.). A third 5.1 cm (2 in.) diameter cold rolled steel cylinder

was placed above the blocks at the midpoint of the block and parallel to the supports as shown in Figure 3.23 (b).

The flexural strength or modulus of rupture of the SCEBs and Adobes were determined in general accordance with New Mexico Earthen Building Materials Code, Section J of 14.7.4.23 (*NMAC, 2012*). Equation (3.18) was used to calculate the flexural strength of the SCEBs and Adobes.

$$\sigma_f = \frac{3 \times P_f \times L}{2 \times b \times t^2} \tag{3.18}$$

where,
σ_f is the flexural stress, MPa
P_f is the force at failure, N
L is the support span, mm
b is the width of block, mm
t is the thickness of block, mm

Figure 3. 23. (a) SCEB 4 tested for dry MOR on Forney. (b) SCEB 7 tested for dry MOR on Tinius Olsen.

For the saturated modulus of rupture test, the full size SCEBs, 35.6 cm x 25.4 cm x 10.2 cm (14 in. x 10 in. x 4 in.), were used as in the dry modulus of rupture test. After curing, the samples were placed in an oven at 110°C (230°F) for 24 hours and allowed to

cool for at least 4 hours prior to absorption testing. The samples were then placed in a container filled with distilled water and saturated for 24 hours at room temperature. After being saturated for 24 hours, the full size SCEBs were again placed in an oven at 110°C (230°F) for 24 hours and allowed to cool for at least 4 hours prior to MOR testing.

SCEB 1, 2, 3, and 4 were tested on the 1779 kN (400 kip) capacity Forney Machine, Model No. QC-400-D using a loading rate of 3.4 MPa/min (500 psi/min) as shown in Figure 3.24 (a). The blocks: SCEB 5, 6, 7, 8, 9, SAB and AB were tested using the (1779 kN) 400 kip capacity Tinius Olsen machine, Model No. 139000 using a loading rate of 3.4 MPa/min (500 psi/min) as shown in Figure 3.24 (b). If the loading rate of 3.4 MPa/min (500 psi/min) was deemed to be too fast, the speed of testing as recommended by ASTM C67 (*ASTM, 2012*) was used to guide testing.

The saturated flexural strength of the SCEBs were calculated using Equation (3.18). The flexural strength was compared with the New Mexico Earthen Building Materials Code, Section K of 14.7.4.23 which requires a strength of 0.35 MPa (50 psi) when units are tested in fully saturated state (*NMAC, 2012*).

Figure 3. 24. (a) Saturated SCEB 4 tested for MOR on Forney. (b) Saturated SCEB 7 tested for MOR on Tinius Olsen.

3.4.4 Absorption

A limitations of SCEBs and Adobes is that while in contact with water swelling of the clayey soil within the blocks occurs and can cause erosion of the block. Therefore, it is a necessary material property to understand the amount of water absorption. For the absorption test, half-block specimens, 35.6 cm x 12.7 cm x 10.2 cm (14 in. x 5 in. x 4 in.) were used to determine the amount of water absorbed during 24 hours.

For all testing, the SCEBs were cured for 28 days in a plastic wrapped pallet and stored in the UNM Structures Laboratory at a temperature of 25°C (77°F) and relative humidity of 20%. Once the full size SCEB units were cured, the blocks were cut using a brick saw to half size, 35.6 cm x 12.7 cm x 10.2 cm (14 in. x 5 in. x 4 in.). Then, the half size SCEBs were placed in an oven at 110°C (230°F) for 24 hours and allowed to cool for at least 4 hours prior to absorption testing. Then, the SCEBs and Adobes were weighed and placed in a container filled with distilled water and saturated for 24 hours at room

temperature as shown in Figure 3.25. Five samples of each of the blocks were tested. ASTM C67 (*ASTM, 2012*) was used to guide testing. After being submerged for 24 hours, the blocks were wiped and weighed. The amount of water absorption was calculated using Equation (3.19).

(a) (b)

Figure 3. 25. (a) SAB half block Absorption testing. (b) SCEB 7 half block Absorption testing.

$$Absorption = \frac{(W_s - W_{d)}}{W_d} \ 100 \tag{3.19}$$

where,
Absorption is the amount of water absorbed by each specimen, %.
W_s is the saturated weight of the specimen after submersion in distilled water, g.
W_d is the dry weight of the specimen, g.

3.4.5 Initial Rate of Absorption (IRA)

As previously stated, a limitation of SCEBs and Adobes is the swelling potential of the soil while in contact with water. Therefore, IRA is also a necessary material property

to understand the rate of water absorption. For the IRA test, full size SCEB blocks, 35.6 cm x 25.4 cm x 10.2 cm (14 in. x 10 in. x 4 in.) were used for the initial rate of absorption test. ASTM C67 (*ASTM, 2012*) was used to guide testing.

For all testing, the SCEBs were cured for 28 days in a plastic wrapped pallet and stored in the UNM Structures Laboratory at a temperature of 25°C (77°F) and relative humidity of 20%. Then, the full size SCEBs were placed in an oven at 110°C (230°F) for 24 hours and allowed to cool for at least 4 hours prior to absorption testing. Then, the SCEBs and Adobes were weighed and placed in a container filled with distilled water up to 0.3175 cm (1/8 in.) above the 0.635 cm (¼ in.) supports for 1 minute as shown in Figure 3.26 (a). Five samples of each of the blocks were tested. After absorption for 1 minute, the blocks were wiped and weighed. Initial rate of absorption (IRA) is the amount of water absorbed in one minute over 193.55 cm^2 (30 in^2) of the block and the IRA was calculated using Equation (3.20).

$$IRA = \frac{W}{L(B)}\ 193.55 \tag{3.20}$$

where,
IRA is the initial rate of absorption which is the gain in weight of specimen corrected to basis of 193.55 cm^2, g/min/193.55 cm^2.
W is the actual gain in weight of the specimen, g.
L is the length of specimen, cm.
B is the width of specimen, cm.

After the SCEB and Adobe blocks were weighed and the IRA calculated, the blocks were then placed in the oven at 110°C (230°F) for 24 hours and allowed to cool for at least 4 hours as shown in Figure 3.26 (b). The blocks were then used for the dry modulus of rupture testing.

(a)

(b)

Figure 3. 26. (a) SCEB 7 IRA. (b) SCEBs in oven after IRA testing.

3.4.6 Sorptivity

The SCEBs were cured for 28 days in a plastic wrapped pallet and stored in the UNM Structures Laboratory at a temperature of 25°C (77°F) and relative humidity of 20%. After the blocks were fully cured, the full size SCEBs, 35.6 cm x 25.4 cm x 10.2 cm (14 in. x 10 in. x 4 in.) were cut using a brick saw into 100 mm x 100 mm x 50 mm (3.9 in. x 3.9 in. x 2.0 in.) specimens. SCEB 4, 5, 7 and SAB were the only blocks tested. Two samples of each of the blocks were tested for statistical purposes. ASTM C1585 (*ASTM, 2013*) was used to guide testing.

The 100 mm x 100 mm x 50 mm (3.9 in. x 3.9 in. x 2.0 in.) specimens were conditioned according to the sample conditioning from ASTM C1202 (*ASTM, 2012*). First the SCEB and Adobe specimens were weighed as shown in Figure 3.27 (a). Then, the specimens were placed in a sealed desiccator, the vacuum was started and the specimens were left for 3 hours as shown in Figure 3.27 (c). A separatory funnel was filled with distilled water and placed near the desiccator. While still under vacuum, the stopcock was opened and distilled water was allowed to drain into the desiccator until the specimen was inundated with water as shown in Figure 3.27 (d). The specimen was left under vacuum saturation for at least 18 hours. After the 18 hours, the specimen was removed from the vacuum as shown in Figure 3.27 (e) and taken out of the desiccator. The specimen was then weighed. Using ASTM C1585 (*ASTM, 2013*), the specimen was then placed in an environmental chamber at a temperature of 50°C (122°F) and relative humidity of 80% for 3 days as shown in Figure 3.27 (f) and (g). The environmental chamber used in this research was a glass desiccator with a saturated solution of potassium bromide which was placed in an oven of 50°C (122°F). After 3 days, the specimen was placed inside a sealable

container for 15 days in a room at a temperature of 25°C (77°F) as shown in Figure 3.27 (h).

After 15 days, the absorption procedure began. The specimen was removed from the storage container and the mass of the conditioned specimen was recorded as shown in Figure 3.27 (b). Then, the top and sides of the specimen were sealed with a plastic sheet and duct tape as shown in Figure 3.27 (i). This allowed for water absorption by capillary action. A container with ability to maintain a constant water level was used and two specimen supports were placed at the bottom of the container. The water level was maintained at a level of 2 +/- 1 mm above to top of the supports. The mass was recorded at intervals described in Table 1 of ASTM C1585 (*ASTM, 2013*) as shown in Figure 3.27 (j). The absorption, *I* was calculated using Equation (3.21) and plotted against the square root of time. The initial rate of water absorption is defined as the slope of the line that is best fit to the plot from 1 minute to 6 hours. If the data between 1 minute and 6 hours is not linear, then the initial rate of absorption cannot be determined. The secondary rate of water absorption is defined as the slope of the line that is best fit to absorption plotted against the square root of time of points from 1 day until 7 days. Also if the data between day 1 and day 7 is not linear, then the secondary rate of absorption cannot be determined.

$$I = \frac{m_t}{a\,(d)} \tag{3.21}$$

where,
I is the absorption, mm.
m_t is the change in specimen mass at time, g.
a is the exposed area of the specimen, mm^2.
d is the density of the water, g/mm^3.


2:1 10%
Trial 1
2:1 TRIAL 1
2:1 10%
Trial 2
2:1 TRIAL 2
UNH 12-4
2:1 w/10%
Trial 1
UNH 12-4
2:1 w/10%
Trial 2

(a)


UNH 12-4
2:1 w/10%
Trial 1
UNH 12-4
2:1 w/10%
Trial 2

(b)


UNH 12-4
2:1 w/10%
Trial 2

(c)

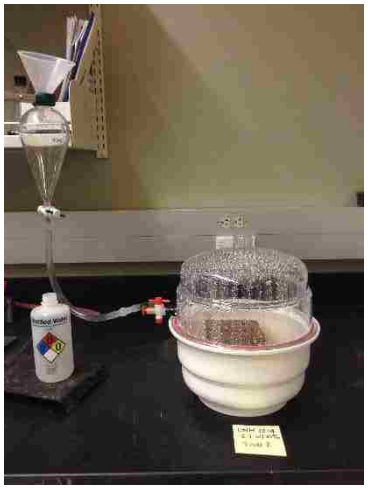

(d)


UNH 12-4
2:1 w/10%
Trial 2

(e)

(f)


UNH 12-4
2:1 w/10%
Trial 1
UNH 12-4
2:1 w/10%
Trial 2

(g)


UNH 12-4
2:1 w/10%
Trial 2

(h)

(i) (j)

Figure 3. 27. (a) SCEB 7 before vacuum saturation. (b) SCEB 7 after vacuum saturation. (c) SCEB 7 under vacuum. (d) SCEB 7 under vacuum saturation. (e) SCEB 7 after saturation. (f) SCEB 7 in environmental chamber. (h) SCEB 7 in glass desiccator after being in environmental chamber for 3 days. (i) SCEB 7 at beginning of Sorptivity testing (j) SCEB 7 at end of Sorptivity testing.

3.4.7 Apparent block density

The apparent density/unit weight of each block specimen was determined using a method given by Dr. Mahmoud Taha. The apparent density testing of the specimens was performed by Conner Rusch. After the blocks were fully cured, the full size SCEBs, 35.6 cm x 25.4 cm x 10.2 cm (14 in. x 10 in. x 4 in.) were cut using a brick saw into 50 mm x 50 mm x 50 mm (2 in. x 2 in. x 2 in.) specimens. SCEB 1, 2, 3, 4, 5, 6, 7, SAB and AB were the only blocks tested. Three samples of each of the blocks were tested for statistical purposes.

The 50 mm x 50 mm x 50 mm (2 in. x 2 in. x 2 in.) blocks were placed in an oven at 110°C (230°F) for 24 hours and allowed to cool for at least 4 hours prior to testing. Then, the SCEBs and adobes were weighed. Then, the specimens were placed in a 400 mL (13.5 US fl. oz.) beaker with filled with 150 mL (5.07 US fl. oz.) of distilled water as

shown in Figure 3.28 (a) and (b). The vertical displacement of the water level was measured as shown in Figure 3.29. This was used to calculate the volume of the specimen using Equation (3.22).

$$\gamma = \frac{m}{A\,(\Delta h)} \tag{3.22}$$

where,
γ is the apparent density, g/cm^3.
m is the dry specimen mass, g.
A is the cross-sectional area of the beaker, cm^2.
Δh is the change in water level, cm.

Figure 3. 28. (a) 400 mL beaker filled with 150 mL distilled water. (b) Specimen placed in 400 mL beaker.

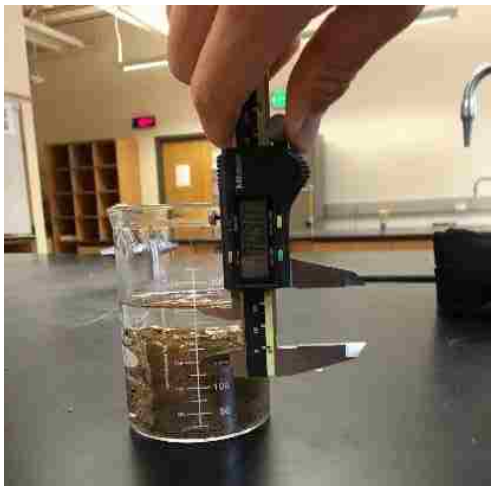

Figure 3. 29. Measuring the vertical displacement of the water level once the specimen is placed in the beaker.

3.5 Prism Construction

In order to understand the interaction of the block and mortar joint, prisms were constructed and tested for prism compression, creep, bond strength, and shear strength. In this research, prisms are composed of 2 or 3 SCEB or Adobe blocks and 1.27 cm (0.5 in.) mortar joint (s). ASTM C270 (*ASTM, 2014*) was used as a guide for choosing the mortar for use in the prisms. Type S mortar was used for prism construction. The proportions by volume for the sand, cement, and lime are listed in Table 3.3.

Table 3. 3. Proportions by volume for Type S Mortar.

Mortar Type	Sand (by volume)	Cement (by volume)	Lime (by volume)
S	4.5	1	0.5

ASTM C1072 (*ASTM, 2013*) was used as a guide to construct the prisms. An alignment jig, mortar template, and drop hammer were designed, built, and used in accordance with ASTM C1072 (*ASTM, 2013*) as shown in Figure 3.30 (a) and (b).

For the prism construction, full size SCEBs, 35.6 cm x 25.4 cm x 10.2 cm (14 in. x 10 in. x 4 in.) were cut using a brick saw into 12.7 cm x 12.7 cm x 10.2 cm (5 in. x 5 in. x 4 in.) blocks after being cured. In preparation for prism construction, the type S mortar was mixed. Then, the block was wetted and mortar was placed on top in the mortar joint template as shown in Figure 3.30 (a) to produce a 1.27 cm (0.5 in.) mortar joint. A second block was placed on top of the mortar joint and then the drop hammer was placed atop the prism as shown in Figure 3.30 (b). The drop hammer was released to produce a bond between the moist block and mortar. The prism was then placed in a plastic bag for 24 hours as shown in Figure 3.30 (c). Holes were poked into the plastic bag after 24 hours and the prisms were placed in the curing room as shown in Figure 3.30 (d). In order to allow the cement to hydrate while also not permitting the blocks to be exposed to a moist

environment, the prisms were kept in the plastic bags with holes. The prisms were kept in the curing room for 7 days to allow for the mortar to hydrate and cure. Then the prisms were removed from the curing room and placed in the UNM Structures Laboratory at a temperature of 25°C (77°F) and relative humidity of 20%.

(a)

(b)

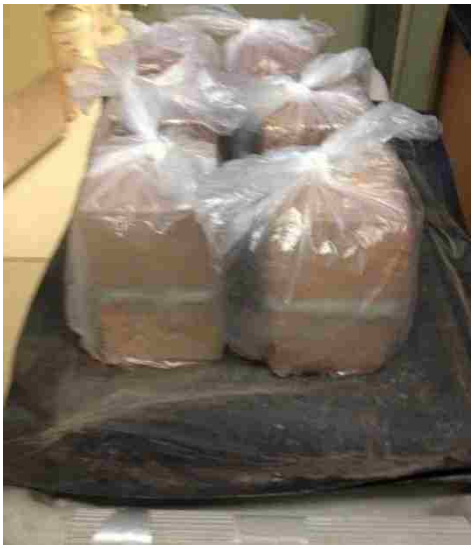

(c)

(d)

Figure 3. 30. (a) Prism being constructed in Alignment Jig with mortar template. (b) Using drop hammer in Alignment Jig. (c) Prism wrapped in plastic to set 24 hours before going into curing room. (d) Prism in curing room.

3.5.1 Mortar Flowability

The workability or flow of the mortar was determined using ASTM C1437 (*ASTM, 2013*) to guide testing. Using Table 3.3 in ASTM C1437 to mix the proportions of sand, cement, and lime for type S mortar, water was added until the mortar was at a good workability level as shown in Figure 3.31 (a). Then the mortar was placed in the flow mold in two layers. The first layer of about 25 mm (1 in.) was placed in the mold and tamped 20 times with the tamper. Then, the rest of the mold was filled with mortar and tamped 20 times with the tamper. Using the straightedge of the tamper, the surface was leveled as shown in Figure 3.31 (b). The flow table was cleaned and the flow mold was removed. The flow table was dropped 25 times in 15 seconds and the diameter of the mortar was measured with the caliper along the four lines scribed on the table as shown in Figure 3.31 (c). The flow was calculated by adding the four diameter readings and the total was recorded as the flow in percent.

(a) (b) (c)

Figure 3. 31. (a) Mixing sand, cement, and lime for mortar mix and adding water. (b) Placing mortar in flow mold on the flow table and using tamper level the surface. (c) Using the caliper to measure the diameter of the mortar.

3.5.2 Mortar Compression

The compressive strength of the cement mortar was determined using ASTM C109 (*ASTM, 2013*) to guide testing. While the prisms were being constructed, mortar used for prism construction was obtained to make six - 50 mm (2 in.) mortar cubes for each mortar batch. The mortar was placed in two specimen molds to make six 50 mm cubes(2 in.). The cubes were then compacted by tamping in two layers using 32 strokes per layer as shown in Figure 3.32 (a). Then, the mortar was leveled and the cubes were allowed to cure one day in the molds as shown in Figure 3.32 (b). Then the cubes were stripped from the molds and placed in the curing room as shown in Figure 3.32 (c). Three cubes were left in the curing room for 7 days and the remaining three cubes were left in the curing room for 28 days. Then, the 7 day and 28 day mortar cube specimens were tested using the 1779 kN (400 kip) capacity Tinius Olsen machine, Model No. 139000 using a loading rate of 53379 N/min (12000 lbf/min) as shown in Figure 3.33.

(a) (b) (c)

Figure 3. 32. (a) Tampering mortar into mortar cube mold in two layers. (b) Leveling mortar in mortar cube mold. (c) Mortar cubes being stripped from molds.

Figure 3. 33. 50mm cube specimen tested for mortar compression on the Tinius Olsen Machine.

3.6 Prism Testing

3.6.1 Prism Compression Testing

Prism compressive strength was determined using ASTM C1314 (*ASTM, 2014*) to guide testing. Once the prisms were constructed and allowed to cure in the curing room for 7 days, the prisms were removed from the plastic bags and allowed to dry for at least 24 hours. Then, the prisms were tested using the 1779 kN (400 kip) capacity Tinius Olsen machine, Model No. 139000 using a loading rate of 4445 to 20000 N/min (1000 to 4500 lbf/min) so that the specimen fails before 2 minutes as shown in Figure 3.34. The prisms were tested in the flat position and a 15.2 cm x 15.2 cm x 1.3 cm (6 in. x 6 in. x 1.5 in.) cold rolled steel plate was used between the prism and the upper spherical bearing area attached to the upper head of the machine.

Figure 3. 34. SCEB 7 prism compression on Tinius Olsen machine.

After testing the mode of failure was determined using Figure 4 from ASTM C1314 (*ASTM, 2014*). The corrected net compressive strength was determined using Equation (3.23).

$$f_{mt} = \frac{F}{A}\,(CF) \tag{3.23}$$

where,
f_{mt} is the corrected compressive strength, MPa.
F is the applied force, N.
A is the cross-sectional area of the top face of prism top block, mm^2.
CF is the correction factor for height to thickness ratio for each prism using Table 1 of ASTM C1314.

3.6.2 Creep Testing

Two prisms each comprised of two SCEB 7 blocks with a Type S mortar joint were tested to determine the effect of creep on a SCEB prism. Each prism was placed on a Carver Automatic Hydraulic Presses Model: Mini-C loading frame as shown in Figure 3.35. Each prism experienced a constant load of 20% of its compressive strength capacity. The prisms are loaded to a constant load of 13.3 kN (3000 lbs). The displacement of the prism over 56 days was measured using three Linear Voltage Displacement Transducers (LVDTs). The LVDTs were placed to measure displacement in the top block, bottom block, and bottom block plus mortar joint as shown in Figure 3.36. LVDT 1 measured the

displacement of the bottom block and the mortar joint displacement. LVDT 2 measured the bottom block displacement and LVDT 3 measured the top block displacement. The data acquisition system used was Campbell Scientific.

The LVDTs used were DC-EC 125 which are DC LVDTs. The LVDTs operated on a nominal +/- 15V DC supply and delivered a linear response of +/- 10V DC. The DC-EC 125 LVDT had a sensitivity of 3.15VDC/mm. Since the LVDTs measure voltage, the measured displacement was calculated using the Equation (3.24).

$$d = G\ (V_{CH+} - V_{CH-}) \tag{3.24}$$

where,
d is the displacement, mm.
G is gain or sensitivity (3.15 VDC/mm).
V_{CH+} is the positive voltage measurement, VDC.
V_{CH-} is the negative voltage measurement, VDC.

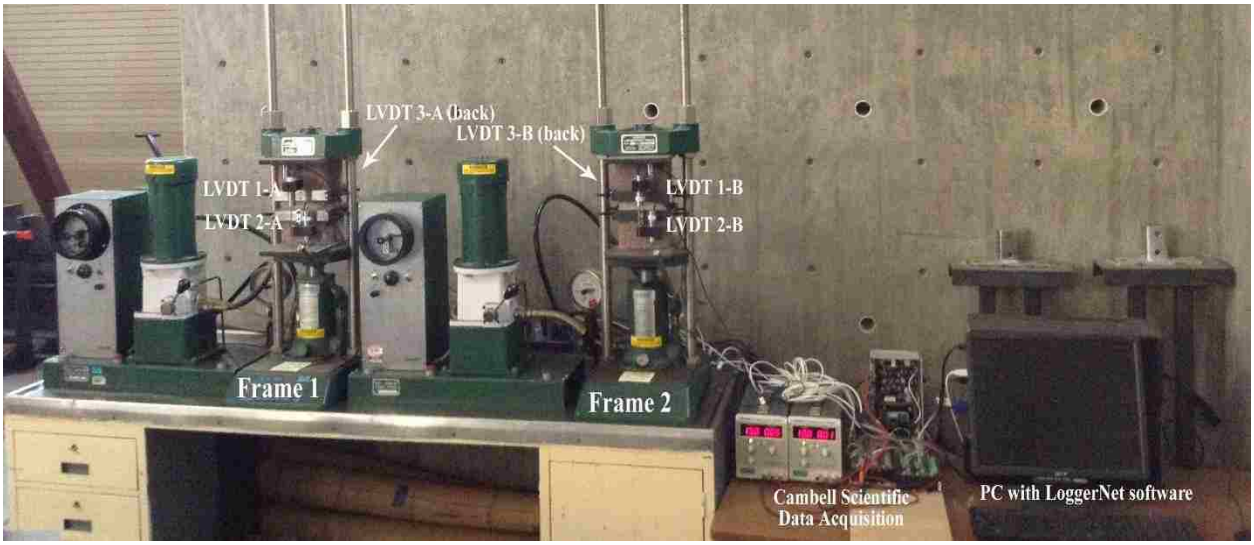

Figure 3. 35. SCEB 7 prisms placed on the Carver Press and displacement measured using the Campbell Scientific Data Acquisition.

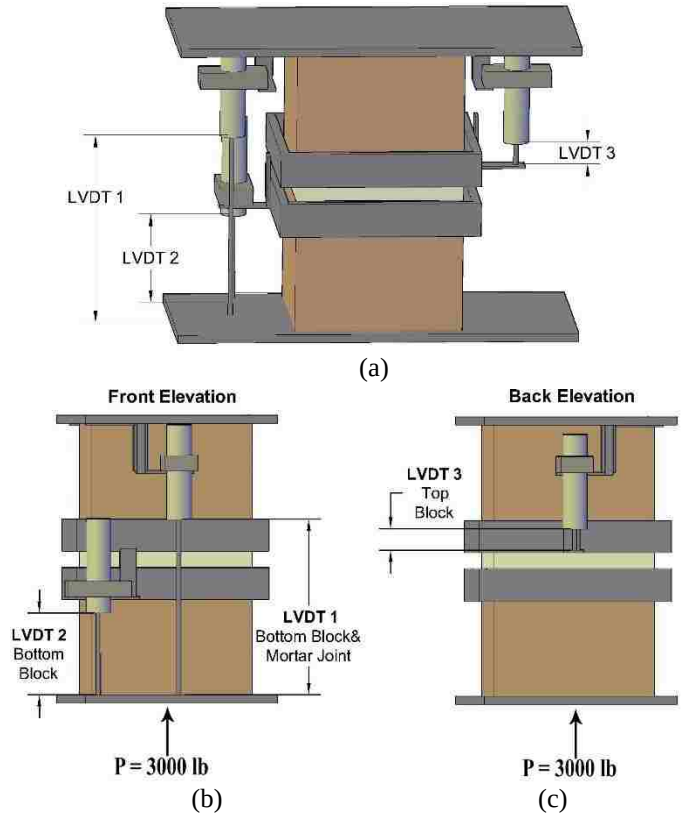

Figure 3. 36. (a) LVDT Layout for Frame 1 and 2. (b) Front Elevation of Frame showing LVDT 1 measures bottom block and mortar joint displacement and LVDT 2 measure bottom block displacement. (c)Back Elevation of Frame showing LVDT 3 measures top block displacement.

The creep coefficient and the creep compliance were the desired parameters from the collected data. In Equation (3.27), the creep coefficient, Φ is the ratio of maximum creep strain to the initial elastic strain, which was determined from experimental results. The initial elastic strain was determined using Equation (3.25) and the maximum creep strain was determined using Equation (3.26). The creep compliance was determined using Equation (3.28).

$$\varepsilon_{el} = \frac{\Delta L(0)}{L_0} \tag{3.25}$$

ε_{el} is the initial elastic strain, mm/mm
$\Delta L(0)$ is the total measured displacement at time 0, mm
L_0 is the original height of the specimen, mm

$$\varepsilon_c(t) = \frac{\Delta L(t)}{L_0} - \varepsilon_{el} \quad (3.26)$$

where,
ε_c is the creep strain over time, mm/mm
t is time, days
ΔL(t) is the total measured displacement at measure time, mm
L_0 is the original height of the specimen, mm

$$\Phi = \frac{\varepsilon_{c,max}}{\varepsilon_{el}} \quad (3.27)$$

where,
Φ is the creep coefficient
$\varepsilon_{c,max}$ is the max creep strain, mm/mm
ε_{el} is the initial elastic strain, mm/mm

$$J(t) = \frac{\varepsilon_c(t)}{\sigma} \quad (3.28)$$

where,
J is the creep compliance
$\varepsilon_c(t)$ is the creep strain over time, mm/mm
σ is the applied stress, MPa

Creep testing of the blocks can be compared to a consolidation test in soil mechanics. Consolidation is a method where a long term static load is applied to the soil specimen and the soil decreases in volume by the expulsion of water. According to Terzaghi & Peck (*1948*), consolidation can occur in two stages. The primary consolidation stage where the consolidation stress is transferred from the pore water to the soil, and the second consolidation stage where compression of soil takes place at slow rate that is caused by creep. Creep is the viscous behavior of the clay-water system.

3.6.3 Bond Strength

Masonry flexural bond strength was determined using ASTM C1072 (*ASTM, 2013*) to guide testing. The bond wrench testing apparatus was designed and constructed by the author and the University of New Mexico Machine Shop in accordance with ASTM C1072

(*ASTM, 2013*) as shown in Figure 3.37 (a). Once the 3 block prisms were constructed and allowed to cure in the curing room for 7 days, the prisms were removed from the plastic bags and allowed to dry for at least 24 hours. Then, the prisms were placed in the bond wrench testing apparatus and the prisms were tested in the flat position. The mortar joint to be tested was placed slightly above the lower clamping bracket. If the location of the mortar joint to be tested was not sufficient, then the adjustable prism base support was used to raise or lower the prism as needed. Once the prism was secured by the lower clamping bracket, then the upper clamping bracket (torque wrench) was placed above the top block of the prism such that the center line of the torque wrench arm is centered on the block. and the clamping bolts were tightened to secure the specimen as shown in Figure 3.37 (b). Once the prism was tightly secured in place in the bond wrench testing apparatus, then the Enerpac P-392 hand pump connected to an Enerpac RC-106, 101 kN (22.7 kip) single acting steel hydraulic cylinder was used to apply an eccentric load to the upper clamping bracket. Load was applied manually at a slow rate until failure of the bond and the maximum applied stress applied was measured on the pressure gage.

The gross area flexural strength (bond strength) was calculated using Equation (3.29). The distance from the center of the prism to the loading point, L and the distance from the center of the prism to the centroid of the loading arm, L_1 are shown in Figure 3.38.

$$F_g = \frac{6\,(PL + P_l L_l)}{bd^2} - \frac{(P + P_l)}{bd} \tag{3.29}$$

where,
F_g = gross area flexural tensile strength, psi
P = maximum applied load, lbf
P_l = weight of loading arm, lbf
L = distance from center of prism to loading point, in.
L_l = distance from center of prism to centroid of loading arm, in.

b = cross-sectional width of the mortar-bedded area, perpendicular to the loading arm of the upper clamping area, in.
d = cross-sectional depth of the mortar-bedded area, parallel to the loading arm of the upper clamping area, in.

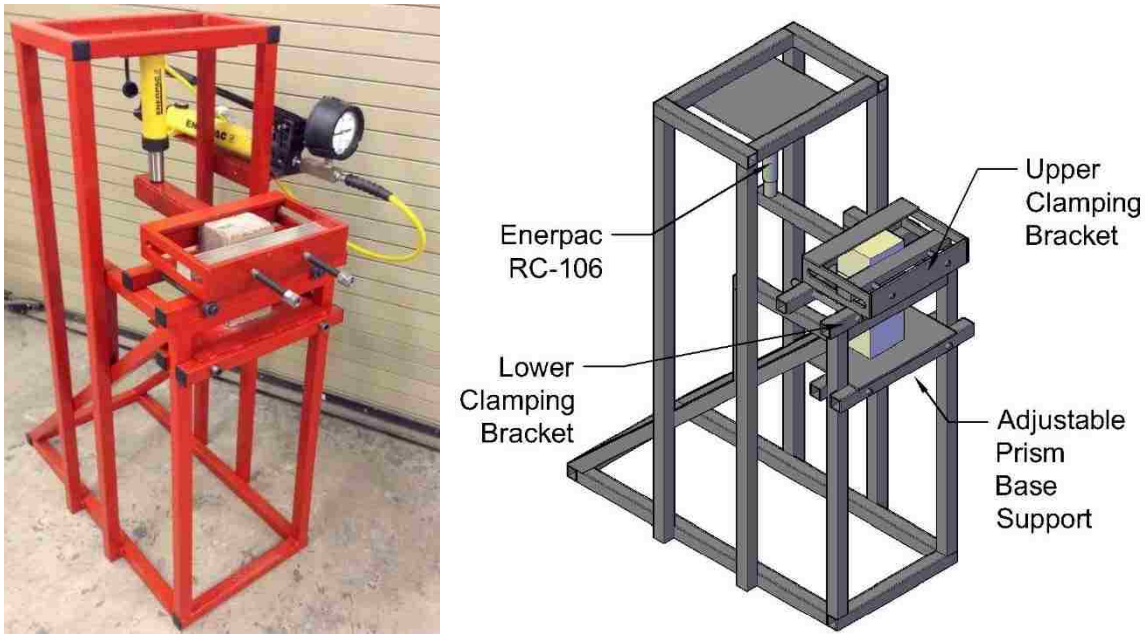

(a) (b)

Figure 3. 37. (a) Bond Wrench Test Apparatus designed and constructed per ASTM C1072. (b) Diagram of Bond Wrench Test Apparatus showing the upper and lower clamping brackets, Enerpac RC-106 and the adjustable prism base support.

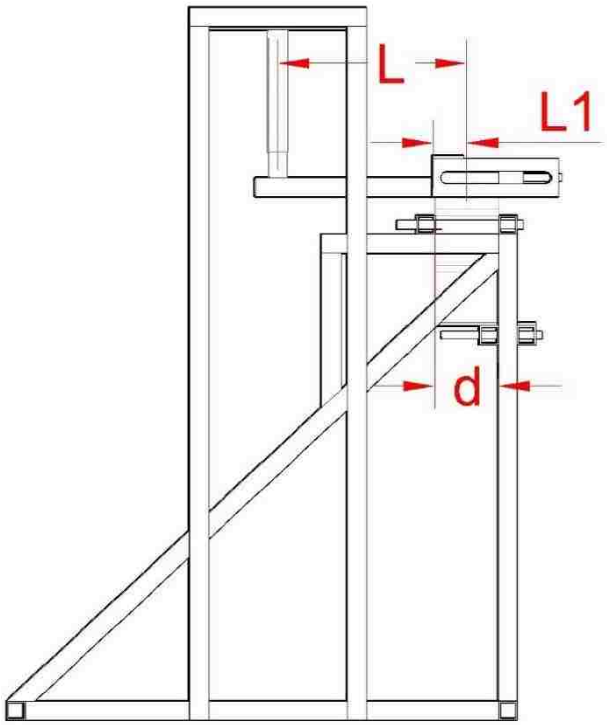

Figure 3. 38. Bond Wrench Test Apparatus showing the location of L, L_1, and d.

3.6.4 Shear Testing

The shear strength of SCEB prisms was determined in accordance with British Standards, BS EN 1052-3 (*BSI, 2002*). The shear testing apparatus was designed and constructed by the author and the University of New Mexico Machine Shop in accordance with BS EN 1052-3 (*BSI, 2002*). Once the 3 block prisms were constructed and allowed to cure in the curing room for 7 days, the prisms were removed from the plastic bags and allowed to dry for at least 24 hours.

Procedure A from BS EN 1052-3 was used to determine the shear strength of the units by using a predetermined precompression load on the prism per the standard. Each prism specimen was supported at the bottom with two, 25.4 mm x 127 mm (1 in x 5 in.) mild steel plates and at the top with one, 12.7 mm x 127 mm (0.5 in. x 5 in.) mild steel

plate as shown in Figure 3.39. The diameter of the roller bearings were 12.7 mm (0.5 in.) mild steel. The precompression force was applied using an Enerpac P-392 hand pump connected to an Enerpac RCS-302, 295 kN (66.3 kip) hydraulic cylinder. A precompression pressure of 0.3 MPa (44 psi) was used for testing. The precompression force and the shear force acting on the prism are shown in Figure 3.40.

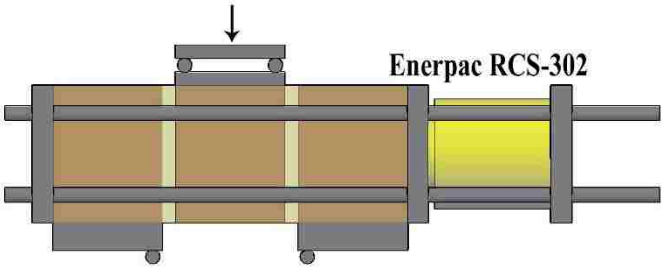

Figure 3. 39. Schematic of 3 block prism in shear testing apparatus with Enerpac RCS-302 loading cyclinder.

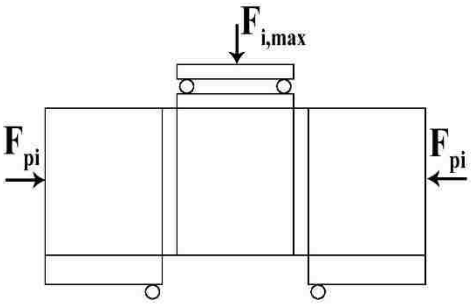

Figure 3. 40. Schematic of 3 block prism with precompression force, F_{pi} and shear force, $F_{i,max}$.

Once the prism was cured, the prism was placed in the shear testing apparatus and the precompression load was applied. Then, the prism was placed in the 1779 kN (400 kip) capacity Tinius Olsen machine, Model No. 139000. The shear force was applied at the top plate on the center block of the prism as shown in Figure 3.41 and 3.42. A loading rate of 0.1 MPa/min (14.5 psi/min) was used.

For each specimen, the shear strength and precompression stress were calculated using Equation (3.30) and (3.31). The average cross sectional area of the top block and center block was calculated using Equation (3.32) and the average cross sectional area of the bottom block and center block was calculated using Equation (3.33). The average cross sectional area of all three block are calculated using Equation (3.34).

$$f_{voi} = \frac{F_{i,max}}{(A_t + A_b)} \tag{3.30}$$

where,
f_{voi} is the shear strength of an individual sample, MPa.
$F_{i,max}$ is the max shear force, N.
A_t is the average cross-sectional area of block 1 and 2, between the top mortar joint, in^2.
A_b is the average cross-sectional area of block 2 and 3, between the bottom0 mortar joint, in^2.

$$f_{pi} = \frac{F_{pi}}{A_{average}} \tag{3.31}$$

where,
f_{pi} is the precompressive stress of an individual sample, MPa.
F_{pi} = precompressive force , N.
$A_{average}$ is the average area of blocks 1,2, and 3, mm^2.

$$A_t = \frac{(A_{block1} + A_{block2})}{2} \tag{3.32}$$

where,
A_t is the average cross-sectional area of block 1 and 2, between the top mortar joint, in^2.
A_{block1} is the area of block 1, mm^2.
A_{block2} is the area of block 2, mm^2.

$$A_b = \frac{(A_{block2} + A_{block3})}{2} \tag{3.33}$$

where,
A_b is the average cross-sectional area of block 2 and 3, between the bottom mortar joint, in^2.
A_{block2} is the area of block 2, mm^2.
A_{block3} is the area of block 3, mm^2.

$$A_{average} = \frac{(A_{block1} + A_{block2} + A_{block3})}{3} \tag{3.34}$$

where,
$A_{average}$ is the average area of blocks 1,2, and 3, mm^2.
A_{block1} is the area of block 1, mm^2.
A_{block2} is the area of block 2, mm^2.
A_{block3} is the area of block 3, mm^2.

Figure 3. 41. Shear testing apparatus in the Tinius Olsen machine.

Figure 3. 42. SAB prism in shear testing apparatus in the Tinius Olsen machine.

3.7 Wall Construction

The SCEB wall panels were constructed by George Shendo and David Chinana from the Jemez Community Development Corporation. The full size SCEBs, 35.6 cm x 25.4 cm x 10.2 cm (14 in. x 10 in. x 4 in.) were cut by a brick saw into 17.8 cm x 12.7 cm x 5.1 cm (7 in. x 5 in. x 2 in.) blocks. Twenty-seven, 17.8 cm x 12.7 cm x 5.1 cm blocks

were used to construct one wall panel. There were four wall panels constructed of SCEB 7 blocks and Type S mortar. The Type S mortar was prepared in larger quantities and a wheel barrow was used for mixing as shown in Figure 3.43 (a). The wall was constructed by experienced masons as shown in Figure 3.43 (b) and Figure 3.44 (a). The completed walls are shown in Figure 3.44 (b).

(a) (b)

Figure 3. 43 (a) Type S mortar mix used for wall construction. (b) Wall being constructed by JCDC.

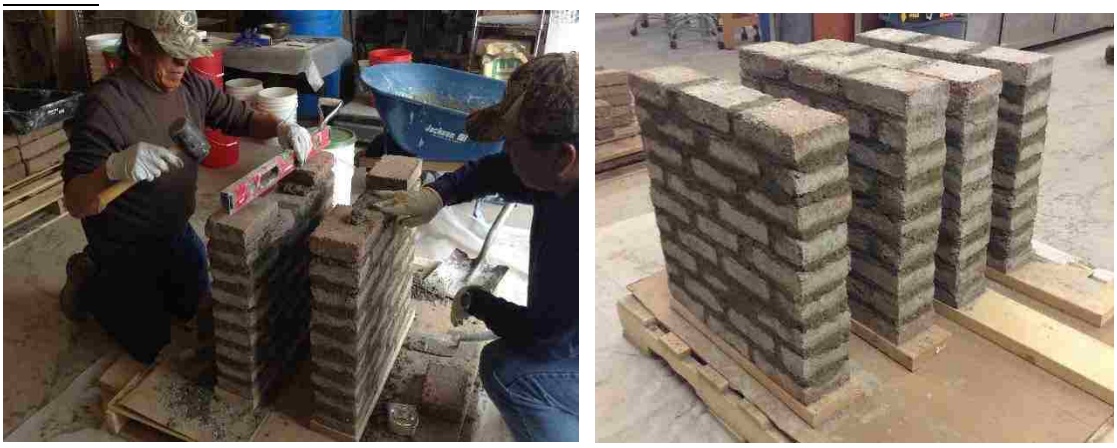

(a) (b)

Figure 3. 44 (a) Wall being constructed by JCDC. (b) Completed SCEB 7 walls.

3.8 Wall Testing

In order to determine the structural behavior of the wall, the shear strength of the masonry assemblage was determined by loading the walls in compression along the diagonal. ASTM E519 (*ASTM, 2010*) was used to guide testing. The experiment was performed under a controlled environment in the Structures Laboratory at a temperature of 25°C (77°F) and relative humidity of 20%. Four approximately 570 x 570 x 127 mm^3 (22 x 22 x 5 $in.^3$) SCEB 7 wall panels were placed in a loading shoe at the top and bottom of the wallet and tested under diagonal compression as shown in Figure 3.45 (a). The diagonal compression test was performed on the 534 kN (120 kip) capacity Instron machine, Model No. AW2568-3 as shown in Figure 3.45 (b). A displacement rate of 0.24 mm/min (0.009 in/min) was used for testing. The vertical displacement was measured using LVDT 3-1 and the horizontal displacement was measure using LVDT 4-1 as shown in Figure 3.46.

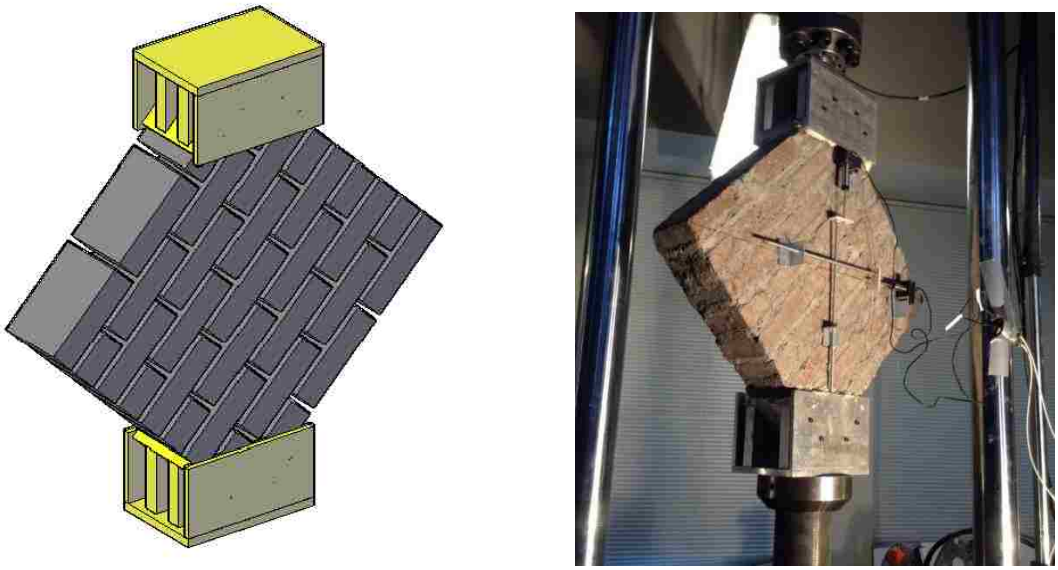

(a) (b)

Figure 3. 45. (a) Schematic of SCEB 7 wall panel in loading shoes. (b) SCEB 7 wallet tested under diagonal compression in the Instron machine with LVDT 3-1 and LVDT 4-1 measuring the vertical and horizontal displcacement.

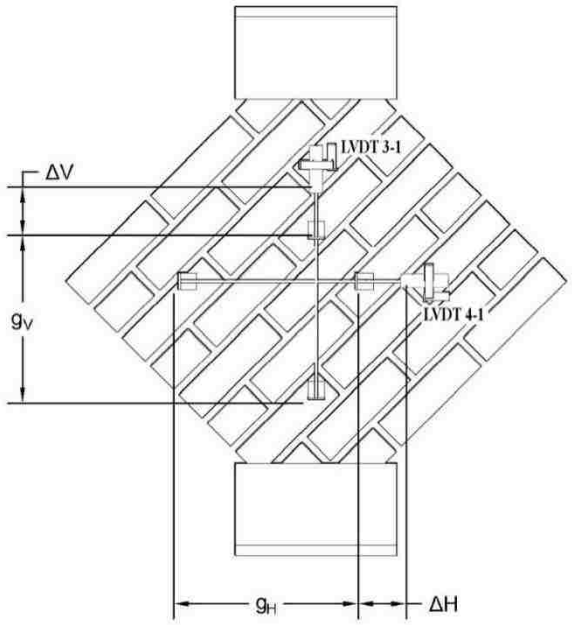

Figure 3. 46. LVDT 3-1 and LVDT 4-1 placed on SCEB 7 wallet to measure vertical and horizontal displacement.

The shear stress was calculated using Equation (3.35). The net area of the wall was calculated using Equation (3.36). The shearing strain was calculated using Equation (3.37) in order to determine the modulus of rigidity using Equation (3.38). The vertical shortening, the vertical gage length, the horizontal extension, and the horizontal gage length used for calculating the shearing strain are shown in Figure 3.46.

$$S_s = \frac{0.707\mathrm{P}}{\mathrm{A_n}} \tag{3.35}$$

where,
S_s is the shear stress on net area, MPa.
P is the applied load, N.
A_n is the net area of the specimen, mm^2.

$$A_n = \frac{(w+h)}{2}\, t \tag{3.36}$$

where,
A_n is the net area of the specimen, mm^2.
w is the width of the specimen, mm.
h is the height of the specimen, mm.
t is the total thickness of the specimen, mm.

$$\gamma = \frac{\Delta V}{g_V} + \frac{\Delta H}{g_H} \tag{3.37}$$

where,
γ is the shearing strain, mm/mm.
ΔV is the vertical shortening, mm.
g_V is the vertical gage length, mm.
ΔH is the horizontal extension, mm.
g_H is the horizontal gage length, mm.

$$G = \frac{S_S}{\gamma} \tag{3.38}$$

where,
G is the modulus of rigidity, MPa.
S_s is the shear stress on net area, MPa.
γ is the shearing strain, mm/mm.

CHAPTER 4: RESULTS AND DISCUSSION

4.1 Introduction

This chapter presents the experimental results from the soils testing and provides a process for selection to determine the soil suitability for use in SCEB block production. In addition, it presents the results from tests determining the mechanical properties of SCEB blocks and assemblies. The mechanical properties of SCEBs are compared to that of commercially available adobe bricks as well as earthen building materials found in the literature.

4.2 Soil Testing

Tests were performed on native soils obtained from Jemez Pueblo for use as the clayey soil in the SCEB soil mixture. Sands purchased locally for use in SCEB production were also tested. The soils were tested in four phases.

Phase 1 included testing the clay(ey) soil from the initial 13 sites and the down selection of two "suitable" soils. A soil was deemed "suitable" if it met the soil criteria discussed in the following section, the soil was located at a site determined by the client with an ease of access to obtain material, and had a sufficient quantity of material available to excavate determined by the geologists from the Colorado State Division of Earth and Mineral Development. When the two "suitable" soils were being mined from their dig sites for use in block production, it was observed in the field there was variability in the soil within each site. Therefore, it was determined to investigate the soils within each site further. In Phase 2, there were 26 soils tested from the two chosen sites. These were down selected to three acceptable soils for use in SCEB production. While in Phase 3, there was additional testing on 13 soils from the two chosen sites to identify soils which can be used

for future use in SCEB production. In Phase 4, two of the soils identified as appropriate for use in SCEBs from Phase 2 were mixed with sands. Mixture ratios were developed and tested.

4.2.1 Phase 1 Soil Testing

In Phase 1, samples were obtained from 13 dig locations within the Jemez Pueblo. The samples and their locations were provided by Functional Earth Consulting, LLC. Received samples were given a specimen identification as shown in Table 4.1. The results of the natural moisture content for soil specimens as received from the site and the specific gravity for the soil specimens are presented in Appendix A.1.

Due to its importance in determining the strength of SCEBs, the particle size distribution was obtained for the 13 samples. The soil fraction results are shown in Table 4.2 and the particle size distribution curves are displayed in Figure 4.1. In identifying a suitable soil, the first criteria is if there are more than 50% fines in the samples. The specimens highlighted in Table 4.2 meet that criteria.

Table 4. 1. Soil Specimen ID for Phase I soils testing.

Specimen ID	Jemez Site ID	Dig Date
UNM 1	JEZ15	11/18/2014
UNM 2	JEZ16	11/18/2014
UNM 3	JEZ17	11/18/2014
UNM 4	JEZ19	11/18/2014
UNM 5	JEZ20	11/18/2014
UNM 6	JEZ21	11/19/2014
UNM 7	JEZ22	11/19/2014
UNM 8	JEZ23	11/19/2014
UNM 9	JEZ24	11/19/2014
UNM 10	JEZ25	11/19/2014
UNM 11	JEZ26	11/19/2014
UNM 12	JEZ27	11/19/2014
UNM 13	JEZ28	11/19/2014

Table 4. 2. Soil fractions for Phase 1.

Specimen ID	% Gravel	%Sand	% Fines (Silt & Clay)
	>2mm	<2mm/>0.075mm	<0.075mm
UNM 1	1.34%	86.20%	12.46%
UNM 2	0.38%	21.64%	77.98%
UNM 3	0.24%	2.56%	97.20%
UNM 4	1.34%	52.90%	45.76%
UNM 5	1.10%	78.16%	20.74%
UNM 6	0.12%	19.86%	80.02%
UNM 7	0.60%	12.42%	86.98%
UNM 9	1.58%	30.04%	68.38%
UNM 10	0.22%	32.12%	67.66%
UNM 11	0.02%	22.02%	77.96%
UNM 12	0.16%	17.32%	82.52%
UNM 13	0.00%	36.78%	63.22%

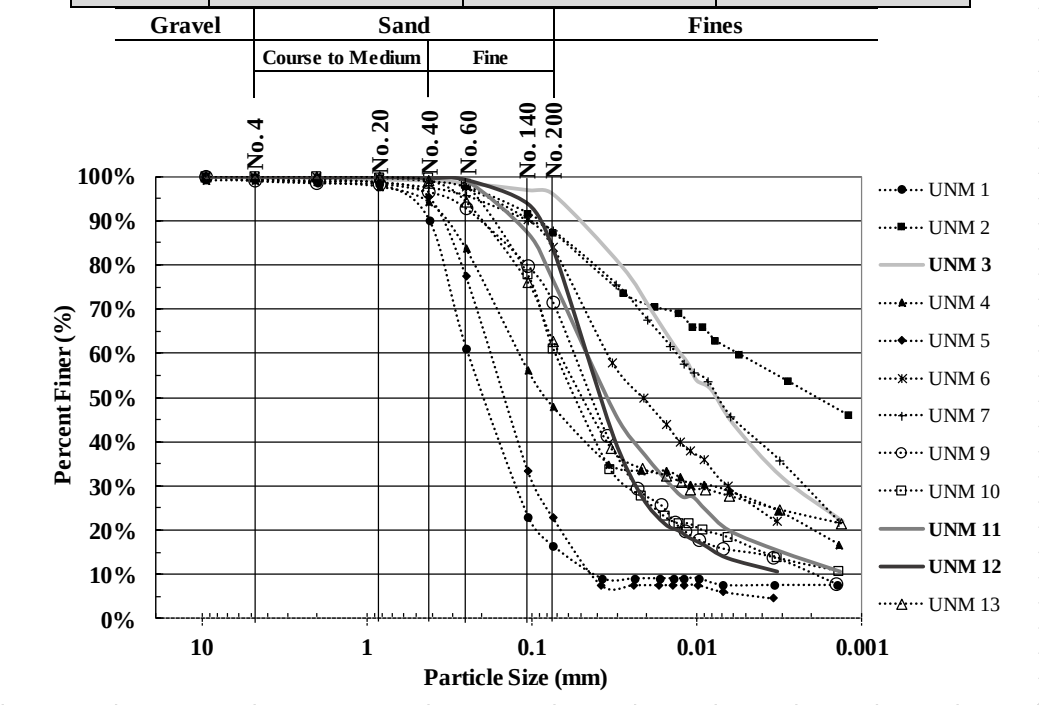

Figure 4. 1. Particle Size Distribution curves for soils in Phase 1.

Atterberg limits tests were then performed on all soil samples to determine the plasticity index and liquid limits and the results are presented in Table 4.3 and Figure 4.2. The second criteria in determining a suitable soil is the Plasticity Classification is CL or ML. The soil specimens that meet this criteria are highlighted in Table 4.3.

Table 4. 3. Phase 1 Atterberg Limits and Plasticity Classification.

Specimen ID	LL	PL	PI	Plasticity Chart Classification
UNM 1	-	NP	-	-
UNM 2	74	44	30	CH
UNM 3	43	24	19	CL
UNM 4	35	17	18	CL
UNM 5	-	NP	-	-
UNM 6	32	13	19	CL
UNM 7	45	19	26	CL
UNM 8	20	6	14	CL-ML
UNM 9	26	6	20	CL-ML
UNM 10	31	9	22	CL
UNM 11	29	10	19	CL
UNM 12	29	4	25	ML
UNM 13	48	25	23	CL

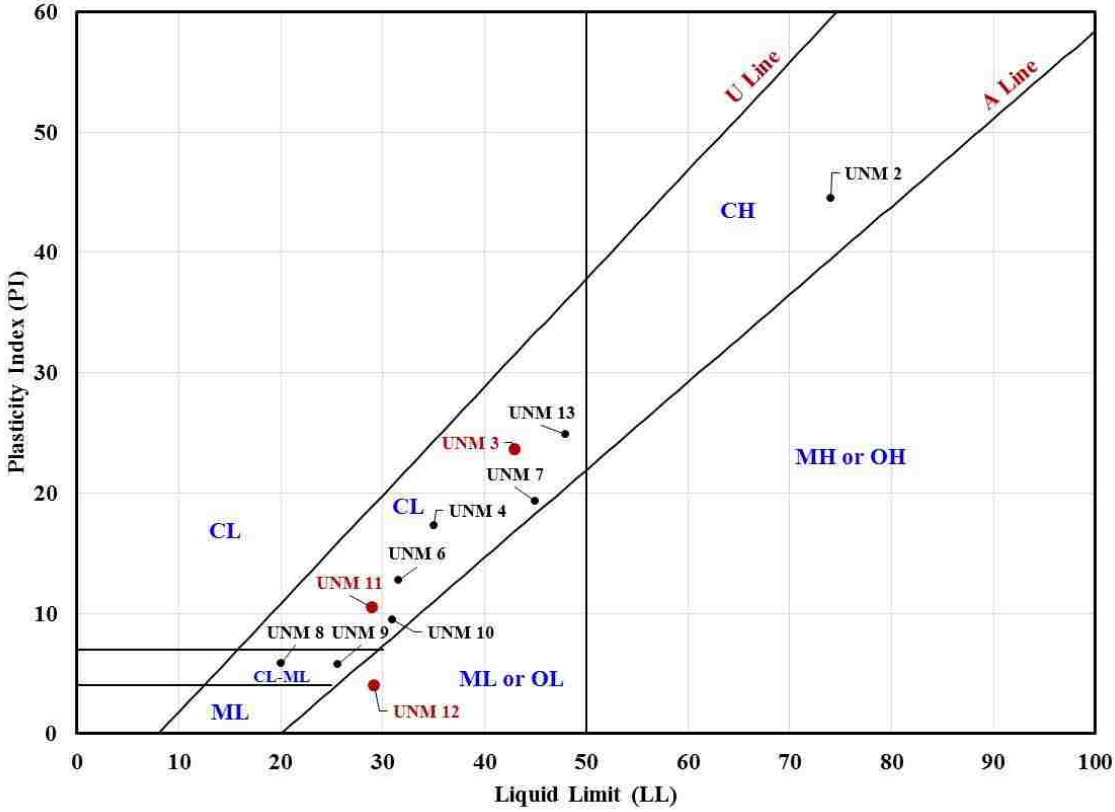

Figure 4. 2. Phase 1 Plasticity Chart.

The soils were then classified according to the Unified Soil Classification System (USCS) and the results are listed in Table 4.4. The third criteria in determining a suitable soil is that the USCS Classification is CL or ML and the soil is located at a site determined

by the client with an ease of access to obtain material as well as a location determined by the geologists from the Colorado State Division of Earth and Mineral Development as a site with an significant amount of soil material. The soil specimens were chosen by the client based on soil suitability per criteria, location and estimated quantity of material available to excavate. The soil specimens that meet this criteria are highlighted in Table 4.4. UNM 3, UNM 11 and UNM 12 were the chosen soil samples.

Table 4. 4. Phase 1 Soil Classification based on USCS methodology.

Specimen ID	**% Passing #200**	**% Retained #200**	**ASTM D 2487 Criteria Assigning Group Symbols and Group Name**		**Soil Classification**
UNM 1	12.46	87.54	Coarse-Grained	Sands with Fines	SM - Silty Sand
UNM 2	77.98	22.02	Fine-Grained	Silts and Clays	CH - Fat Clay with sand
UNM 3	97.20	2.80	Fine-Grained	Silts and Clays	CL - Lean Clay
UNM 4	45.76	54.24	Coarse-Grained	Sands with Fines	SC - Clayey Sand
UNM 5	20.74	79.26	Coarse-Grained	Sands with Fines	SM - Silty Sand
UNM 6	80.02	19.98	Fine-Grained	Silts and Clays	CL - Lean Clay with sand
UNM 7	86.98	13.02	Fine-Grained	Silts and Clays	CL - Lean Clay
UNM 9	68.38	31.62	Fine-Grained	Silts and Clays	CL-ML – Sandy silty clay
UNM 10	67.66	32.34	Fine-Grained	Silts and Clays	CL – Sandy Lean Clay
UNM 11	77.96	22.04	Fine-Grained	Silts and Clays	CL - Lean Clay with sand
UNM 12	82.52	17.48	Fine-Grained	Silts and Clays	ML – Silt with sand
UNM 13	63.22	36.78	Fine-Grained	Silts and Clays	CL – Sandy Lean Clay

Soil samples UNM 3, UNM 11, and UNM 12, were selected to be tested for their swelling potential. The results from testing are shown in Table 4.5. The final criteria for determining the soil suitability is if the Expansion Index Classification is Very Low or Low. The soil specimens that meet this criteria are highlighted in Table 4.5. UNM 11 and UNM 12 are the soil specimens determined suitable for use as the clay(ey) soil in SCEBs.

Table 4. 5. Phase 1 Expansion Index and Classification .

Specimen ID	Expansion Index	Classification
UNM 3	130	High
UNM 11	0	Very Low
UNM 12	3	Very Low

4.2.2 Phase 2 Soil Testing

Results from Phase 1 suggested that sites UNM 11 and UNM 12 contained soils suitable for SCEB production. However, it was determined that there was variability in the soil at each site and warranted further investigation of the soil at each of the two sites. In Phase 2, samples were obtained from five dig locations from each of the UNM 11 and UNM 12 sites. The samples and their locations were provided by Functional Earth Consulting, LLC. Received samples were given a specimen identification as shown in Table 4.6. In the Phase 2 labeling scheme, the letter following the dig location indicates a different depth. The results of the natural moisture content for soil specimens as received from the site are presented in Appendix A.1.

Table 4. 6. Soil Specimen ID for Phase 2 soils testing.

Specimen ID	Jemez Site ID	Dig Date	Location in Bore	Location	
UNM 11-1A	Jez26 -1A	6/9/2015	6 to 8’	N35° 34' 46.344"	W106° 45' 20.736"
UNM 11-1B	Jez26 -1B	6/9/2015	1 to 6’	N35° 34' 46.344"	W106° 45' 20.736"
UNM 11-1C	Jez26 -1C	6/9/2015	1 to 6’	N35° 34' 46.344"	W106° 45' 20.736"
UNM 11-1D	Jez26 -1D	6/9/2015	1 to 6’	N35° 34' 46.344"	W106° 45' 20.736"
UNM 11-2A	Jez26 -2A	6/9/2015	1 to 3’	N35° 34' 47.1"	W106° 45' 19.836"
UNM 11-2B	Jez26 -2B	6/9/2015	1 to 3’	N35° 34' 47.1"	W106° 45' 19.836"
UNM 11-3A	Jez26 -3A	6/9/2015	6’	N35° 34' 47.856"	W106° 45' 18.864"
UNM 11-3B	Jez26 -3B	6/9/2015	8’	N35° 34' 47.856"	W106° 45' 18.864"
UNM 11-4A	Jez26 -4A	6/9/2015	3’	N35° 34' 45.84"	W106° 45' 19.296"
UNM 11-4B	Jez26 -4B	6/9/2015	3’	N35° 34' 45.84"	W106° 45' 19.296"
UNM 11-4C	Jez26 -4C	6/9/2015	7’	N35° 34' 45.84"	W106° 45' 19.296"
UNM 12-1-1A	Jez27 1-1A	6/9/2015	10’	N35° 34' 32.988"	W106° 45' 12.852"
UNM 12-1-2B	Jez27 1-2B	6/9/2015	1 to 6’	N35° 34' 32.988"	W106° 45' 12.852"
UNM 12-2-1A	Jez27 2-1A	6/9/2015	1 to 5’	N35° 34' 31.908"	W106° 45' 12.024"
UNM 12-2-2B	Jez27 2-2B	6/9/2015	1 to 5’	N35° 34' 31.908"	W106° 45' 12.024"
UNM 12-3-1A	Jez27 3-1A	6/9/2015	1 to 3’	N35° 34' 31.872"	W106° 45' 10.008"
UNM 12-3-2B	Jez27 3-2B	6/9/2015	6.5’	N35° 34' 31.872"	W106° 45' 10.008"
UNM 12-4-1A	Jez27 4-1A	6/9/2015	1 to 4.5’	N35° 34' 30.828"	W106° 45' 10.404"
UNM 12-4-2B	Jez27 4-2B	6/9/2015	4.5’ to 10’	N35° 34' 30.828"	W106° 45' 10.404"
UNM 12-5-1A	Jez27 5-1A	6/9/2015	1 to 6’	N35° 34' 30.828"	W106° 45' 13.32"
UNM 12-5-2B	Jez27 5-2B	6/9/2015	7 to 12.5’	N35° 34' 30.828"	W106° 45' 13.32"

The 24 samples were first classified based on particle size analysis. The soil fraction results are shown in Table 4.7 and the particle size distribution curves are displayed in Figure 4.3 and 4.4. The specimens highlighted in Table 4.7 meet the criteria of more than 50% passing #200 sieve.

Table 4. 7. Soil fractions for Phase 2.

Specimen ID	% Gravel	%Sand	% Fines (Silt & Clay)
	>2mm	<2mm/>0.075mm	<0.075mm
UNM 11-1A	50.12%	48.36%	1.52%
UNM 11-1B	12.96%	81.20%	5.84%
UNM 11-1C	24.64%	68.54%	6.82%
UNM 11-1D	11.84%	79.46%	8.70%
UNM 11-2A	0.00%	54.44%	45.56%
UNM 11-2B	0.38%	62.00%	37.62%
UNM 11-3A	6.92%	47.88%	45.20%
UNM 11-3B	6.08%	52.46%	41.46%
UNM 11-4A	0.00%	0.86%	99.14%
UNM 11-4B	0.38%	6.40%	93.22%
UNM 11-4C	1.76%	16.10%	82.14%
UNM 12-1-1A	0.96%	58.88%	40.16%
UNM 12-1-2B	0.28%	37.30%	62.42%
UNM 12-2-1A	3.50%	64.10%	32.40%
UNM 12-2-2B	2.98%	64.70%	32.32%
UNM 12-3-1A	0.02%	0.84%	99.14%
UNM 12-3-2B	0.66%	12.76%	86.58%
UNM 12-4-1A	0.02%	0.52%	99.46%
UNM 12-4-2B	0.44%	13.32%	86.24%
UNM 12-5-1A	3.38%	67.78%	28.84%
UNM 12-5-2B	0.16%	5.98%	93.86%

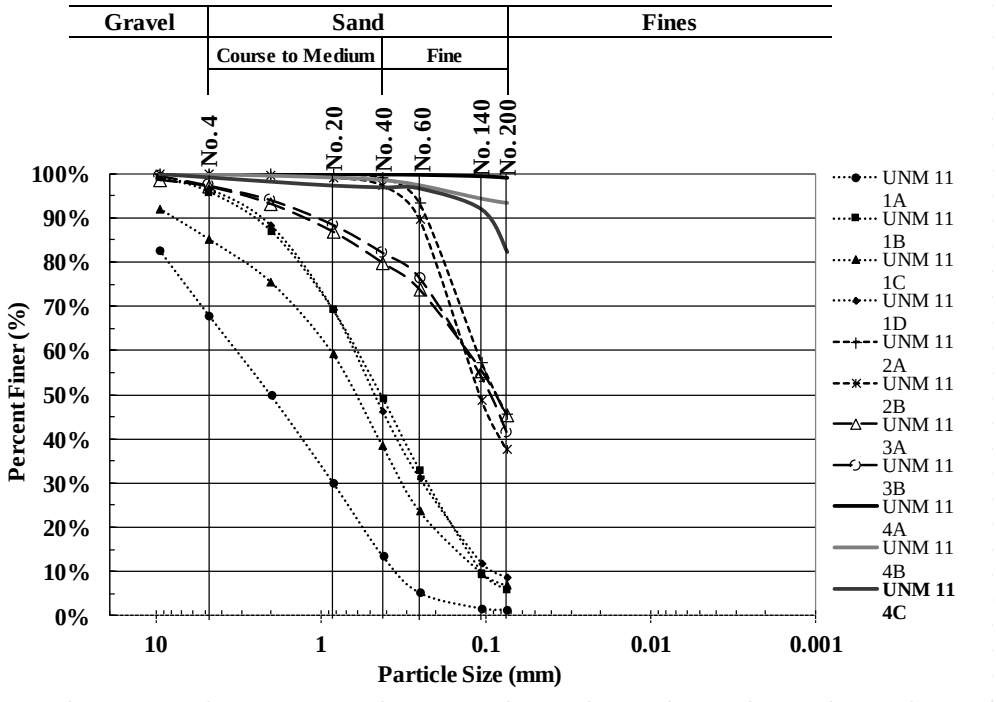

Figure 4. 3. Particle Size Distribution curves for soils in Phase 2 at site, UNM 11.

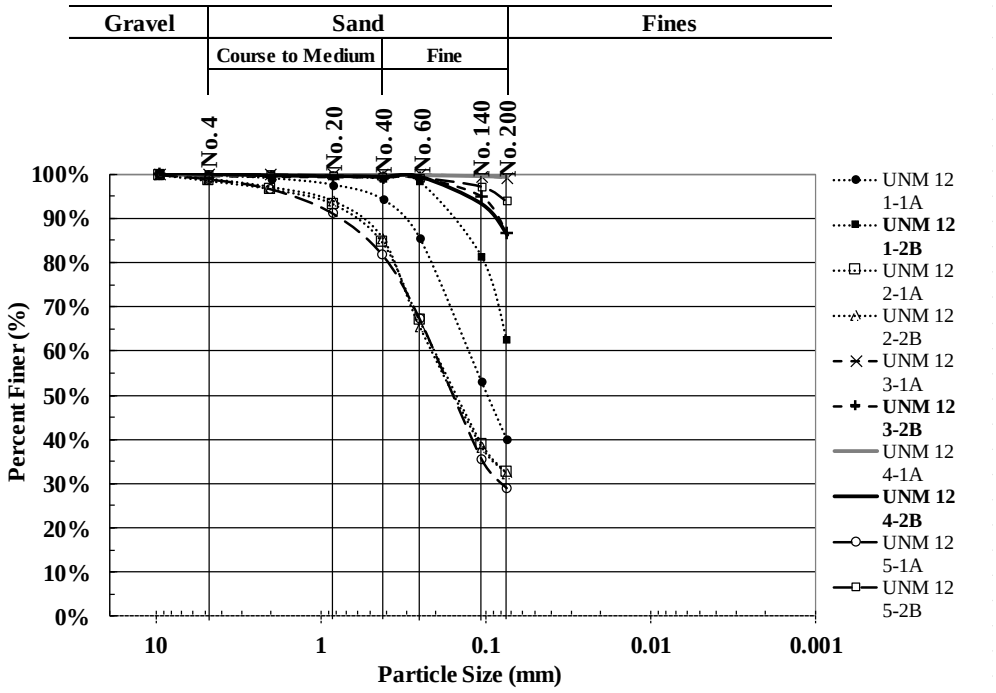

Figure 4. 4. Particle Size Distribution curves for soils in Phase 2 at site, UNM 12.

Atterberg limits were then performed on all soil samples and the results are presented in Table 4.8 and Figure 4.5. The soil specimens that meet the criteria of a Plasticity Classification of CL or ML are highlighted in Table 4.8

Table 4. 8. Phase 2 Atterberg Limits and Plasticity Classification.

Specimen ID	LL	PL	PI	Plasticity Chart Classification
UNM 11-1A	-	NP	-	-
UNM 11-1B	-	NP	-	-
UNM 11-1C	-	NP	-	-
UNM 11-1D	-	NP	-	-
UNM 11-2A	24	0	0	ML
UNM 11-2B	-	NP	-	-
UNM 11-3A	27	20	7	CL-ML
UNM 11-3B	29	20	9	CL
UNM 11-4A	68	30	38	CH
UNM 11-4B	51	23	28	CH
UNM 11-4C	33	24	9	ML
UNM 12-1-1A	-	NP	-	-
UNM 12-1-2B	33	22	11	CL
UNM 12-2-1A	20	0	0	ML
UNM 12-2-2B	19	15	4	ML
UNM 12-3-1A	65	35	30	MH
UNM 12-3-2B	44	20	24	CL
UNM 12-4-1A	76	35	41	MH
UNM 12-4-2B	40	19	21	CL
UNM 12-5-1A	-	NP	-	-
UNM 12-5-2B	53	24	29	CH

Using USCS methodology, the soils were then classified and the results are listed in Table 4.9. The soil specimens that meet the criteria of a USCS Classification which is CL or ML are highlighted in Table 4.9.

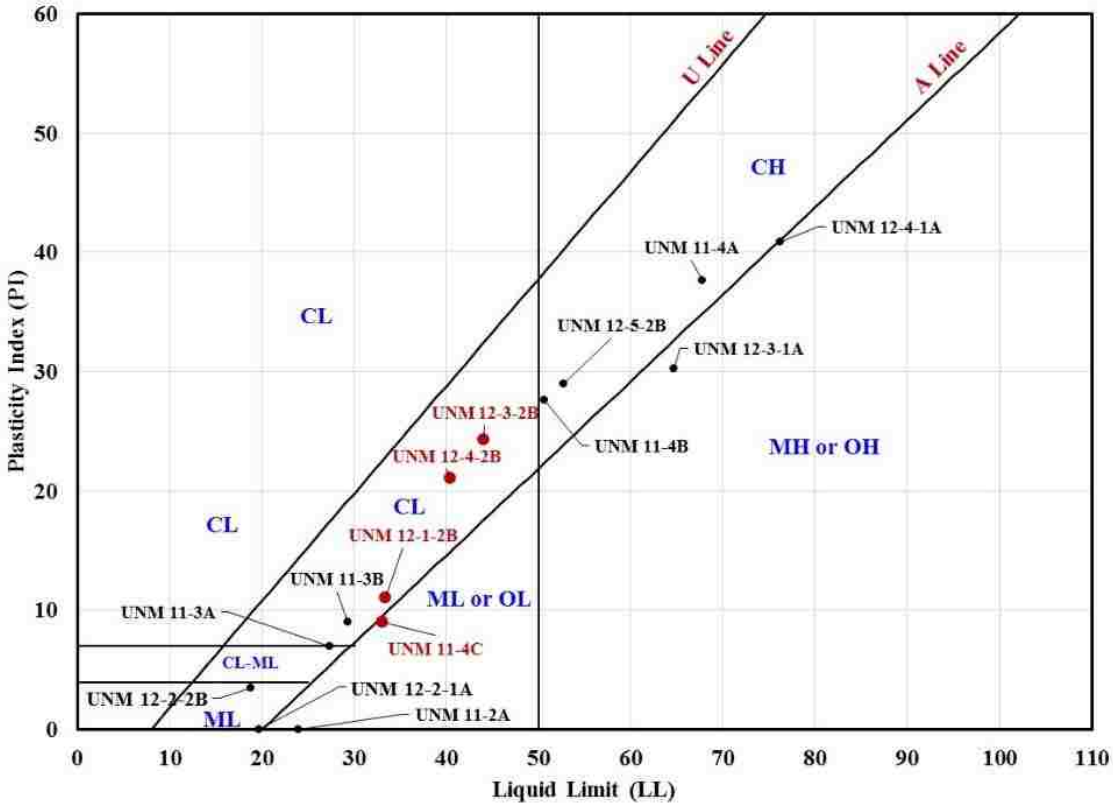

Figure 4. 5. Phase 2 Plasticity Chart.

Table 4. 9. Phase 2 Soil Classification based on USCS methodology.

Specimen ID	% Passing #200	PI	LL	ASTM D 2487 Criteria Assigning Group Symbols and Group Name		Soil Classification
UNM 11-1A	1.52%	-	-	Course-Grained	Clean Sands	**SP** Poorly graded sand
UNM 11-1B	5.84%	0	0	Course-Grained	Sands	**SP - SM** Poorly graded sand with silt
UNM 11-1C	6.82%	0	0	Course-Grained	Sands	**SW - SM** Well-graded sand with silt
UNM 11-1D	8.70%	0	0	Course-Grained	Sands	**SW - SM** Well-graded sand with silt
UNM 11-2A	45.56%	0	24	Course-Grained	Sand with Fines	**SM** Silty sand
UNM 11-2B	37.62%	0	0	Course-Grained	Sand with Fines	**SM** Silty sand
UNM 11-3A	45.20%	7	27	Course-Grained	Sand with Fines	**SC-SM** Silty, Clayey sand
UNM 11-3B	41.46%	9	29	Course-Grained	Sand with Fines	**SC** Clayey sand
UNM 11-4A	99.14%	38	68	Fine-Grained	Silts and Clays	**CH** Fat clay
UNM 11-4B	93.22%	28	51	Fine-Grained	Silts and Clays	**CH** Fat clay
UNM 11-4C	82.14%	9	33	Fine-Grained	Silts and Clays	**ML** Silt with sand
UNM 12-1-1A	40.16%	0	0	Course-Grained	Sand with Fines	**SM** Silty sand
UNM 12-1-2B	62.42%	11	33	Fine-Grained	Silts and Clays	**CL** Sandy lean clay
UNM 12-2-1A	32.40%	0	20	Course-Grained	Sand with Fines	**SM** Silty sand
UNM 12-2-2B	32.32%	4	19	Course-Grained	Sand with Fines	**SM** Silty sand
UNM 12-3-1A	99.14%	30	65	Fine-Grained	Silts and Clays	**MH** Elastic silt
UNM 12-3-2B	86.58%	24	44	Fine-Grained	Silts and Clays	**CL** Lean clay
UNM 12-4-1A	99.46%	41	76	Fine-Grained	Silts and Clays	**MH** Elastic silt
UNM 12-4-2B	86.24%	21	40	Fine-Grained	Silts and Clays	**CL** Lean clay
UNM 12-5-1A	28.84%	0	0	Course-Grained	Sand with Fines	**SM** Silty sand
UNM 12-5-2B	93.86%	29	53	Fine-Grained	Silts and Clays	**CH** Fat clay

UNM 11-4C, UNM 12-1-2B, UNM 12-3-2B, and UNM 12-4-2B are classified as ML or CL and were tested to determine the swelling potential. Table 4.10 shows the expansion index results and highlights the samples recommended for use as the clay(ey) soil in the SCEB production. UNM 11-4C and UNM 12-4-2B were chosen to be used in SCEB production.

Table 4. 10. Phase 2 Expansion Index and Classification .

Specimen ID	Expansion Index	Classification
UNM 11-4C	17	Very Low
UNM 12-1-2B	14	Very Low
UNM 12-3-2B	106	High
UNM 12-4-2B	57	Medium

4.2.3 Phase 3 Soil Testing

In Phase 3, 13 samples were obtained from seven dig locations from the UNM 11 and UNM 12 site locations to further investigate the variability in soils and provide more options for use in SCEB production. The samples and their locations were provided by Functional Earth Consulting, LLC. Received samples were given a specimen identification as shown in Table 4.11 and a letter following the dig location indicates a different depth. The results of the natural moisture content for soil specimens as received from the site and the specific gravity for the soil specimens are presented in Appendix A.1.

The 13 samples were first classified based on particle size analysis. The soil fraction results are shown in Table 4.12 and the particle size distribution curves are displayed in Figure 4.6. The specimens highlighted in Table 4.12 meet the criteria of more than 50% fine-grained soils as recommended for a suitable soil for SCEB production.

Table 4. 11. Soil Specimen ID for Phase 3 soils testing.

Specimen ID	Jemez Site ID	Dig Date	Location in Bore	Location	
UNM 11 1A	JEZ 26 1A	11/19/2015	Top 7'	N35° 34' 44.8"	W106° 45' 17.7"
UNM 11 1B	JEZ 26 1B	11/19/2015	Bottom 7'-11'	N35° 34' 44.8"	W106° 45' 17.7"
UNM 11 2A	JEZ 26 2A	11/19/2015	Top	N35° 34' 45.1"	W106° 45' 19.2"
UNM 11 2B	JEZ 26 2B	11/19/2015	Bottom	N35° 34' 45.1"	W106° 45' 19.2"
UNM 11 4A	JEZ 26 4A	11/19/2015	Top	N35° 34' 43.5"	W106° 45' 16.9"
UNM 11 4B	JEZ 26 4B	11/19/2015	Bottom	N35° 34' 43.5"	W106° 45' 16.9"
UNM 12 1A	JEZ 27 1A	11/19/2015	Top	N35° 34' 31.0"	W106° 45' 11.7"
UNM 12 1B	JEZ 27 1B	11/19/2015	Bottom	N35° 34' 31.0"	W106° 45' 11.7"
UNM 12 2	JEZ 27 2	11/19/2015	-	N35° 34' 30.8"	W106° 45' 5.0"
UNM 12 3A	JEZ 27 3A	11/19/2015	Top 7'	N35° 34' 31.8"	W106° 45' 8.6"
UNM 12 3B	JEZ 27 3B	11/19/2015	Bottom	N35° 34' 31.8"	W106° 45' 8.6"
UNM 12 4A	JEZ 27 4A	11/19/2015	Bottom	N35° 34' 32.8"	W106° 45' 8.5"
UNM 12 4B	JEZ 27 4B	11/19/2015	Top	N35° 34' 32.8"	W106° 45' 8.5"

Table 4. 12. Soil fractions for Phase 3.

Specimen ID	% Gravel	%Sand	% Fines (Silt & Clay)
	>2mm	<2mm/>0.075mm	<0.075mm
UNM 11 1A	1.27	2.41	96.32
UNM 11 1B	2.92	51.70	45.38
UNM 11 2A	13.18	84.05	2.77
UNM 11 2B	12.8	85.60	1.56
UNM 11 4A	3.04	48.94	48.01
UNM 11 4B	3.04	48.94	48.01
UNM 12 1A	0.36	5.66	93.97
UNM 12 1B	1.19	59.77	39.04
UNM 12 2	0.02	2.39	97.58
UNM 12 3A	0.21	1.79	98.00
UNM 12 3B	0.26	4.59	95.15
UNM 12 4A	0.05	1.10	98.86
UNM 12 4B	0.07	5.35	94.58

Atterberg limits tests were then performed on all soil samples and the results are presented in Table 4.13 and Figure 4.7. The soil specimens that meet the criteria of a Plasticity Classification of CL or ML are highlighted in Table 4.13.

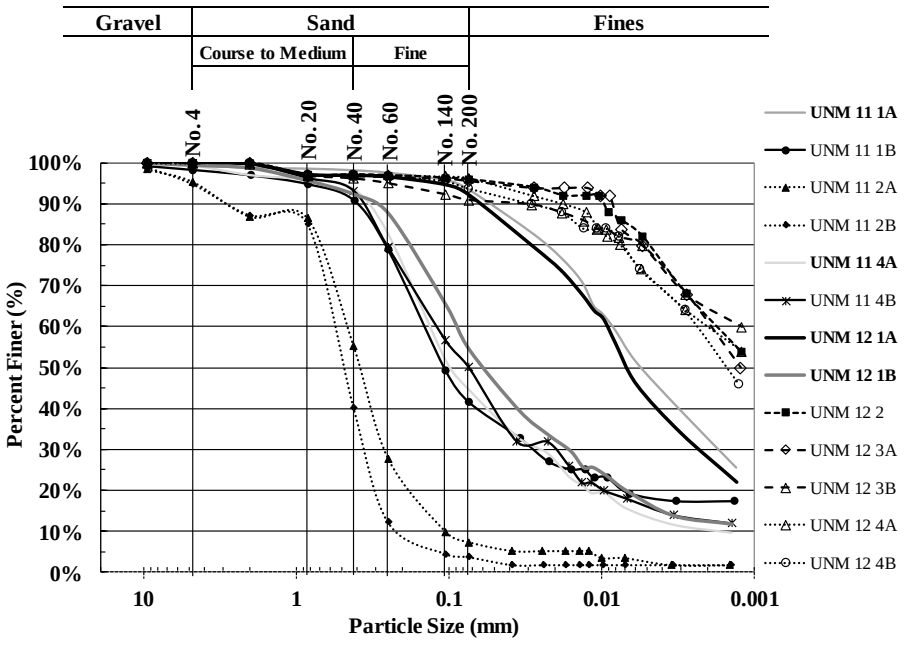

Figure 4. 6. Particle Size Distribution curves for soils in Phase 3.

Table 4. 13. Phase 3 Atterberg Limits and Plasticity Classification.

Specimen ID	LL	PL	PI	Plasticity Chart Classification
UNM 11 1A	46	24	22	CL
UNM 11 1B	-	NP	-	-
UNM 11 2A	-	NP	-	-
UNM 11 2B	-	NP	-	-
UNM 11 4A	24	20	3	ML
UNM 11 4B	-	NP	-	-
UNM 12 1A	43	25	18	CL
UNM 12 1B	29	20	9	CL
UNM 12 2	77	39	38	MH
UNM 12 3A	73	35	38	MH
UNM 12 3B	103	36	67	CH
UNM 12 4A	83	35	48	CH
UNM 12 4B	70	36	34	MH

Using USCS methodology, the soils were then classified and the results are listed in Table 4.14. The soil specimens that meet the criteria of a USCS Classification of CL, SC, or SM are highlighted in Table 4.14.

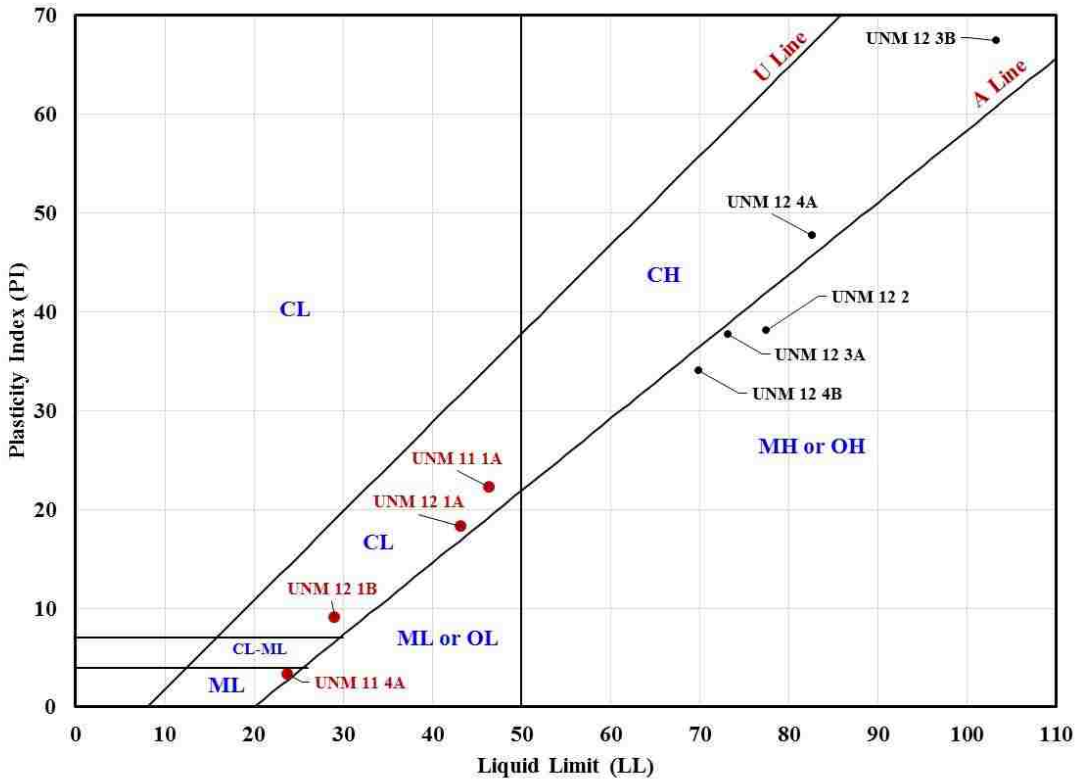

Figure 4. 7. Phase 3 Plasticity Chart.

Table 4. 14. Phase 3 Soil Classification based on USCS methodology.

Specimen ID	% Passing #200	PI	LL	ASTM D 2487 Criteria Assigning Group Symbols and Group Name		Soil Classification
UNM 11 1A	96.3%	46	22	Fine-Grained	Silts and Clays	**CL** Lean Clay
UNM 11 1B	45.4%	-	-	Coarse-Grained	Sands with Fines	**SM** Silty sand
UNM 11 2A	2.8%	-	-	Coarse-Grained	Clean Sands	**SP** Poorly graded sand
UNM 11 2B	1.6%	-	-	Coarse-Grained	Clean Sands	**SP** Poorly graded sand
UNM 11 4A	48.0%	24	3	Coarse-Grained	Sands with Fines	**SM** Silty sand
UNM 11 4B	48.0%	-	-	Coarse-Grained	Sands with Fines	**SM** Silty sand
UNM 12 1A	94.0%	43	18	Fine-Grained	Silts and Clays	**CL** Lean Clay
UNM 12 1B	39.0%	29	9	Coarse-Grained	Sands with Fines	**SC** Clayey sand
UNM 12 2	97.6%	77	38	Fine-Grained	Silts and Clays	**MH** Elastic Silt
UNM 12 3A	98.0%	73	38	Fine-Grained	Silts and Clays	**MH** Elastic Silt
UNM 12 3B	95.2%	103	67	Fine-Grained	Silts and Clays	**CH** Fat Clay
UNM 12 4A	98.9%	83	48	Fine-Grained	Silts and Clays	**CH** Fat Clay
UNM 12 4B	94.6%	70	34	Fine-Grained	Silts and Clays	**MH** Elastic Silt

UNM 11 1A, UNM 11 4A, UNM 12 1A, and UNM 12 1B are classified as CL, SM, and SC. They were tested to determine the swelling potential. Table 4.15 shows the expansion index results and highlights the samples recommended for use as the clay(ey) soil in the SCEB production in the future. These soils are UNM 11 4A, UNM 12 1A, and UNM 12 1B.

Table 4. 15. Phase 3 Expansion Index and Classification .

Specimen ID	Expansion Index	Classification
UNM 11 1A	104	High
UNM 11 4A	1	Low
UNM 12 1A	48	Low
UNM 12 1B	14	Low

4.2.4 Phase 4 Soil Testing

Typically SCEBs are a mixture of four components: clay (ey) soil, sand, stabilizer and water. In Phase 4, the soils used for SCEB production were tested. The clay (ey) soils and sands used for SCEBs were tested and are listed in Table 4.16. These soils were used

in five SCEB mix designs as displayed in Table 4.17. There were two SCEB dry mixes without stabilizer tested (Soil 1 and Soil 2), three SCEB dry mixes including stabilizer tested (SCEB 7, 8 and 9), and one Adobe dry mix tested (Adobe Soil). These block dry mixes are listed in Table 4.18.

Table 4. 16. Specimen Identification for Clay and Sand used in SCEBs.

Specimen ID	Soil Type ID	Jemez Site ID
Clay 1	UNM 11-4	JEZ 26
Clay 2	UNM 12-4	JEZ 27
Sand 1	Vulcan sand	-
Sand 2	Buildology sand	-

In this research, there were 9 SCEBs tested for block mechanical properties. Out of the 9 SCEB mixes, only 4 were investigated for their soil properties: SCEB 4, SCEB 7, SCEB 8, and SCEB 9. SCEB 4 is made up of a dry mix of Soil 1 and SCEB 7, 8, and 9 is made up of a dry mix of Soil 2. The stabilizer used in SCEB mixes are listed in Table 4.18.

Table 4. 17. Summary of Mix Designs used in SCEB.

Mix Design No.	Clay:Sand Ratio (by Volume)	Clay Soil Type ID	Sand Soil Type ID
1	1:1	Clay 1	Sand 1
2	3:2	Clay 1	Sand 1
3	2:3	Clay 2	Sand 2
4	1:1	Clay 2	Sand 2
5	2:1	Clay 2	Sand 2

Table 4. 18. Soil specimen identification for various SCEB mix designs

Specimen ID	Specimen Name	Mix Design No.	Stabilizer	Sieve Sand on #4 Sieve	Grind Clay on #4 Sieve
Soil 1	3:2 Blend, UNM 11-4: Vulcan sand	2	-	-	-
Soil 2	2:1 Blend, UNM 12-4: Buildology sand	5	-	-	-
Adobe Soil	Adobe Soil	-	Asphalt	-	-
SCEB 7	UNM 12-4 2:1 10%	5	Type II Portland Cement	-	x
SCEB 8	UNM 12-4 2:1 10% Sieved	5	Type II Portland Cement	x	x
SCEB 9	UNM 12-4 2:1 10% Unsieved	5	Type II Portland Cement	-	x

The results of the natural moisture content for soil specimens as received from the site and the specific gravity for the soil specimens are presented in Appendix A.1. The grain size distribution of soil samples were determined and a summary of these results are given in Table 4.19. The particle size distribution curves are displayed in Figure 4.8, 4.9, 4.10 and 4.11.

The results for particle size analysis are compared to published grain size distribution results of earthen materials using data summarized in Table 2.1 in Chapter 2. All soils compared from the literature are within a 15% difference from soil results obtained in this research. This is important because the soils used in this research can be compared to work published around the world, indicating a wider impact of the data presented. In an article published by Walker (*2004*), Soil Ic obtained a sand content 0.7% lower than Soil 1 and a fines content 1.1% higher than Soil 1. Soil B3 (*Bharath et al. 2014*) had a sand content 11.7% lower and fines content 13.5% higher than Soil 1. Soil C (*Bei & Papayianni, 2003*) had a sand content 5.1% lower than Soil 2 and a fines content 14.1%

higher than Soil 2. Earth block soil (*Miccoli et al. 2014*) had a sand content 2.4% lower than Soil 2 and a fines content 13.2% higher than Soil 2. The SCEB soil mix design compared with other investigations in the literature, which also used a designed a soil mixture of clayey soil and sand.

The results for particle size analysis are also compared with the Adobe Soil results. The Adobe Soil had a gravel content 68% higher than Soil 1 and 197% higher than Soil 2, a sand content 16% higher than Soil 1 and 40% higher than Soil 2, and a fines content 66% lower than Soil 1 and 78% lower than Soil 2. Therefore, the amount of fines was much lower for the Adobe Soil than Soil 1 and Soil 2.

Table 4. 19. Soil fractions for Phase 4.

Specimen ID	**% Gravel**	**% Sand**	**% Fines**
	>2mm	**<2mm/>0.075mm**	**<0.075mm**
Clay 1	0.14	11.40	88.46
Clay 2	0.48	16.34	83.18
Sand 1	20.86	78.02	1.12
Sand 2	11.90	86.16	1.94
Soil 1	0.08	56.40	43.52
Soil 2	5.98	44.06	49.96
Adobe Soil	12.16	65.98	21.86
SCEB 7	7.52	54.06	38.42
SCEB 8	1.82	54.40	43.78
SCEB 9	4.32	56.76	38.92

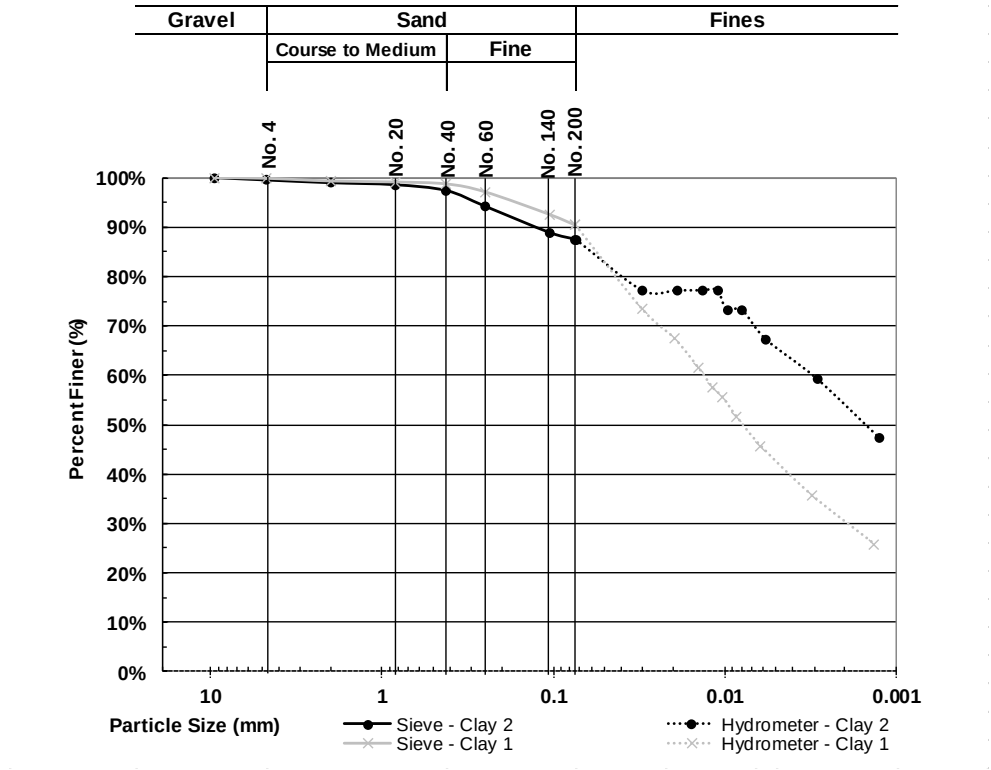

Figure 4. 8. Particle Size Distribution curves for clay(ey) soils in Phase 4.

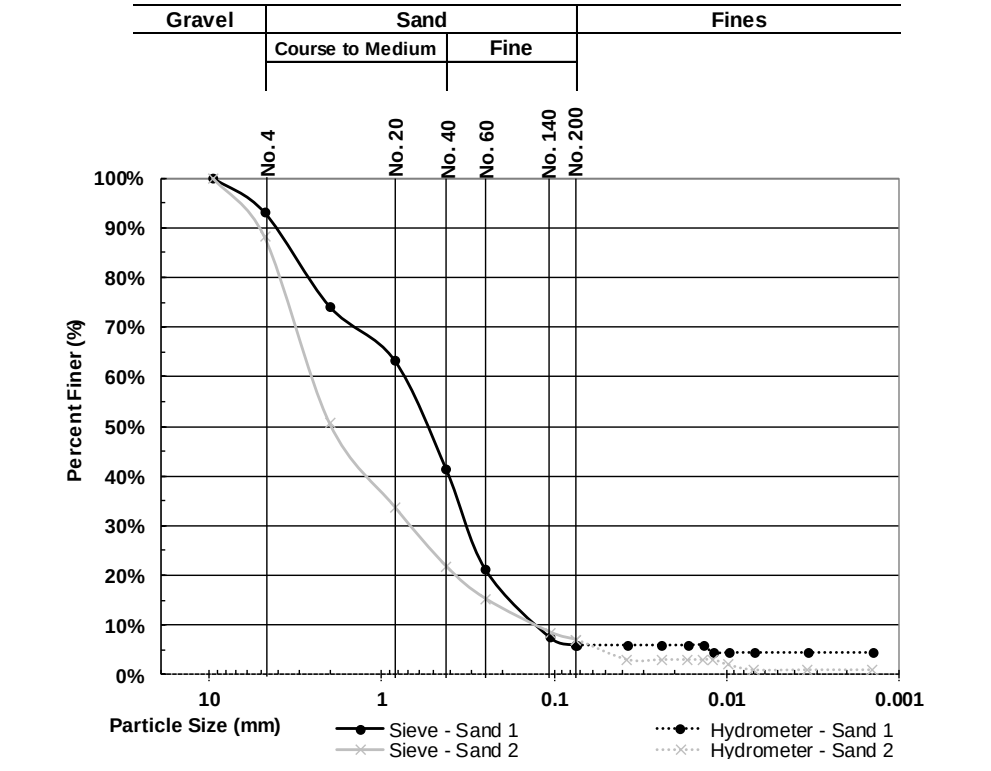

Figure 4. 9. Particle Size Distribution curves for sands in Phase 4.

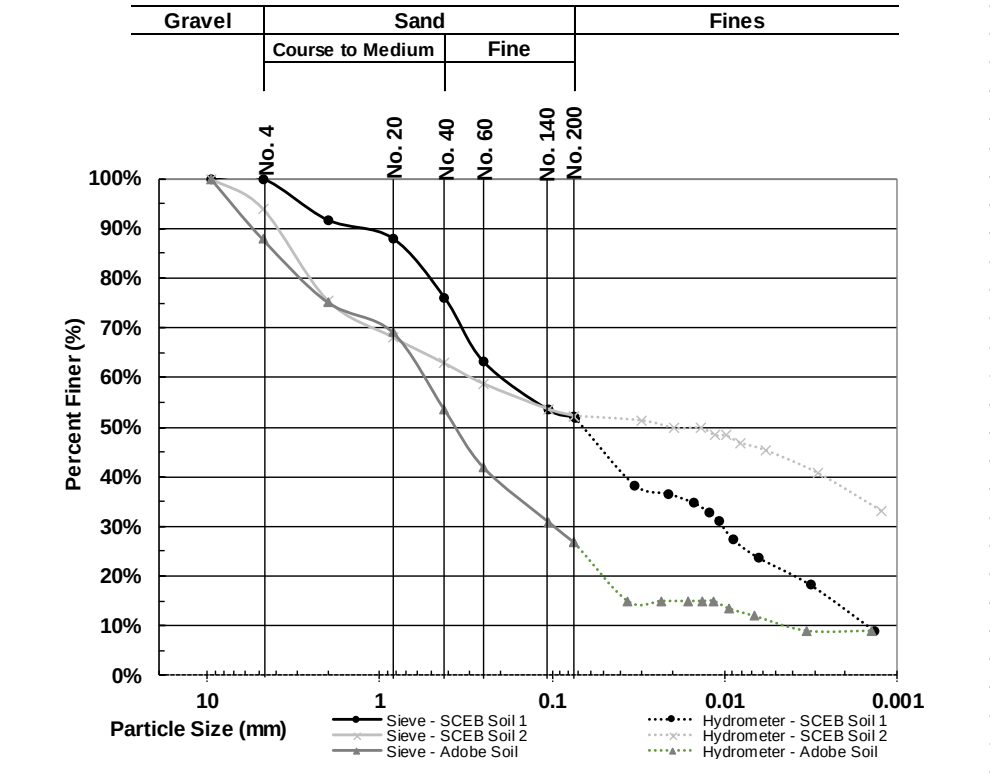

Figure 4. 10. Particle Size Distribution curves for SCEB soil mixes and Adobe soil in Phase 4.

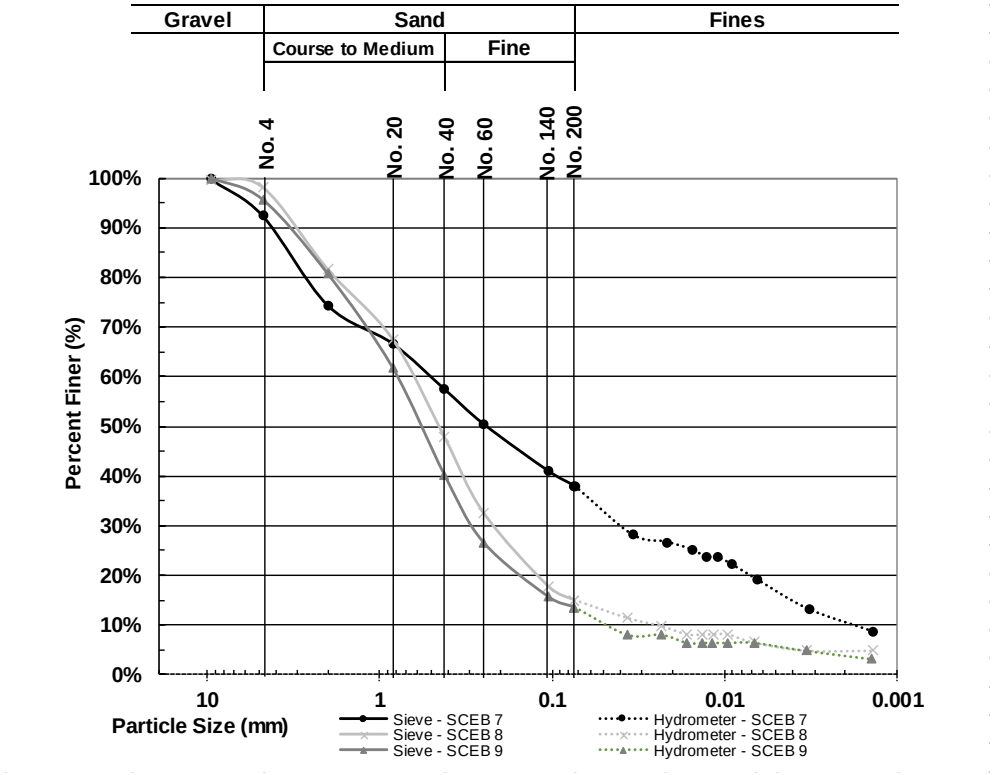

Figure 4. 11. Particle Size Distribution curves for SCEB soils in Phase 4.

Tests to determine the Atterberg limits were performed on all soil samples and a summary of the results are in Table 4.20 and Figure 4.12. Soil 1 classified as Lean Clay (CL), Soil 2 classified as Fat Clay (CH), while the Adobe Soil Classified as Silt (ML). Therefore, Soil 2 has a larger range where the soil behaves plastically than Soil 1. Soil 2 needs more than 50% water content to reach its liquid limit making it a fat clay. The Adobe Soil does not have a plastic limit and does not behave plastically.

The results for Atterberg limits of Soil 1 and Soil 2 are compared to published plasticity results of earthen materials using data summarized in Table 2.1 in Chapter 2. Soil C (*Bei & Papayianni, 2003*) had a liquid limit (LL) 7.4% higher and a plasticity index (PI) 8% lower than Soil 1. Soil Ic (*Walker, 2004*) had a LL 15.4% lower and a PI 11.8% higher than Soil 1. Soil RS1 (*Reddy et al. 2007*) had a LL 3.65% higher and a PI 11.14% lower than Soil 1. Soil B3 (*Bharath et al. 2014*) had a LL 6.9% higher and a PI –2.82% higher than Soil 1. There were no Atterberg limits results similar to Soil 2.

Table 4. 20. Phase 4 Atterberg Limits and Plasticity Classification.

Specimen ID	LL	PI	PL	Plasticity Classification
Clay 1	50	29	21	CH
Clay 2	72	40	32	CH
Sand 1	-	NP	-	-
Sand 2	-	NP	-	-
Soil 1	35	18	17	CL
Soil 2	53	28	25	CH
Adobe Soil	20	0	-	ML
SCEB 7	65	33	32	CH
SCEB 8	-	NP	-	-
SCEB 9	-	NP	-	-

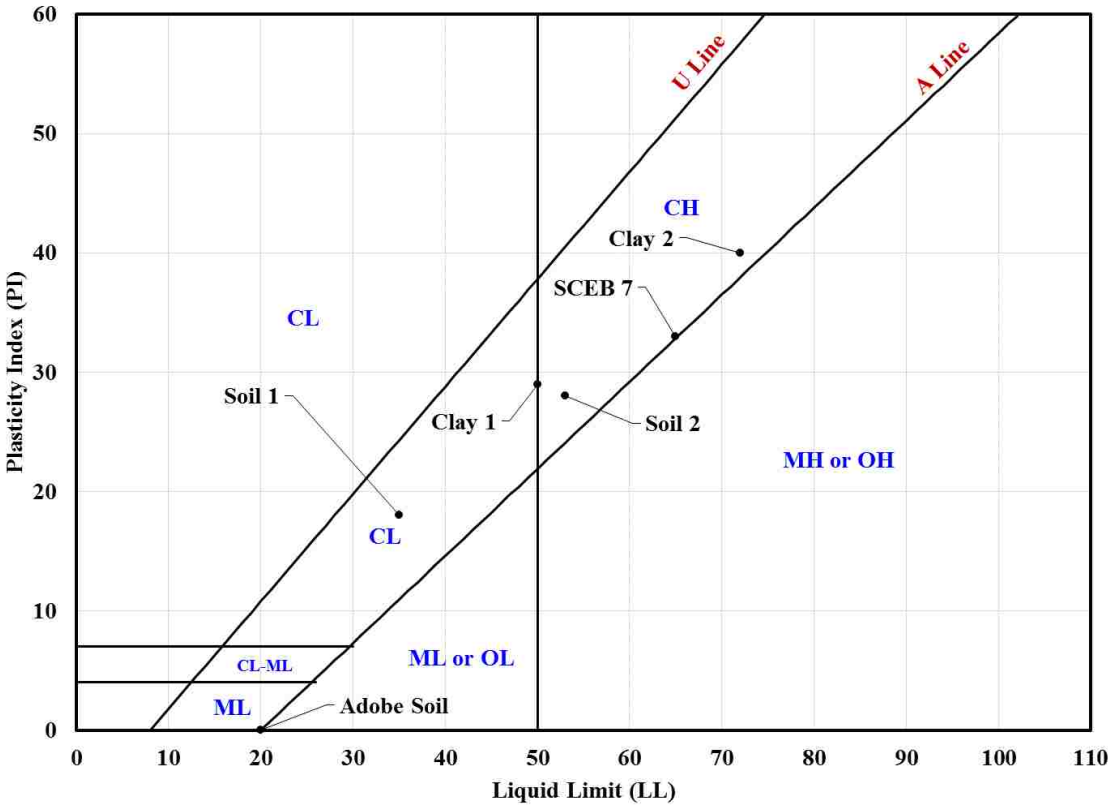

Figure 4. 12. Phase 4 Plasticity Chart.

Using USCS methodology, the soils were then classified and a summary of the results are listed in Table 4.21. Soil 1 and Soil 2 are classified as a Clayey Sand (SC). While, the Adobe Soil is classified as a Silty-Clayey Sand (SM-SC).

The results of USCS soil classification for Soil 1 and Soil 2 are compared to published results of earthen materials using data summarized in Table 2.1 in Chapter 2. Soil Ib and Ic (Walker, 2004), Soil RS1 and NS1 (Reddy et al. 2007), and Soil B3 (Bharath et al. 2014) were classified as SC similar to both Soil 1 and Soil 2.

Table 4. 21. Phase 4 Soil Classification based on USCS methodology.

Specimen ID	**% Passing #200**	**% Retained #200**	**ASTM D 2487 Criteria Assigning Group Symbols and Group Name**		**Cu**	**Cc**	**LL**	**Soil Classification**
Clay 1	88.5	11.5	Fine-Grained	-	-	-	50	CH Fat Clay
Clay 2	83.2	16.8	Fine-Grained	-	-	-	72	CH Fat Clay
Sand 1	2.2	97.8	Coarse-Grained	Clean Sands	4.48	0.86	-	SP Poorly-graded sand
Sand 2	1.9	98.1	Coarse-Grained	Clean Sands	10.71	1.22	-	SW Well-graded sand
Soil 1	43.5	56.5	Coarse-Grained	Sands with Fines	-	-	35	SC Clayey Sand
Soil 2	50.0	50.0	Coarse-Grained	Sands with Fines	-	-	53	SC Clayey Sand
Adobe Soil	21.9	78.1	Coarse-Grained	Sands with Fines	-	-	20	SM-SC-Silty-clayey Sand
SCEB 7	38.4	61.6	Coarse-Grained	Sands with Fines	-	-	65	SC Clayey sand
SCEB 8	43.8	56.2	Coarse-Grained	Sands with Fines	-	-	-	SM-SC-Silty-clayey Sand
SCEB 9	38.9	61.1	Coarse-Grained	Sands with Fines	-	-	-	SM-SC-Silty-clayey Sand

Clay 1, Clay 2, Soil 1, Soil 2, Adobe Soil, and SCEB 7 were tested to determine the swelling potential. Table 4.22 shows the expansion index results and shows that Clay 1 had a “very low” expansion classification while Clay 2 had a “very high” expansion classification. Clay 1 was used in the mix design of Soil 1 and the “very low” expansion classification correlates for both soils. Clay 2 was used in the mix design of Soil 2 and SCEB 7. While Clay 2 had a “very high” expansion classification, the expansion classification for Soil 2 was “low” and SCEB 7 was “very low”. This also demonstrates that the addition of Type II Portland Cement decreases the water content. The Adobe Soil had a “very low” expansion index. A suitable expansion classification was determined based on experience from initial block testing as well as prior knowledge in limiting the expansion of the soils.

The results of swelling potential were not compared to results in literature because there were no results found on the expansion index classification of soils used for earthen materials.

Table 4. 22. Phase 4 Expansion Index and Classification .

Specimen Identification	Expansion Index	Classification
Clay 1	2	Very Low
Clay 2	152	Very High
Soil 1	0	Very Low
Soil 2	21	Low
Adobe Soil	1	Very Low
SCEB 7	8	Very Low

4.2.3.1 Proctor

Tests to determine optimum moisture content of the soil when it will become most dense and achieve its maximum dry density were performed on the soils used for SCEB production. The maximum dry density of the soil was a necessary soil characteristic to obtain in order to calculate the soil mixture ratio by weight. A summary of the results are in Table 4.23. The unit weight of the soil is plotted against water content in Figure 4.13 in order to show the dry density and optimum water content. Figure 4.14 compares the dry density of Clay 1, Clay 2, Sand 1, Sand 2, Soil 1, Soil 2, Adobe Soil, and SCEB 7. Soil 1 obtained a dry density 18% lower than Adobe Soil and Soil 2 obtained a dry density 9% lower than Adobe Soil.

Table 4. 23. Phase 4 Results from Modified Proctor A test.

Specimen Identification	Wet Density, ρw, kN/m³ [lb/ft³]	Dry Density, ρd kN/m³ [lb/ft³]	Optimum Moisture Content (%)
Clay 1	20.8 [132.5]	17.8 [113.5]	16.8
Clay 2	20.2 [128.5]	17.2 [109.8]	17.0
Sand 1	19.7 [125.4]	18.2 [115.6]	8.4
Sand 2	20.3 [129.1]	18.6 [118.2]	9.3
Soil 1	19.6 [124.5]	17.5 [111.3]	11.8
Soil 2	21.6 [137.5]	19.1 [121.6]	13.0
Adobe Soil	22.8 [144.9]	20.9 [133.3]	8.7
SCEB 7	18.8 [119.7]	16.1 [102.7]	14.3

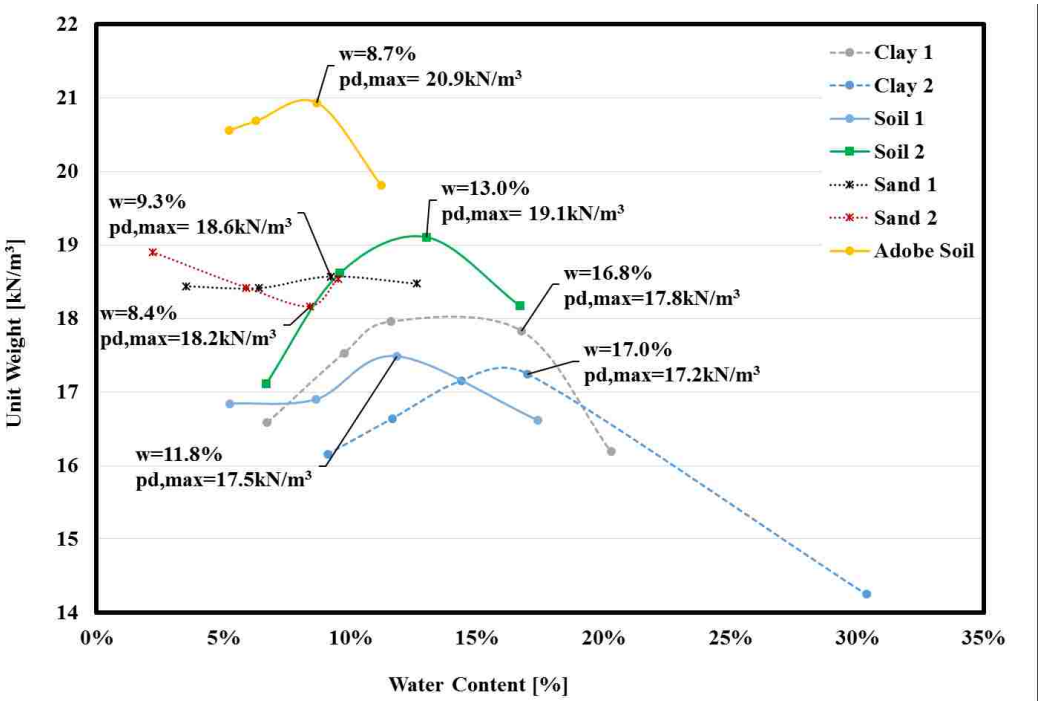

Figure 4. 13. Unit weight plotted against water content to show optimum water content and dry density of soil samples.

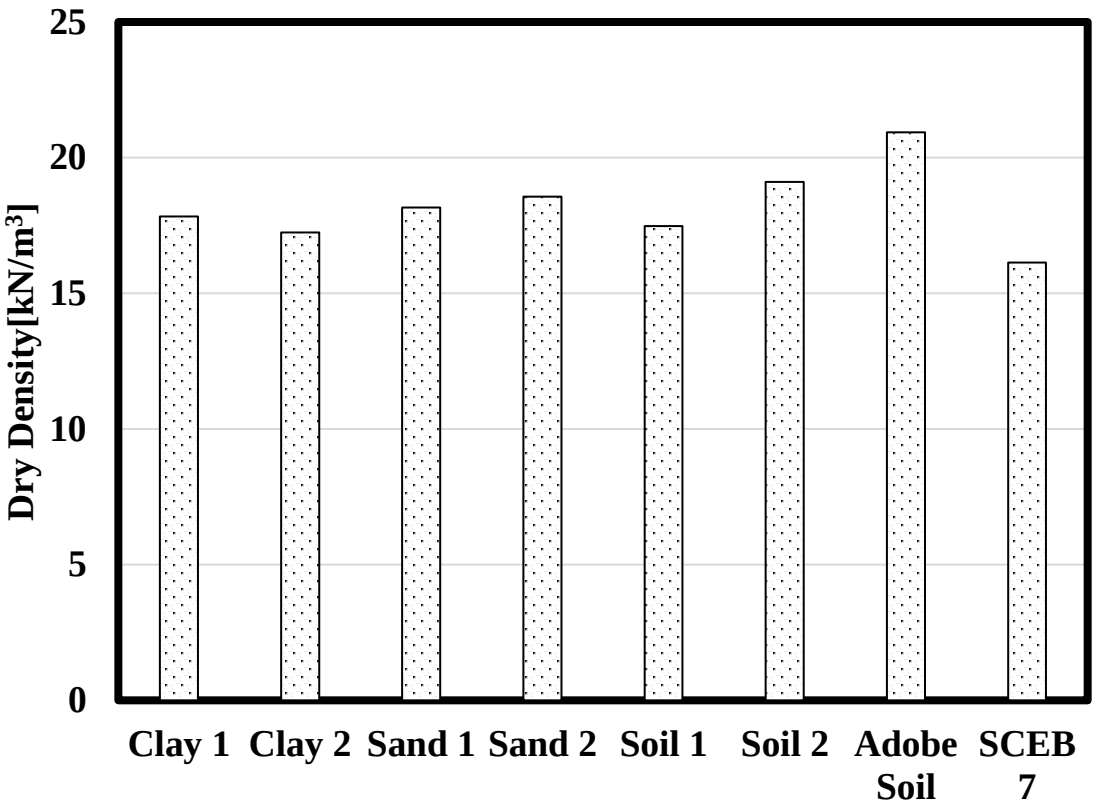

Figure 4. 14. Compares the maximum dry density of the soil specimens.

4.2.3.3 Clay Activity

The clay activity is a single parameter defined by Skempton (*1953*) using the Atterberg limits and the clay content of a soil. The activity can be calculated using Equation (4.1). Skempton listed typical activity values for the clay minerals as defined in Table 4.24.

$$\mathrm{A} = \frac{PI}{clay\ size\ fraction} \tag{4.1}$$

where,
A is the activity of the clay.
PI is the plasticity index, %.
Clay size fraction is the percentage clay size fraction, %.

Table 4. 24. Clay Mineral Acitvity (Skempton, 1953).

Clay Mineral	Activity
Calcite	0.18
Muscovite	0.23
Kaolinite	0.33 – 0.46
Illite	0.9
Ca-Montmorillonite	1.5
Na-Montmorillonite	7.2

Using the particle size analysis and Atterberg limits for the soils in Phase 1, 3, and 4, the activity of the soils were calculated. The results for soils are shown in Table 4.25. The clay activity values for the soils were then plotted in Figure 4.15 with the typical activity values of clay minerals according to Skempton (*1953*).

The clay activity of Clay 1, Clay 2, Soil 1, Soil 2, and Adobe Soil from Phase 4 soil testing were compared with the XRD results below. Using the clay activity values for the soils in Figure 4.15, it can be noted that Clay 1, Clay 2, Soil 2 was Illite, Soil 1 was Ca-montmorillonite, and Adobe Soil was Calcite. The clay mineral identification using XRD for Clay 1, Clay 2, Soil 1, Soil 2, and Adobe Soil was Kaolinite. These two different approaches for clay mineral identification provide reasonable results even though the classification of clay mineralogy for each soil is different. The reason for the difference cannot be identified since that was not the focus of this study. However, the clay activity can be used as an initial indicator of the clay mineralogy.

Table 4. 25. Phase 1, 3, and 4 Clay Activity Results.

Phase	ID	Activity
1	UNM 7	0.26
1	UNM 9	0.94
1	UNM 10	3.23
1	UNM 11	2.25
1	UNM 12	1.04
3	UNM 11 1A	1.48
3	UNM 11 4A	2.33
3	UNM 12 1A	1.61
3	UNM 12 1B	2.33
3	UNM 12 2	1.26
3	UNM 12 3A	1.24
3	UNM 12 3B	1.61
3	UNM 12 4A	1.41
3	UNM 12 4B	1.29
4	Clay 1	0.98
4	Clay 2	0.76
4	Soil 1	1.46
4	Soil 2	0.76
4	Adobe Soil	0.00
4	SCEB 7	3.17

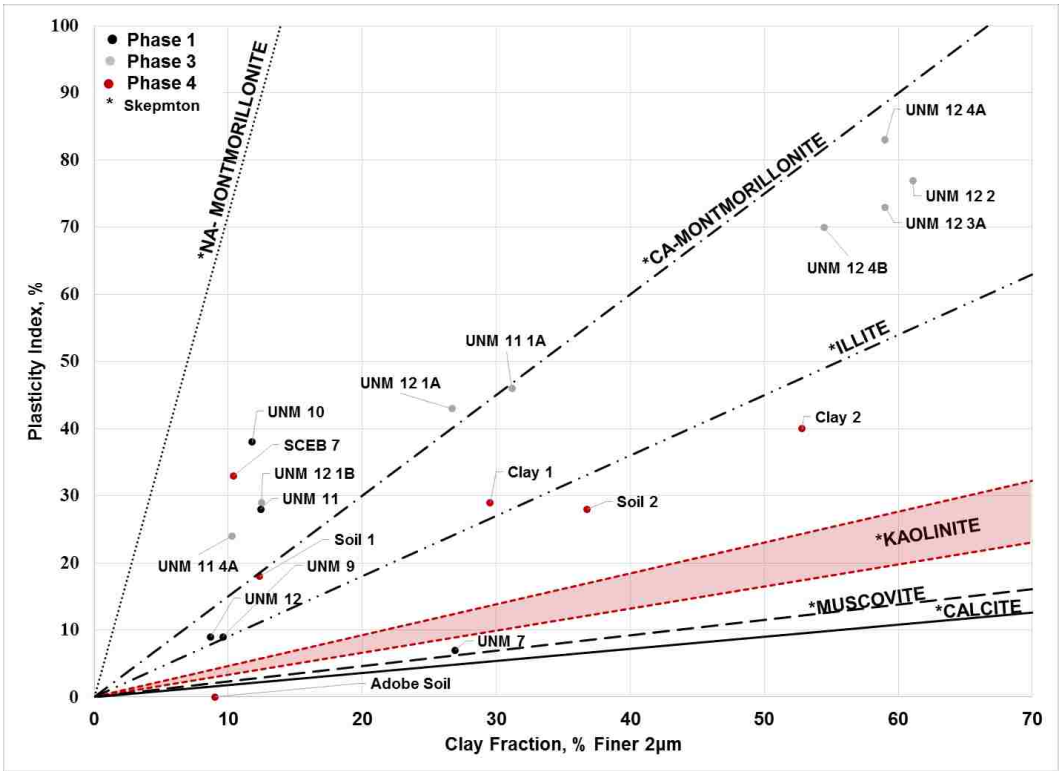

Figure 4. 15. Activity of Clay in Soil Specimens plotted with the typical activity values of clay minerals according to Skempton (1953)

4.2.3.4 X-Ray Diffraction (XRD)

The results of XRD Spectra are shown in Figure 4.16 and Figure 4.17. The minerals were identified by Eric Peterson in the Department of Earth and Planetary Sciences at the University of New Mexico. The Clay Mineral Identification Flow Diagram from the U.S. Geological Survey was used to determine the clay mineral identification. In addition, Moore and Reynolds (*1997*) was also used. Whole pattern fitting was used to calculate the approximate weight as a percentage of the minerals per total weight. The results from quantification of minerals in the soil sample are shown in Table 4.26.

Table 4. 26. Quantification of Minerals using Whole Pattern Fitting by approximate weight.

Specimen Identification		**Clay 1**	**Clay 2**	**Soil 1**	**Soil 2**	**Adobe Soil**
		Mineral Content (%)				
Quartz [SiO_2]	Tectosilicate SiO_2	27.1	26.2	23.7	14.9	24.2
Calcite [$CaCO_3$]	Carbonate	9.1	10.0	5.8	5.3	9.0
Albite [$K_{0.22}Na_{0.78}AlSi_3O_8$]	Tectosilicate Feldspar	12.1	11.7	8.6	5.8	8.6
Microcline [$K(AlSi_3O_8)$]	Tectosilicate Feldspar	5.3	6.3	4.1	2.9	14.4
Muscovite [$KAl3(Si3O_{10})(F,OH)_2$]	Phyllosilicate Mica group	7.3	10.2	4.5	7.6	1.6
Kaolinite [$Al_2Si_2O_5(OH)_4$]	Phyllosilicate Clay group	5.3	2.2	2.8	1.7	-
Amorphous and Others	-	31.4	33.4	50.4	61.8	41.7
Gypsum [$CaSO_4(2H_2O)$]	Sulfate	-	-	-	-	0.6
Tridymite [SiO_2]	Tectosilicate SiO_2	2.4	-	-	-	-
Predominant Clay Mineral		Kaolinite	Kaolinite	Kaolinite	Kaolinite	Kaolinite

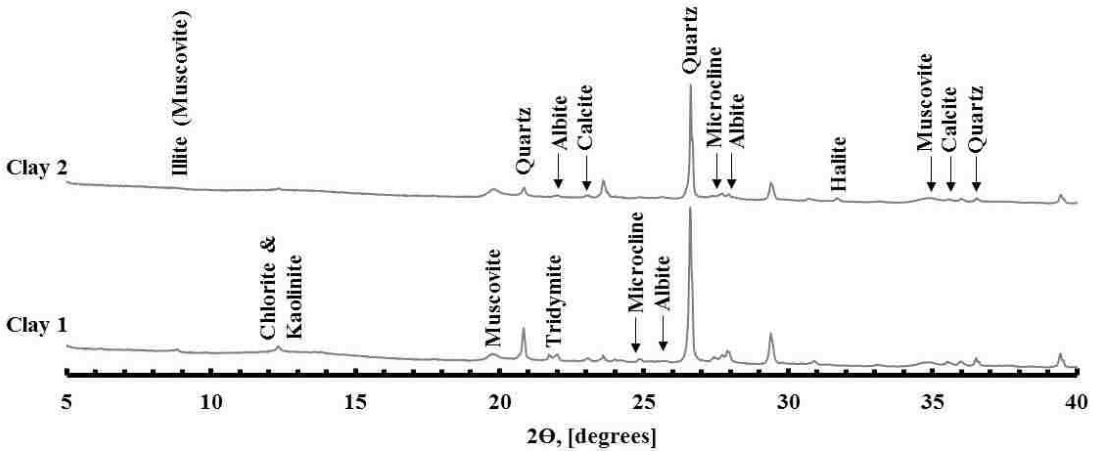

Figure 4. 16. Clay 1 and Clay 2 XRD Spectra.

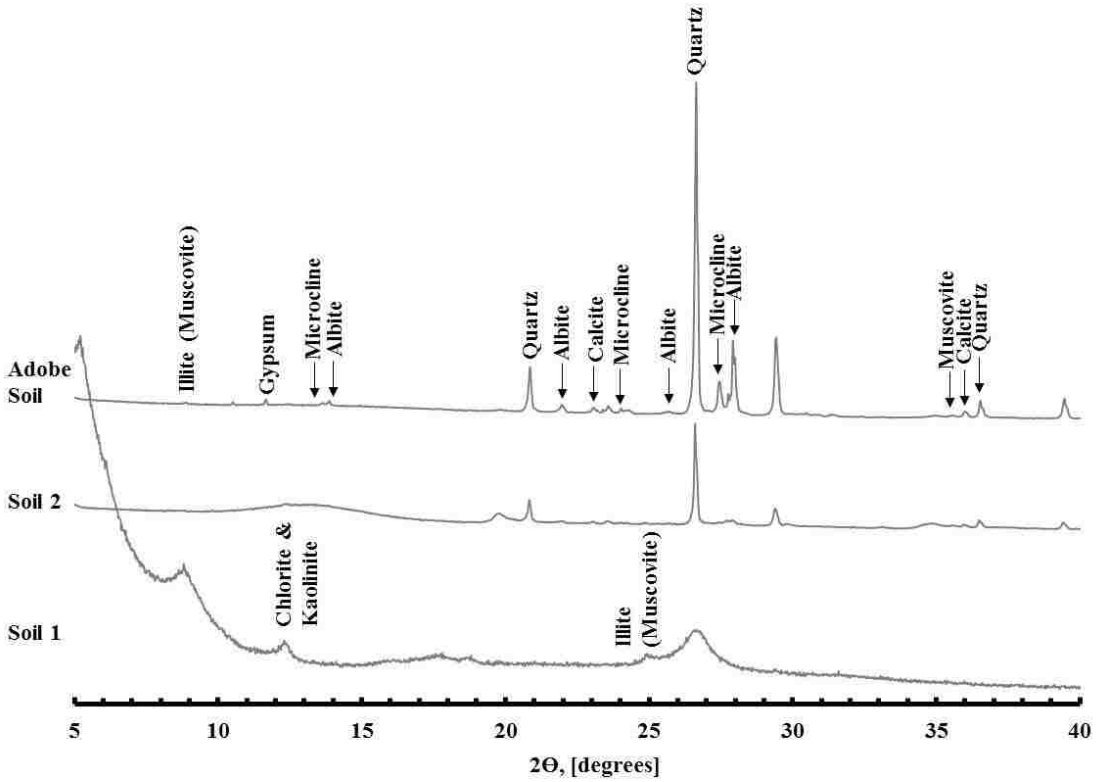

Figure 4. 17. SCEB Soil 1 and 2 and Adobe Soil XRD Spectra.

The dominant material classified in all specimens was quartz. Quartz is a tectosilicate. A tectosilicate is a framework silicate composed of all four oxygens of a SiO_4 tetrahedron that are shared by adjoining tetrahedron (*Klein and Dutrow, 2007*). Quartz is

a common and abundant mineral which is present in many igneous and metamorphic rocks (*Klein and Dutrow, 2007*).

The presence of calcite was identified in all soil specimens. Caliche is composed of calcite which is a carbonate commonly associated with clay minerals. Calcite is the primary mineral in sedimentary and igneous rocks (*Klein and Dutrow, 2007*). The most common use for calcite is for the production of cements and lime to be used as mortars. Portland cement is composed of about 75% calcium carbonate (*Klein and Dutrow, 2007*).

Muscovite is a common phyllosilicate part of the Mica group (*Klein and Dutrow, 2007*). It is common in metamorphic rocks. It has high dielectric and heat-resisting properties (*Klein and Dutrow, 2007*). Illite is an alkali-deficient mica near the muscovite composition (*Klein and Dutrow, 2007*).

Kaolinite is a common phyllosilicate part of the clay mineral group (*Klein and Dutrow, 2007*). Kaolinite is a common mineral which is formed at low temperatures and pressures in sedimentary rocks (*Klein and Dutrow, 2007*).

Microcline and albite are alkali feldspars. Each belong to the tectosilicates. Microcline belongs to the K-felspars while Albite belongs to the Plagioclase feldspars (*Klein and Dutrow, 2007*). Microcline feldspars are often used to make porcelain (*Klein and Dutrow, 2007*). Albite feldspar is found in igneous, metamorphic, and sedimentary rocks (*Klein and Dutrow, 2007*). Albite is used in ceramics as well.

Gypsum is a common mineral found in sedimentary rocks (*Klein and Dutrow, 2007*). It is the most common sulfate. This material, when mixed with water, slowly absorbs the water, crystallizes and then hardens (*Klein and Dutrow, 2007*). Uncalcined gypsum is used as a retarder in Portland cement (*Klein and Dutrow, 2007*).

Tridymite is a tectosilicate and occurs commonly in certain siliceous volcanic rocks (*Klein and Dutrow, 2007*).

The results of XRD for Soil 1 and Soil 2 are compared to published results of earthen materials using data summarized in Table 2.1 in Chapter 2. Soil Ia, Ib, and Ic (*Walker, 2004*) and Soil RS1, NS1, and NS2 (*Reddy et al. 2007*) were documented to have kaolinite as the predominant clay material in the soils.

Maskell et al. (2014) used X-ray diffraction to determine the mineralogy of a soil used for CEBs. Table 4.27 lists the mineral content. The literature shows similar results to the XRD for SCEB soils. There is a large quartz presence however, the soil from literature has a higher clay mineral content with, Kaolinite, Illite, and Smecitite. The soils determined for use in SCEB listed in Table 4.26 have a larger feldspar presence than clay minerals.

Table 4. 27. Clay Mineralogy for a CEB (Maskell et al. 2014).

Specimen Identification	**Mineral Content (%)**
Quartz	39
Kaolinite	31
Illite	16
Chlorite	3
Smectite	3
Hematite	3
Siderite	2

4.2.3.5 Scanning Electron Microscopy (SEM)

The clay particle size was also investigated by scanning electron microscopy (SEM) for Clay 2 only. The SEM has an energy dispersive X-ray detection system (EDS), which allows for the spectral analysis of X-rays generated from the specimen directly under the

electron beam (*Klein and Dutrow, 2007*). The full spectral X-ray maps of Clay 2 is shown in Figure 4.18 (a).

The Clay 2 EDS spectrum is portrayed as a plot of x-ray counts vs. energy (in keV) in Figure 4.18 (b). Energy peaks correspond to the various elements in the soil sample. The EDS Spectrum shows a large amount of Silicon (Si). There is also evidence of Aluminum (Al), Sodium (Na), and Calcium (Ca). As shown Figure 4.18 (c), the EDS map of Clay 2 shows a distribution of Silicon (Si). The EDS map of Clay 2 shows a distribution of Aluminum (Al) as shown in Figure 4.18 (d) and Figure 4.18 (e) shown a distribution of Sodium (Na). The EDS map of Clay 2 shows a distribution of Calcium (Ca) as shown in Figure 4.18 (f). The evidence of these elements seems appropriate. The large amount of Silicon in Clay 2 is evident in the following minerals: Quartz, Albite, Microcline, and Kaolinite. The evidence of Calcium in Clay 2 is due to the mineral Calcite. The minerals, Albite, Muscovite, and Kaolinite are present in Clay 2 and they also have traces of the element Aluminum. The amount of Sodium in Clay 2 is evident in the mineral Albite which is present in Clay 2.

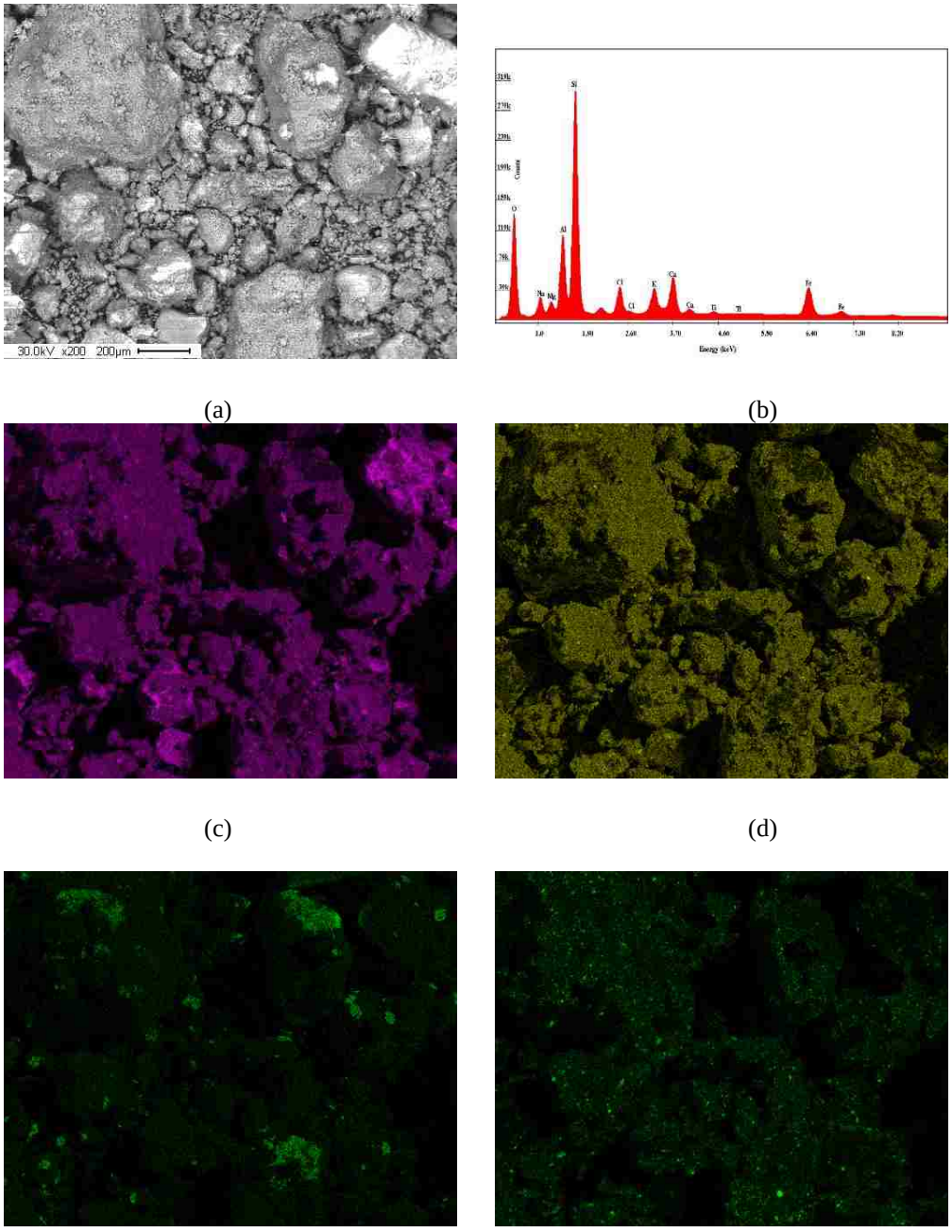

(a) (b)

(c) (d)

(e) (f)

Figure 4. 18. (a) SEM image. (b) EDS Spectrum. (c) EDS map of Clay 2 showing distribution of Silicon (Si). (d) EDS map of Clay 2 showing distribution of Aluminum (Al). (e) EDS map of Clay 2 showing distribution of Sodium (Na). (f) EDS map of Clay 2 showing distribution of Calcium (Ca).

4.3 Block Testing

There were 9 Stabilized Compressed Earth Blocks (SCEBs) tested to determine dry and saturated compressive strength, dry and saturated flexural strength, water absorption,

the initial rate of absorption, sorptivity, modulus of elasticity and Poisson's ratio. The SCEBs were compared to the results from commercial Adobe blocks purchased from New Mexico Earth Inc. There were two types of adobe tested: unstabilized and stabilized as listed in Table 3.2 in Chapter 3.

4.3.1 SCEB Mixture Proportions

The clay (ey) soil samples used for earth block production are Clay 1 and Clay 2 and the sands used are Sand 1 and Sand 2 as shown in Phase 4 soil testing. The mix design using these soils are listed in Table 4.28. The clay to sand ratio by volume was converted to ratio by weight using the dry density determined for the soils in Phase 4 soils testing. Equation (4.2) was used to determine the weight for each volume ratio.

$$V = \frac{W}{\rho_d} \tag{4.2}$$

where,
V is the volume, m^3.
W is the weight, kN.
ρ_d is the dry density, kN/m^3

Table 4. 28. Summary of Mix Designs used in SCEB.

Mix Design No.	Clay:Sand Ratio (by Volume)	Clay:Sand Ratio (by Weight)	Clay Soil Type ID	Sand Soil Type ID
1	1:1	0.98:1	Clay 1	Sand 1
2	3:2	2.95:2	Clay 1	Sand 1
3	2:3	2:3.22	Clay 2	Sand 2
4	1:1	0.93:1	Clay 2	Sand 2
5	2:1	1.86:1	Clay 2	Sand 2

There were 9 different SCEBs tested. The mix designs for the SCEBs are listed in Table 4.29. There were also two adobe blocks tested from NM Earth, Inc. The unstabilized adobe block (AB) and the stabilized adobe block (SAB).

It should be noted the large increase in stabilizer from 6% Type II Portland cement in SCEB 6 to 10% Type II Portland cement in SCEB 7. The reason for the increase was due to time constraints of the project and the variability of the soil within each site. The intent was to design a "robust" SCEB soil mixture that would be able to take into account the soil variability. There are a variety of elements that are influenced by the amount of Portland cement included in the SCEB. A lower amount of Portland cement is desired in SCEBs for environmental considerations and to lower the unit cost of the block. However, a larger amount of Portland cement in SCEBs can improve the durability and strength of the block, increase the bond strength, and also allow for soil variability.

Table 4. 29. SCEB Specimen Identification and Mixture Design.

Specimen ID	Specimen Name	Mix Design No.	Clay:Sand Ratio (by volume)	Stabilizer	Production Date
SCEB 1	UNM 11-4-1L	1	1:1	1% Type S Lime	8-25-15
SCEB 2	UNM 11-4-4L	2	3:2	4% Type S Lime	9-1-15
SCEB 3	UNM 11-4-5C	2	3:2	5% Type II Portland Cement	9-8-15
SCEB 4	UNM 11-4-6C	2	3:2	6% Type II Portland Cement	9-10-15
SCEB 5	UNM 12-4 2:3 6%	3	2:3	6% Type II Portland Cement	1-27-16
SCEB 6	UNM 12-4 1:1 6%	4	1:1	6% Type II Portland Cement	1-27-16
SCEB 7	UNM 12-4 2:1 10%	5	2:1	10% Type II Portland Cement	2-18-16
SCEB 8	UNM 12-4 2:1 10% Sieved	5	2:1	10% Type II Portland Cement	3-2-16
SCEB 9	UNM 12-4 2:1 10% Unsieved	5	2:1	10% Type II Portland Cement	3-2-16

It should be noted that SCEB 7 and SCEB 9 specimens were basically the same block except that SCEB 9 was mixed in a concrete mixer. Also, the water content for SCEB 9 at time of mixing was 13.1% and SCEB 7 was 12.3%.

4.3.2 Unconfined Compressive Strength

The unconfined compression test was performed to determine the dry compressive strength of the SCEBs and commercial adobe blocks. Five specimens of each SCEB and adobe blocks were tested and the average compressive strength was calculated for each block. The results from testing are listed in Table 4.30. The three SCEBs with the highest dry compressive strength are SCEB 3, 4, and 7 and are highlighted in Table 4.30.

Table 4. 30. Dry unconfined compressive strength results and coefficient of variation (cov).

Specimen ID	**Average Compressive Strength, MPa [psi]**	**COV (%)**
SCEB 1	5.6 [815]	16
SCEB 2	3.8 [557]	13
SCEB 3	10.1 [1465]	15
SCEB 4	11.9 [1740]	18
SCEB 5	6.9 [996]	8
SCEB 6	6.1 [883]	16
SCEB 7	8.8 [1280]	7
SCEB 8	7.8 [1138]	19
SCEB 9	6.5 [938]	45
SAB	1.8 [263]	9
AB	2.8 [406]	13

The results are plotted in Figure 4.19. SCEB 4 had the maximum measured dry compressive strength of 11.9 MPa (1740 psi) which is 6.6 times greater than the commercial stabilized adobe block (SAB). SCEB 3 obtained a compressive strength 5.6 times greater than SAB and SCEB 7 had a dry compressive strength 4.9 times greater than SAB. SCEB 4 was stabilized with 6% Portland cement, SCEB 3 was stabilized with 5% Portland cement, and SCEB 7 was stabilized with 10% Portland cement. Therefore, it is

interesting to note that SCEB 4 obtained a higher compressive strength than SCEB 7 even though SCEB 7 had 50% percent more Portland cement stabilizer than SCEB 4. Soil 1 (SCEB 4) had about 50% higher Quartz and Kaolinite mineral content than Soil 2 (SCEB 7). While Soil 2 (SCEB 7), had about a 50% higher Muscovite (Illite) mineral content than Soil 1 (SCEB 4). Therefore, the difference in dry compressive strength of SCEB 4 than SCEB 7 may be because of the difference in mineral content.

The results for dry compressive strength of SCEBs and adobe blocks are compared to published mechanical strength results of earthen materials using data summarized in Table 2.1 of Chapter 2. The results for blocks vary. Therefore, Soil Ic (*Walker, 2004*) and Soil B3 (*Bharath et al. 2014*) have soil properties similar to Soil 1 and can be compared to SCEB 4. Soil C (*Bei & Papayianni, 2003)* and Earth Block Soil (*Miccoli et al. 2014*) have soil properties similar to Soil 2 and can be compared to SCEB 7, 8 and 9. In an article published by Walker (*2004*), Soil Ic had a dry compressive strength of 21.9 MPa (3176.3 psi) and Soil B3 (*Bharath et al. 2014*) had a dry compressive strength of 6.08 MPa (881.8 psi) which can be compared to SCEB 4 with a strength of 11.9 MPa (1725.9 psi). SCEB 4 had a strength 65% higher than Soil B3 and 59% lower than Soil Ic. Soil C (*Bei & Papayianni, 2003)* had a dry compressive strength of 4.46 MPa (646.8 psi) and Earth Block Soil (*Miccoli et al. 2014*) had a dry compressive strength of 5.21 MPa (775.6 psi) which can be compared to SCEB 7 with a dry compressive strength of 8.8 MPa (1276.3 psi). SCEB 7 had a strength 66% higher than Soil C and 51% higher than Earth Block Soil. The differences in dry compressive strength of the earthen blocks can be contributed to differences in stabilizer content and construction techniques.

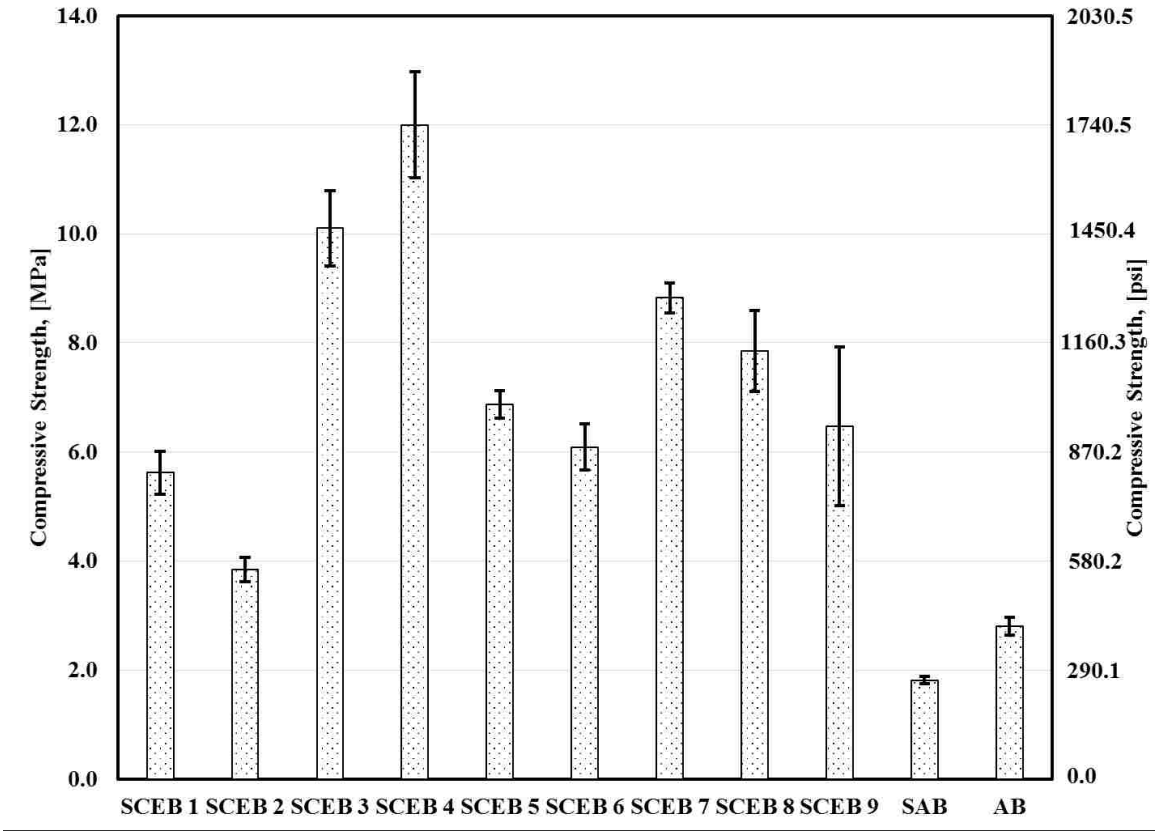

Figure 4. 19. Plot of dry unconfined compressive strength results.

The saturated unconfined compressive strength was compared with the New Mexico Earthen Building Materials Code, Section J of 14.7.4.23 minimum saturated compressive strength of 2.1 MPa (300 psi) (*NMAC, 2009*). Each SCEB and adobe block had 5 specimens of each mix design that were tested for statistical purposes The average compressive strength was calculated for each block tested and the results for the saturated compressive strength of SCEBs and adobes are detailed in Table 4.31. SCEB 4, 7, and 9 meet the minimum saturated compressive strength requirement according to the NM Earthen Building Materials Code and are highlighted in Table 4.31.

Table 4. 31. Saturated unconfined compressive strength results and coefficient of variation.

Specimen ID	Average Compressive Strength, MPa [psi]	COV (%)
SCEB 1	-	-
SCEB 2	-	-
SCEB 3	1.15 [166]	34
SCEB 4	2.19 [319]	17
SCEB 5	-	-
SCEB 6	-	-
SCEB 7	7.43 [1077]	17
SCEB 8	1.57 [227]	16
SCEB 9	7.12 [1032]	42
SAB	1.28 [185]	4
AB	-	-

SCEB 1, 2, and AB did not withstand the 24 hour saturation test. Therefore, these blocks were not able to be tested for the saturated compressive strength. The results are plotted in Figure 4.20. SCEB 7 had the highest measured saturated compressive strength of 7.43 MPa (1077.6 psi) which is 3.5 times greater than the NM Earthen Building Materials Code minimum strength of 2.1 MPa (300 psi). It was demonstrated that SCEB 4, 7, 8, and 9 had a higher saturated compressive strength than commercial stabilized adobe blocks (SAB). SCEB 7 had a saturated compressive strength 5.8 times greater than SAB. SCEB 9 had a saturated compressive strength 4.26% lower than SCEB 7. While, SCEB 4 had a saturated compressive strength 3.3 times lower than SCEB 7. In the saturated compressive strength test, SCEB 7 had a higher strength than SCEB 4. While in the dry compressive strength test, SCEB 7 had a lower strength SCEB 4. As it was previously considered, the difference in mineral content as well as the amount of Portland cement stabilizer contributed to these differences.

The results for saturated compressive strength of SCEB and adobe blocks are compared to published mechanical strength results of earthen materials using data summarized in Table 2.1 of Chapter 2. Soil Ic and Soil B3 have soil properties similar to

Soil 1 and can be compared to SCEB 4. Earth Block Soil have soil properties similar to Soil 2 and can be compared to SCEB 7, 8 and 9. Soil Ic (*Walker, 2004*) had a saturated compressive strength of 6.2 MPa (899.2 psi) and Soil B3 (*Bharath et al. 2014*) had a saturated compressive strength of 4.44 MPa (643.9 psi) which can be compared to SCEB 4 with a strength of 2.19 MPa (317.6 psi). SCEB 4 had a strength 96% lower than Soil B3 and 68% lower than Soil Ic. Earth Block Soil (*Miccoli et al. 2014*) had a dry compressive strength of 5.73 MPa (831.1 psi) which can be compared to SCEB 7 with a dry compressive strength of 7.43 MPa (1077.6 psi). SCEB 7 had a strength 26% higher than Earth Block Soil.

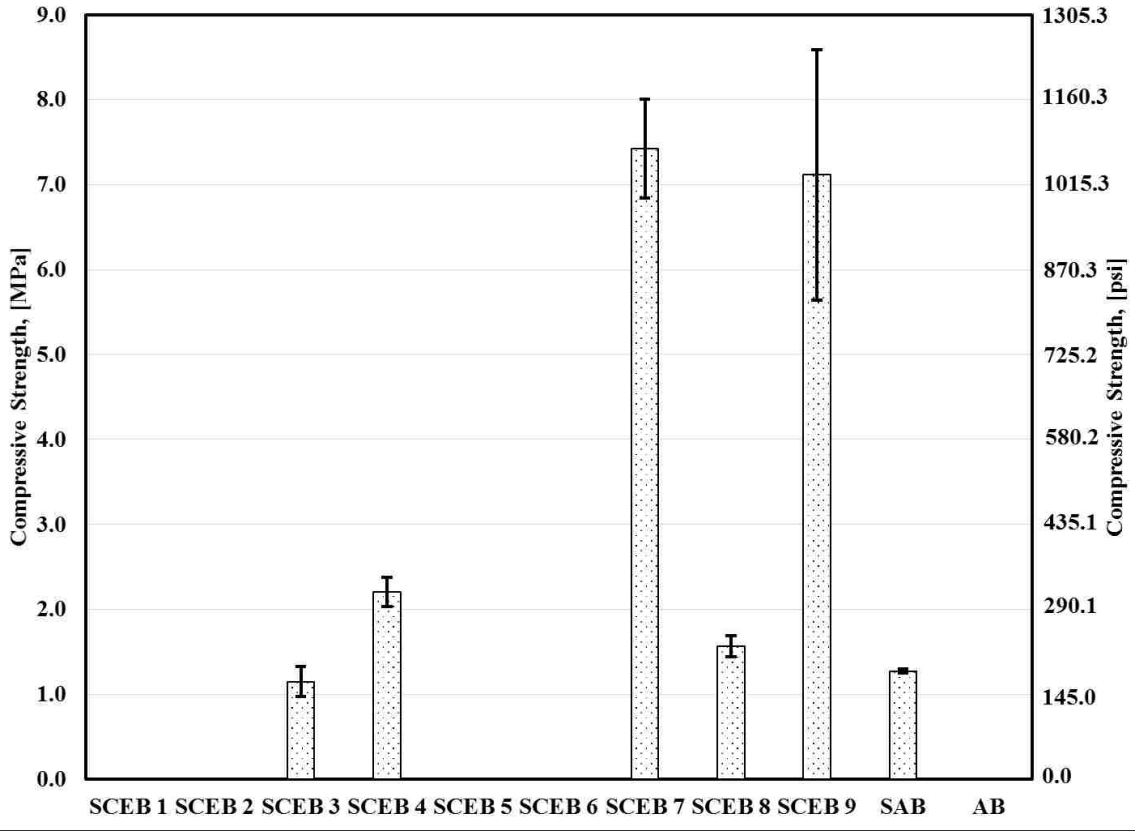

Figure 4. 20. Plot of saturated unconfined compressive strength results.

4.3.3 Modulus of Elasticity and Poisson's Ratio

The modulus of elasticity which is the ratio of the applied stress to the strain produced by the material was determined using the data obtained from the dry compression testing of SCEB and adobe blocks. The force and displacement data points of SCEB 5, 6, 7, 8, 9, SAB and AB were used to calculate the stress and strain data points and plotted in Figure 4.21. The linear portion of the curve is the elastic region and the slope of the line is the modulus of elasticity. The modulus of elasticity for SCEB 5, 6, 7, 8, and 9 were determined and are listed in Table 4.32.

SCEB 7 and 9 had the steepest slope and obtained modulus of elasticity values of 1275 MPa (184.9 ksi) and 1282 MPa (185.9 ksi), respectively as highlighted in Table 4.32. A steeper slope means a greater modulus of elasticity as well indicating a stiffer material. The greater modulus of elasticity means that a larger stress is necessary to obtain a set strain value. SCEB 5, 6, and 8 also had steep slopes indicating more brittle material behavior. In contrast, a lower modulus of elasticity value indicates that it is a less stiff material and that a smaller stress is needed to obtain a set stress value. SAB and AB obtained lower modulus of elasticity values of 94 MPa (13.6 ksi) and 239 MPa (34.6 ksi), respectively. However, as shown in Figure 4.20, SAB and AB reached larger strain values than SCEB 5, 6, 7, 8, and 9. SAB extended to the furthest strain value. This may have been due to the addition of asphalt as the binder in the material giving it more elasticity than SCEB 5, 6, 7, 8, and 9. SCEB 7 had a modulus of elasticity 13.5 times larger than SAB. While SAB reached a strain value within the elastic region 2.5 times larger than SCEB 7.

The results for modulus of elasticity of SCEBs and adobe blocks are compared to published mechanical strength results of earthen materials using data summarized in Table 2.1 of Chapter 2. Earth Block Soil had soil properties similar to Soil 2 and can be compared to SCEB 7, 8 and 9. Earth Block Soil (*Miccoli et al. 2014*) had a modulus of elasticity value of 2197 MPa which can be compared to SCEB 7 with a value of 1275 MPa (184.9 ksi). SCEB 7 had a modulus of elasticity 53% lower than Earth Block Soil. As a result, the Earth Block Soil can be determined to be a stiffer block than SCEB 7.

Table 4. 32. Summary of Results for SCEB and Adobe blocks Modulus of Elasticity.

Specimen ID	Modulus of Elasticity, MPa [ksi]
SCEB 5	909 [132]
SCEB 6	816 [118]
SCEB 7	1275 [185]
SCEB 8	800 [116]
SCEB 9	1282 [186]
SAB	94 [14]
AB	239 [35]

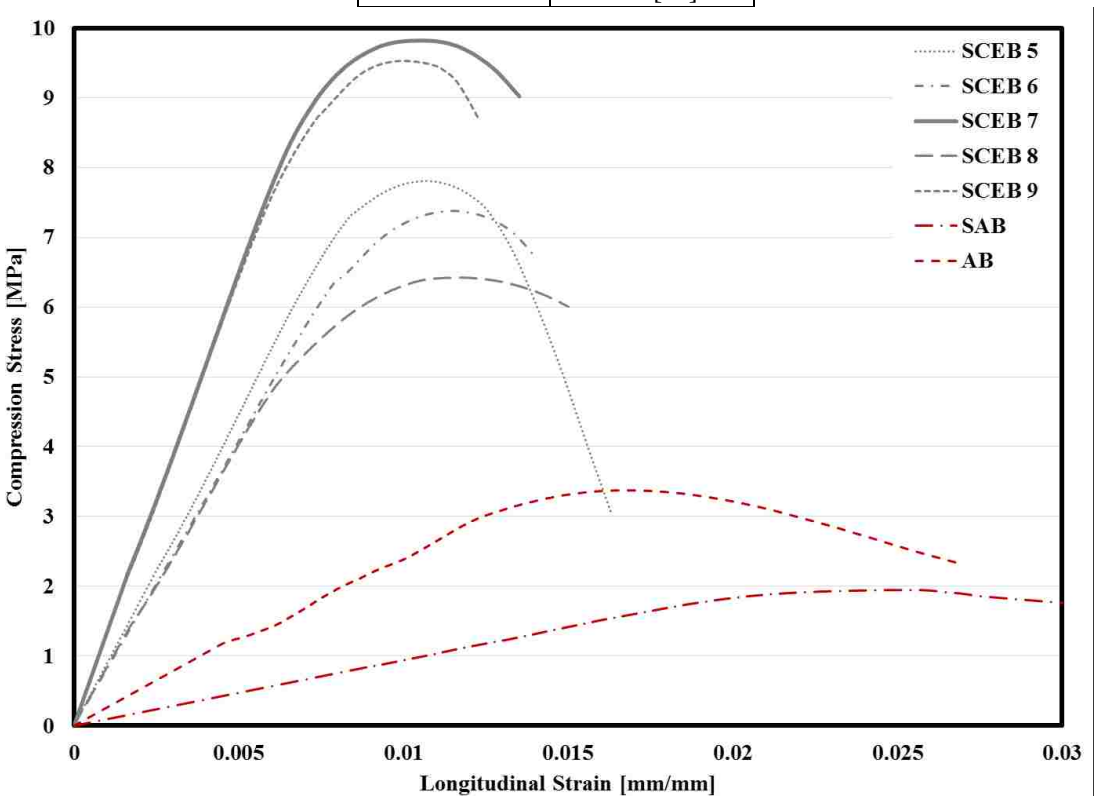

Figure 4. 21. Compression Stress vs. Longitudinal Strain plot of SCEB and Adobe blocks.

Poisson's ratio is a material property and is the ratio of transverse (vertical) strain to longitudinal (horizontal) strain in the along the vertical direction. Poisson's ratio was determined only for SCEB 7 and the value obtained is listed in Table 4.33. The results for Poisson's ratio of SCEB 7 are compared to published mechanical strength results of earthen materials using data summarized in Table 2.1 of Chapter 2. Earth Block Soil had soil properties similar to Soil 2 and can be compared to SCEB 7. Earth Block Soil (*Miccoli et al. 2014*) had a Poisson's ratio of 0.45 which is 63% higher than the value of SCEB 7.

Table 4. 33. Poisson's Ratio of SCEB 7.

Specimen ID	Poisson Ratio
SCEB 7	0.233

4.3.4 Modulus of Rupture

The SCEB and Adobe blocks ability to resist flexural stress were quantified by determining the modulus of rupture. Five specimens of each SCEBs and adobe blocks were tested and the average dry modulus of rupture was calculated for each block. The results are listed in Table 4.34. The two SCEBs with the highest dry compressive strength are SCEB 4, and 7 and are highlighted in Table 4.34.

Table 4.34. Dry Modulus of Rupture results and coefficient of variation.

Specimen ID	Average MOR, MPa [psi]	COV (%)
SCEB 1	0.30 [43]	12
SCEB 2	0.17 [24]	28
SCEB 3	0.48 [69]	13
SCEB 4	0.93 [135]	17
SCEB 5	0.18 [26]	28
SCEB 6	0.13 [19]	64
SCEB 7	0.91 [132]	28
SCEB 8	0.48 [69]	31
SCEB 9	0.51 [74]	15
SAB	0.49 [71]	9
AB	0.65 [94]	37

The results are plotted in Figure 4.22. SCEB 4 had the maximum average modulus of rupture of 0.93 MPa (134.9 psi) which is 62% greater than the commercial stabilized adobe block (SAB). SCEB 7 had the maximum average modulus of rupture of 0.91 MPa (131.9 psi) which is 60% greater than SAB. SCEB 4 had a dry modulus of rupture 2% greater than SCEB 7.

The results for the dry flexural strength of SCEBs and adobe blocks are compared to published mechanical strength results of earthen materials using data summarized in Table 2.1 of Chapter 2. Soil Ic had soil properties similar to Soil 1 and can be compared to SCEB 4. Soil Ic (*Walker, 2004*) had a dry flexural strength of 1.37 MPa (198.7 psi) and can be compared to SCEB 4 with a dry flexural strength of 0.93 MPa (134.9 psi). Soil Ic had a dry flexural strength 38% greater than SCEB 4.

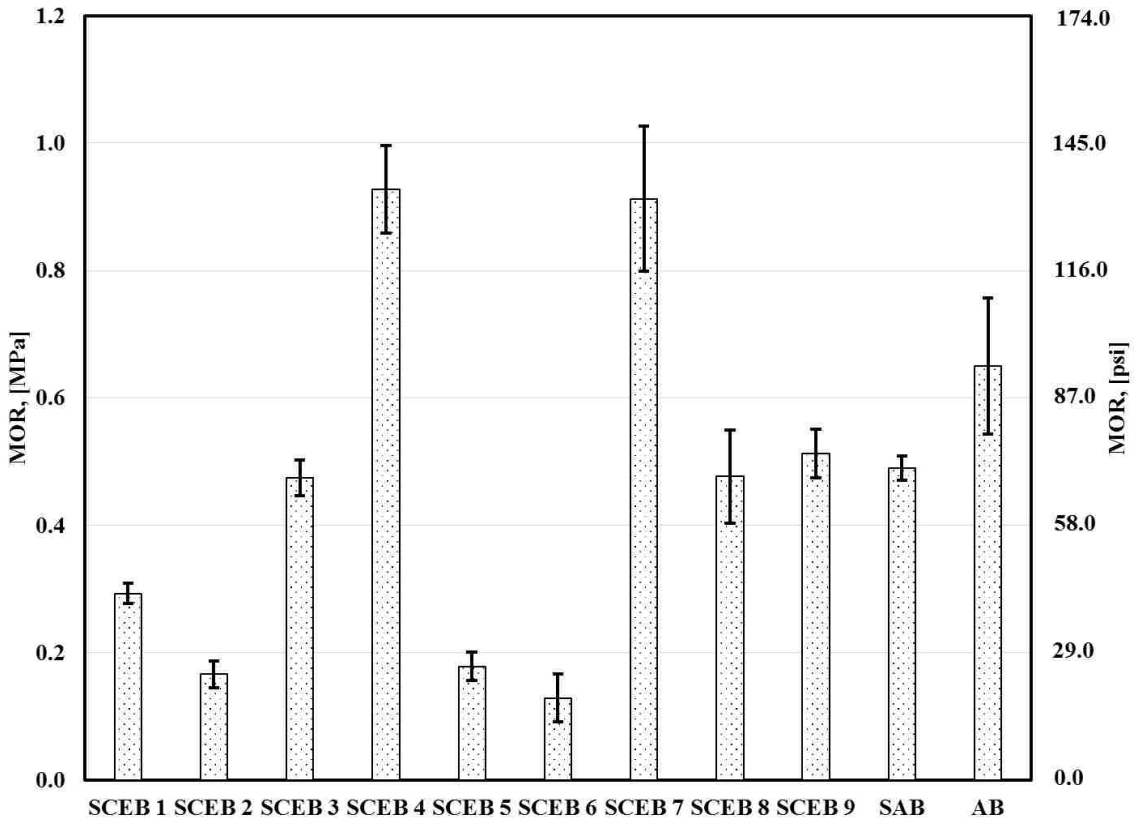

Figure 4. 22. Dry modulus of rupture results plotted.

The saturated modulus of rupture was determined for SCEB and Adobe blocks. Five specimens of each SCEBs and adobe blocks were tested and the average saturated flexural strength was calculated for each block. The saturated flexural strength was compared with the New Mexico Earthen Building Materials Code, Section J of 14.7.4.23 minimum saturated flexural strength of 0.35 MPa (50 psi) (*NMAC, 2009*). The results are listed in Table 4.35. SCEB 4 and 7 meet the minimum saturated compressive strength requirement according to the NM Earthen Building Materials Code and are highlighted in Table 4.35.

Table 4. 35. Saturated Modulus of Rupture results and coefficient of variation.

Specimen ID	Average MOR, MPa [psi]	COV (%)
SCEB 1	-	-
SCEB 2	-	-
SCEB 3	-	-
SCEB 4	0.43 [63]	8
SCEB 5	-	-
SCEB 6	-	-
SCEB 7	0.75 [109]	11
SCEB 8	0.23 [33]	52
SCEB 9	0.33 [48]	50
SAB	0.41 [60]	8
AB	-	-

SCEB 1, 2, 3, 5, 6, and AB did not withstand the 24 hour saturation test. Therefore, these blocks were not able to be tested for the saturated flexural strength. The results are plotted in Figure 4.23. SCEB 7 had the highest measured saturated compressive strength of 0.75 MPa (108.8 psi) which is 2.1 times greater than the NM Earthen Building Materials Code minimum strength of 0.35 MPa (50 psi). Also, SCEB 4 and 7 had a higher saturated compressive strength than commercial stabilized adobe blocks (SAB). SCEB 7 had a saturated flexural strength 59% greater than SAB. SCEB 4 had a saturated flexural strength 54% lower than SCEB 7.

The results for the saturated flexural strength of SCEB and adobe blocks are compared to published mechanical strength results of earthen materials using data summarized in Table 2.1 of Chapter 2. Soil RSI and NS1 had soil properties similar to Soil 2 and each were stabilized with 8% Portland cement. Therefore, Soil RS1 and NS1 can be compared to SCEB 7. Soil RS1 (*Reddy et al. 2007*) had a saturated flexural strength of 1.21 MPa (175.5 psi) and Soil NS1 (*Reddy et al. 2007*) had a saturated flexural strength of 0.95 MPa (137.8 psi). Soil RS1 had a saturated flexural strength 47% greater than SCEB 7and Soil NS1 had a saturated flexural strength 24% greater than SCEB 7.

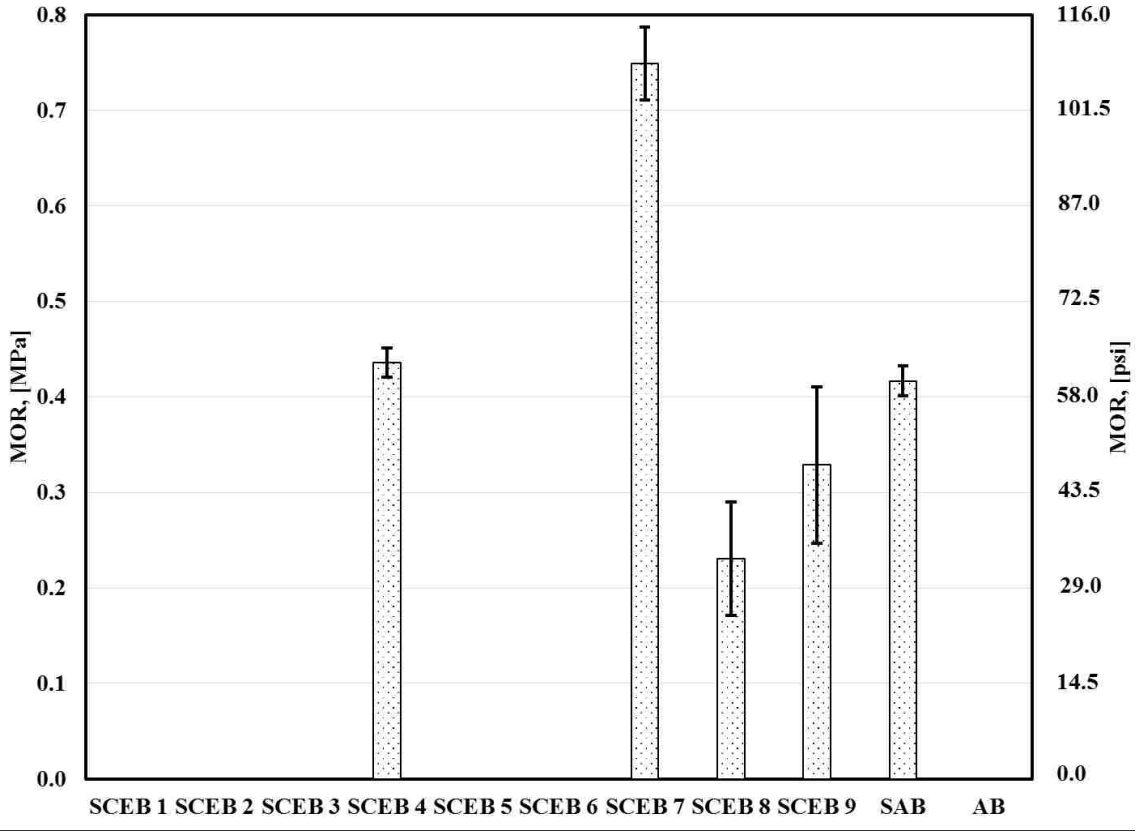

Figure 4. 23. Saturated modulus of rupture results plotted.

4.3.5 Absorption

A necessary material property is to measure the amount of water absorption over 24 hours. Five specimens of each SCEBs and adobe blocks were tested and the average percent water absorption was calculated for each block. The results are listed in Table 4.36. The three SCEBs that endured the absorption test are SCEB 4, 7, and 9 and are highlighted in Table 4.36.

Table 4. 36. Absorption results and coefficient of variation.

Specimen ID	Average Absorption, %	COV, %
SCEB 1	-	-
SCEB 2	-	-
SCEB 3	-	-
SCEB 4	9.4	29
SCEB 5	-	-
SCEB 6	-	-
SCEB 7	8.5	27
SCEB 8	-	-
SCEB 9	5.7	108
SAB	1.5	12
AB	-	-

SCEB 1, 2, 3, 5, 6, 8, and AB did not withstand the 24 hour saturation test. The results are plotted in Figure 4.24. SCEB 9 had the lowest measured percentage water absorption of 5.7%. Also, SCEB 4 and 7 measure a water absorption of 9.4% and 8.5%, respectively. SCEB 9 had an amount of water absorption 3.8 times greater than SAB. SCEB 7 had an amount of water absorption 5.7 times greater than SAB and SCEB 4 had an amount of water absorption 6.3 times greater than SAB.

The results for the amount of water absorption of SCEBs and adobe blocks are compared to published mechanical strength results of earthen materials using data summarized in Table 2.1 of Chapter 2. Soil B3 had soil properties similar to Soil 1 and

was stabilized with 8% Portland cement and 3% lime which can be compared to SCEB 4. Soil B3 (*Bharath et al. 2014*) had an amount of water absorption of 12.35% which can be compared to SCEB 4 which had a water absorption of 9.4%. Soil RSI and NS1 have soil properties similar to Soil 2 and each were stabilized with 8% Portland cement. Therefore, Soil RS1 and NS1 can be compared to SCEB 7 and 9. Soil RS1 (*Reddy et al. 2007*) had a percentage water absorption of 12.02% and Soil NS1 (*Reddy et al. 2007*) had a percentage water absorption of 14.97%. All SCEBs obtained an amount of water absorption less than the comparable block in the literature.

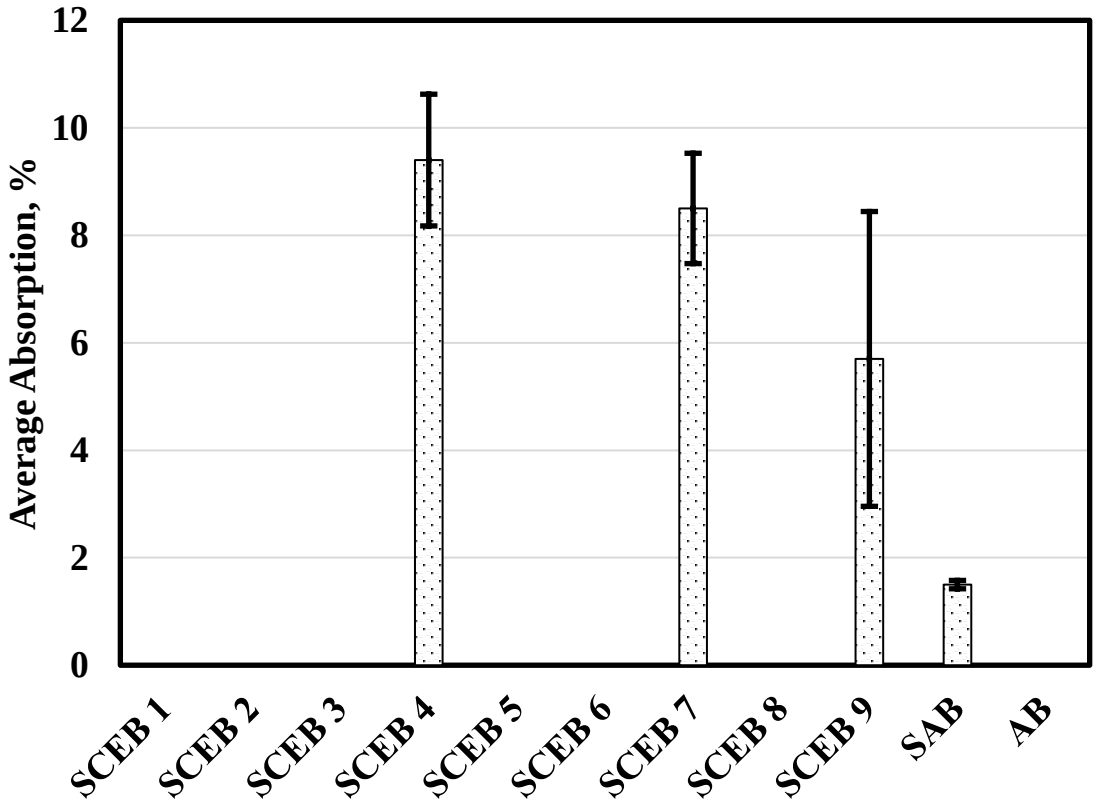

Figure 4. 24. Absoprtion results plotted.

4.3.6 Initial Rate of Absorption (IRA)

The initial rate of water (IRA) absorption is the gain in weight of a specimen corrected to basis of 193.55 cm^2 and was measured for SCEBs and adobe blocks. Five specimens of each SCEBs and adobe blocks were tested and the IRA was calculated for each block. The results are listed in Table 4.37. The three SCEBs that had the lowest measured IRA are SCEB 3, 4, and 7 and are highlighted in Table 4.37.

Table 4. 37. Initial rate of absoprtion results and coefficient of variation.

Specimen ID	Average IRA, g/min/193.55 cm^2 [g/min/30 in^2]	COV, %
SCEB 1	-	-
SCEB 2	-	-
SCEB 3	36.1 [36.1]	137
SCEB 4	44.7 [44.7]	61
SCEB 5	96.2 [96.2]	13
SCEB 6	94.6 [94.6]	14
SCEB 7	41.1 [41.1]	13
SCEB 8	66.3 [66.3]	17
SCEB 9	56.6 [56.6]	11
SAB	4.6 [4.6]	32
AB	-	-

SCEB 1, 2, and AB did not withstand the IRA testing. The results are plotted in Figure 4.25. SCEB 3 had the lowest IRA of 36.1 g/min/193.55 cm^2. Also, SCEB 4 and 7 measure a low IRA of 44.7 g/min/193.55 cm^2 and 41.1 g/min/193.55 cm^2, respectively. All SCEBs measured a higher IRA than SAB which had an IRA of 4.6 g/min/193.55 cm^2. SCEB 3 had an IRA 7.8 times greater than SAB. SCEB 4 had an IRA 9.7 times greater than SAB and SCEB 7 had an IRA 8.9 times greater than SAB.

The results for the amount of initial rate of water absorption of SCEB and adobe blocks are compared to published mechanical strength results of earthen materials using data summarized in Table 2.1 of Chapter 2. Soil B3 had soil properties similar to Soil 1

and was stabilized with 8% Portland cement and 3% lime which can be compared to SCEB 3 and 4. Soil B3 (*Bharath et al. 2014*) had an IRA of 14.8 g/min/193.55 cm^2 which can be compared to SCEB 3 and 4. SCEB 3 measured an IRA 2.4 times greater than Soil B3. SCEB 4 measured an IRA 3 times greater than Soil B3. Soil RSI and NS1 have soil properties similar to Soil 2 and each were stabilized with 8% Portland cement. Therefore, Soil RS1 and NS1 can be compared to SCEB 7. Soil RS1 (*Reddy et al. 2007*) had an IRA of 62.1 g/min/193.55 cm^2 and Soil NS1 (*Reddy et al. 2007*) had an IRA of 36.2 g/min/193.55 cm2. SCEB 7 obtained an IRA 34% lower than Soil RS1 and 20% higher than Soil NS1.

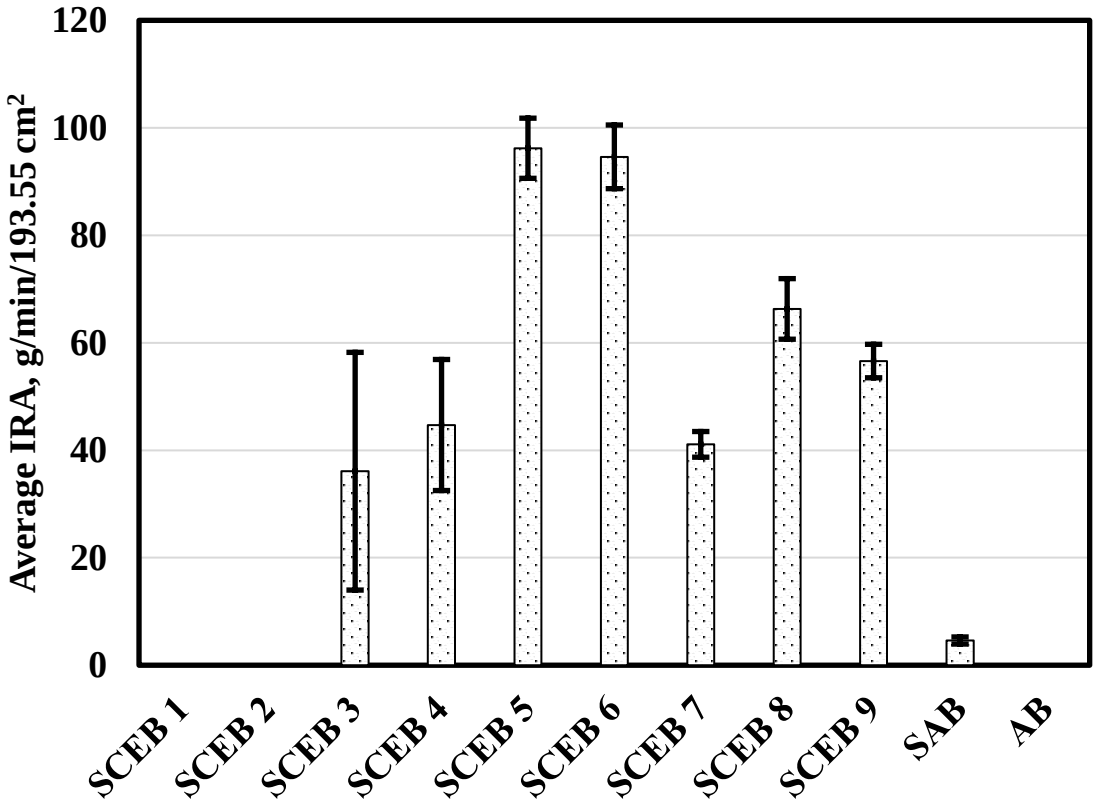

Figure 4. 25. Initial rate of absoprtion results plotted.

4.3.7 Sorptivity

SCEB 4, SCEB 5, SCEB 7, and SAB were tested for sorptivity. SCEB 4 and SCEB 7 were the only specimens to withstand the sample conditioning of vacuum saturation. The absorption, "I" was calculated and plotted against the square root of time. The results from sorptivity testing of SCEB 4 are plotted on Figure 4.27 and of SCEB 7 are plotted on Figure 4.28.

The initial rate of water absorption is defined as the slope of the line that is best fit to the plot from 1 minute to 6 hours as shown in Figure 4.26. If the data between 1 minute and 6 hours is not linear, then the initial rate of absorption cannot be determined. The secondary rate of water absorption is defined as the slope of the line that is best fit to "I" plotted against the square root of time of points from 1 day until 7 days as shown in Figure 4.25. Also if the data between 1 day and 7 days is not linear, then the secondary rate of absorption cannot be determined. Since the data for SCEB 4 and SCEB 7 were not linear, the initial rate of absorption and secondary rate of absorption could not be determined.

The results for the sorptivity testing of SCEBs and adobe blocks were not compared to the literature since there were no published results found for sorptivity testing of earthen materials.

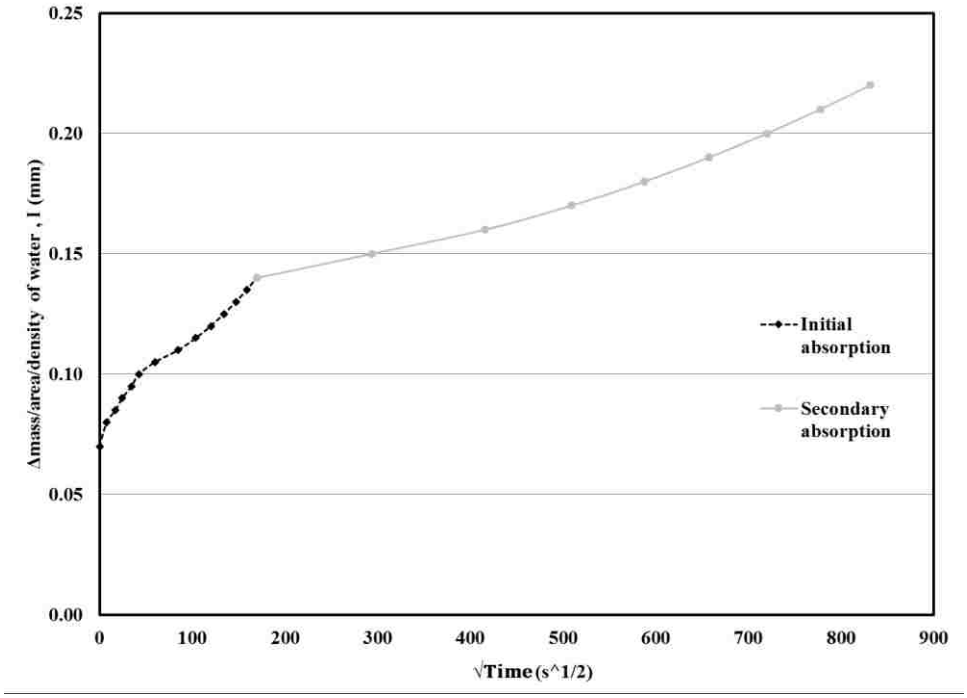

Figure 4. 26. Example Plot of the Typical Data in Sorptivity Testing.

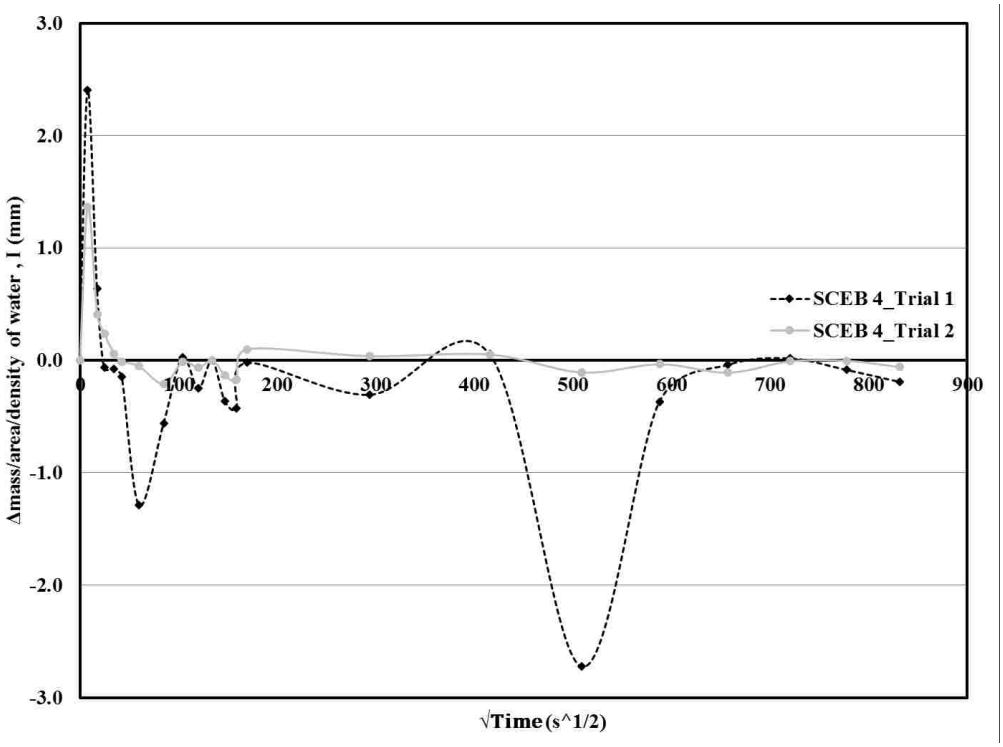

Figure 4. 27. Plot of SCEB 4 data in Soprtivity Testing.

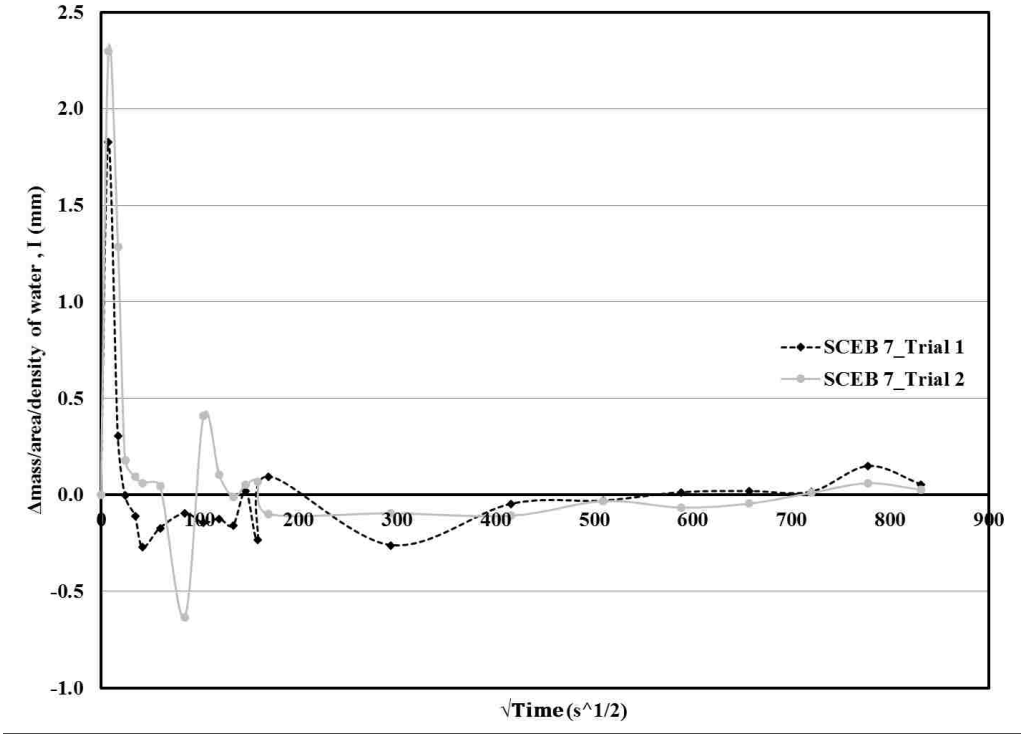

Figure 4. 28. Plot of SCEB 7 data in Soprtivity Testing.

4.3.8 Apparent block density

Density is a characteristic property. The apparent block density of a specimen is its mass divided by its volume. SCEB 1, 2, 3, 4, 5, 6, 7, and SAB and AB were tested to determine the apparent block density. The apparent block density test results were provided by Conner Rusch and are shown in Table 4.38. The three SCEBs that had the highest measured apparent density are SCEB 4, 5, and 6 and are highlighted in Table 4.38.

Table 4. 38. Apparent Block Density results and coefficeint of variation.

Specimen ID	Average Apparent block density, kg/m^3 [lb/ft^3]	COV, %
SCEB 1	2003 [125.0]	3
SCEB 2	1987 [124.1]	3
SCEB 3	1976 [123.3]	1
SCEB 4	2168 [135.3]	2
SCEB 5	2277 [142.1]	4
SCEB 6	2124 [132.6]	2
SCEB 7	2063 [128.8]	1
SCEB 8	-	-
SCEB 9	-	-
SAB	1851 [115.5]	1
AB	1890 [118.0]	0

The results are plotted in Figure 4.29. The SCEBs with the highest apparent density were SCEB 4 with a density of 2168 kg/m^3 (135.3 lb/ft^3), SCEB 5 with a density of 2277 kg/m^3 (142.1 lb/ft^3), and SCEB 6 with a density of 2124 kg/m^3 (132.6 lb/ft^3). SCEB 5 had the highest apparent density and was compared with the adobe results. SAB had an apparent density of 1851 kg/m^3 (115.5 lb/ft^3) which was 20.6% lower than SCEB 5. AB had an apparent density of 1890 kg/m^3 (118.0 lb/ft^3) which was 18.6% lower than SCEB 5.

The results of apparent density for SCEB are compared to published results of earthen materials using data summarized in Table 2.1 in Chapter 2. Soil Ia, Ib, and Ic (*Walker, 2004*) have soil properties similar to Soil 1and can be compared to SCEB 4. SCEB 4 obtained a dry density 15.8% higher than Soil Ia (*Walker, 2004*), 9.1% higher than Soil Ib (*Walker, 2004*), and 11.5% higher than Soil Ic (*Walker, 2004*). Soil RS1, Soil NS1, Soil NS2 (*Reddy et al. 2007*), Soil OMC (*Lawson et al. 2011*), and Soil C (*Bei & Papayianni, 2003*) have soil properties similar to Soil 2 and can be compared to SCEB 7. SCEB 7 obtained a dry density 11.7% higher than Soil RS1 (*Reddy et al. 2007*), 12.8% higher than Soil NS1 (*Reddy et al. 2007*), 14.4% higher than Soil NS2 (*Reddy et al. 2007*),

9.7% higher than Soil OMC (*Lawson et al. 2011*), and 1.8% lower than Soil C (*Bei & Papayianni, 2003*).

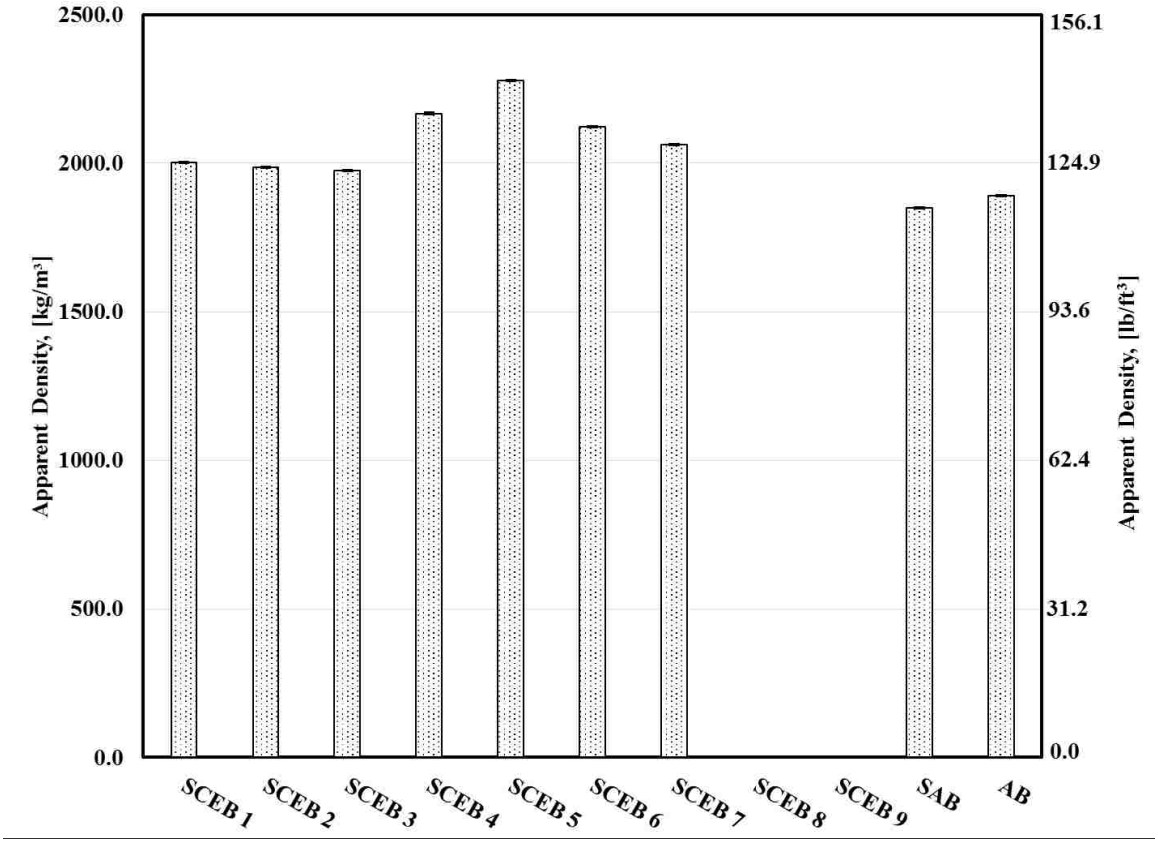

Figure 4. 29. Apparent block density results plotted.

4.4 Prism Testing

In order to understand the interaction of the block and mortar joint, prisms were constructed and tested for prism compression, creep, bond strength, and shear strength. In this research, prisms are composed of 2 or 3 SCEBs or Adobe blocks and 1.27 cm (0.5 in.) mortar joint(s). Type S mortar was used for the mortar join in prism construction.

4.4.1 Mortar Flowability and Compression

When prisms were constructed, the type S mortar was mixed. The workability or flow of the mortar was calculated and the temperature of the mortar was measured. The flowability and temperature results are listed in Table 4.36 for each date of mortar mixing. The flowability of the type S mortar mixes varied from 76% to 101%, which has a coefficient of variation of 37%. It was found in the literature that the flowability of masonry prisms were maintained at 100% (*Venkatarama Reddy and Uday Vyas, 2008*).

Table 4. 39. Type S Mortar Flowability and Compressive Strength results.

		ASTM C109		**ASTM C1437**	
Mortar Type	**Date Mixed**	**Average 7 day strength, MPa [psi]**	**Average 28 day strength, MPa [psi]**	**Flowability (%)**	**Temp (°F)**
S	3/17/16	20.1 [2917]	21.6 [3142]	76%	-
S	3/22/16	14.9 [2163]	19.0 [2758]	77%	-
S	3/28/16	26.9 [3907]	33.2 [4813]	101%	-
S	4/4/16	22.1 [3209]	23.3 [3376]	95%	62
S	4/13/16	23.5 [3403]	26.3 [3813]	77%	68
S	4/13/16	20.6 [2988]	26.9 [3905]	81%	68
S	4/13/16	22.5 [3261]	26.2 [3797]	80%	65
Average		20.4 [2957]	24.2 [3506]	84%	66
COV (%)		17%	18%	37%	54%

For each mortar batch, the compressive strength of the type S mortar was determined for the 7 day strength and 28 day strength. While the prisms were being constructed, mortar used for prism construction was obtained to make six - 50 mm (2 in.) mortar cubes for each mortar batch. Three cubes were used for 7 day compressive strength testing and the remaining three cubes were used for 28 day compressive strength testing. The average 7 day compressive strength and 28 day compressive strength were calculated and the results for mortar compressive strength testing are listed in Table 4.39 for each mortar batch. The results are plotted in Figure 4.30 to demonstrate the range in values of compressive strength of each mortar batch and plotted in Figure 4.31 to show

the compressive strength results and coefficient of variation for each mortar batch. The coefficient of variation for the 7 mortar batches for 7 day compressive strength was 17% and for the 28 day compressive strength was 18%.

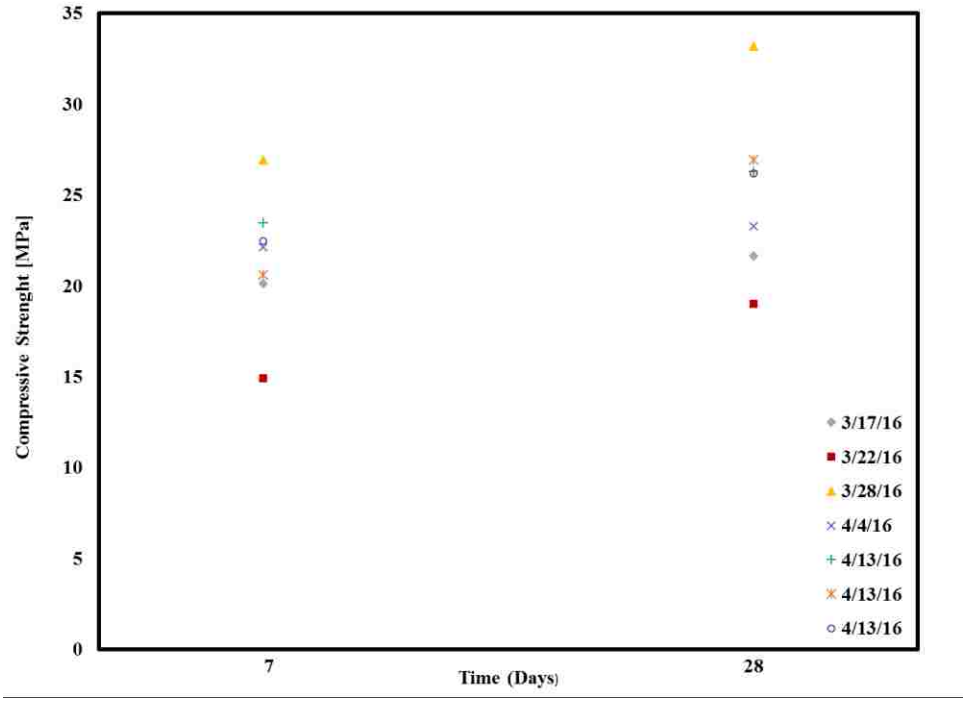

Figure 4. 30. 7 day and 28 day Mortar compressive strength plot of results.

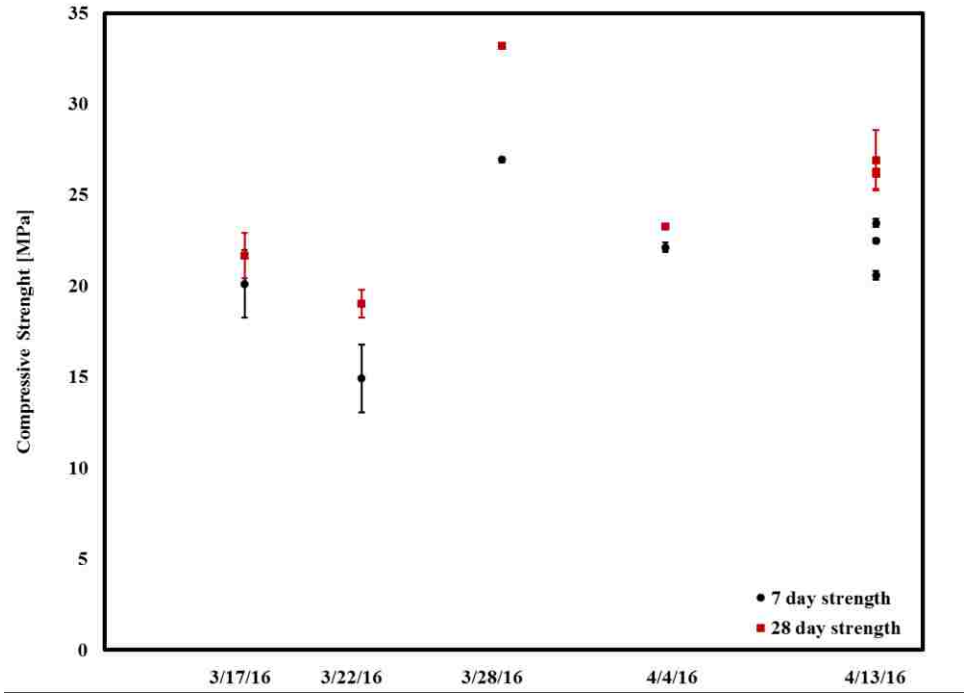

Figure 4. 31. 7 day and 28 day Mortar compressive strength plot of results and coefficient of variation.

The type S mortar was used for prism construction. There were 7 mortar batches to make prisms for compression testing, bond wrench testing, bond shear testing, creep and wall testing. The mortar batches used for constructing prisms and assemblies are listed in Table 4.40.

Table 4. 40. Type S mortar batch used for construction of respective prism and assemblies testing.

Mortar Date Mixed	Prism Compression	Prism Bond Wrench	Prism Bond Shear	Prism Creep	Wall
3/17/16	(5) SAB, (5) SCEB 7			(2) SCEB 7	
3/22/16	(5) AB, (5) SCEB 5, (5) SCEB 4				
3/28/16			(5) SCEB 7		(4) SCEB 7 Wallets
4/4/16	(1) SCEB 5	(1) SAB	(5) SAB		
4/13/16	(1) SCEB 5	(4) SAB			
4/13/16		(5) SAB, (7) SCEB 7			
4/13/16	(1) SCEB 5	(1) SAB, (3) SCEB 7			

4.4.2 Prism Compression

A prism constructed with two SCEBs or adobe blocks and type S mortar was tested to determine the prism compressive strength. Five specimens of each SCEBs and adobe prisms were tested and the average was calculated. The results for average compressive strength of SCEB 4, 5, 7, SAB, and AB are listed in Table 4.41. The two SCEBs with the highest average compressive strength are SCEB 4 and 7 and are highlighted in Table 4.41.

Table 4. 41. Prism compressive strength test results and coefficient of variation.

Prism Specimen ID	**Average Compressive Strength, MPa [psi]**	**COV (%)**
SCEB 4	4.8 [702]	8%
SCEB 5	1.5 [219]	10%
SCEB 7	4.2 [602]	22%
SAB	1.0 [141]	15%
AB	1.2 [181]	33%

The results are plotted in Figure 4.32. SCEB 4 obtained the maximum average compressive strength with a value of 4.8 MPa (696.2 psi). SCEB 7 measured an average prism compressive strength of 4.2 MPa (609.2 psi) which is 13% lower than SCEB 4. The SCEBS are compared to the stabilized adobe block (SAB) which obtained an average compressive strength value of 1.0 MPa (145.0 psi). The average compressive strength value of SCEB 4 was 4.8 times higher than SAB and SCEB 7 was 4.2 times greater than SAB.

The results for the prism compressive strength testing of SCEBs and adobe prisms were not compared to the literature since there were no published results found for prism compressive strength testing of earthen materials.

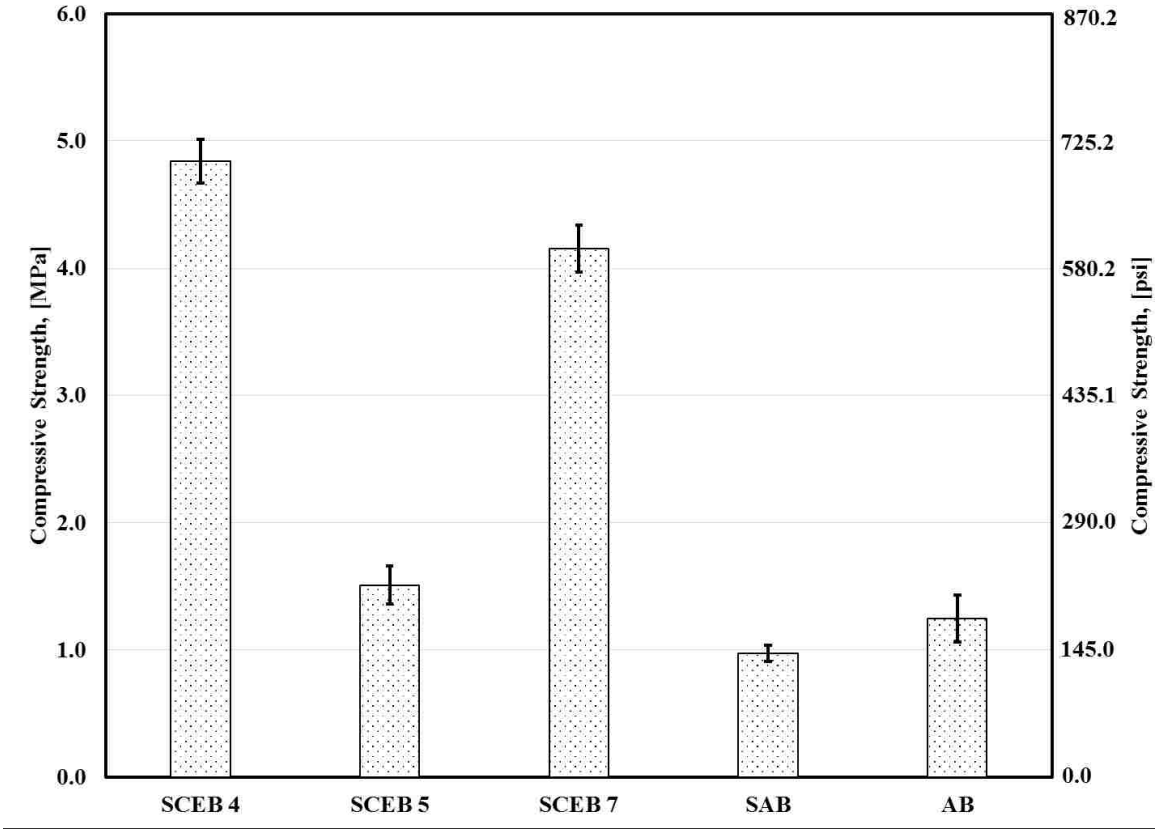

Figure 4. 32. Prism compressive strength test results plotted.

4.4.3 Bond Strength

Masonry flexural bond strength was determined for SCEB 7 and SAB. The prisms were constructed of 3 blocks and a type S mortar. Five specimens of each SCEBs and adobe prisms were tested. The average bond flexural strength was calculated for SCEB 7 and SAB and the results are listed in Table 4.42 and are plotted in Figure 4.33. SCEB 7 obtained a bond flexural strength 43% lower than SAB, which obtained a value of 76 kPa (7.1 psi). The higher flexural bond strength of adobe block, SAB can be attributed to the higher surface roughness of the SAB block improving the bond between the block and mortar.

Table 4. 42. Bond Flexural strength results and coefficeint of variation.

Prism Specimen ID	Average Bond Strength, kPa [psi]	COV (%)
SCEB 7	49.0 [7.1]	60
SAB	76.0 [11.0]	38

The results for the bond strength of SCEBs are comparable to published bond strength results of earthen materials using data summarized in Table 2.2 of Chapter 2. Soil IV (*Walker, 1999*) had soil properties similar to Soil 2 and the block was stabilized with 10% Portland cement. Therefore, Soil IV was compared to SCEB 7. Soil IV (*Walker, 1999*) had a bond strength of 50 kPa (7.3 psi) which is 2% higher than the bond strength for SCEB 7. A clay fired brick masonry with a similar mortar mix obtained a bond strength of 460 kPa (66.7 psi) (*Reda and Shrive, 2000*). SCEB 7 obtained a bond strength 9 times less than clay fired brick masonry.

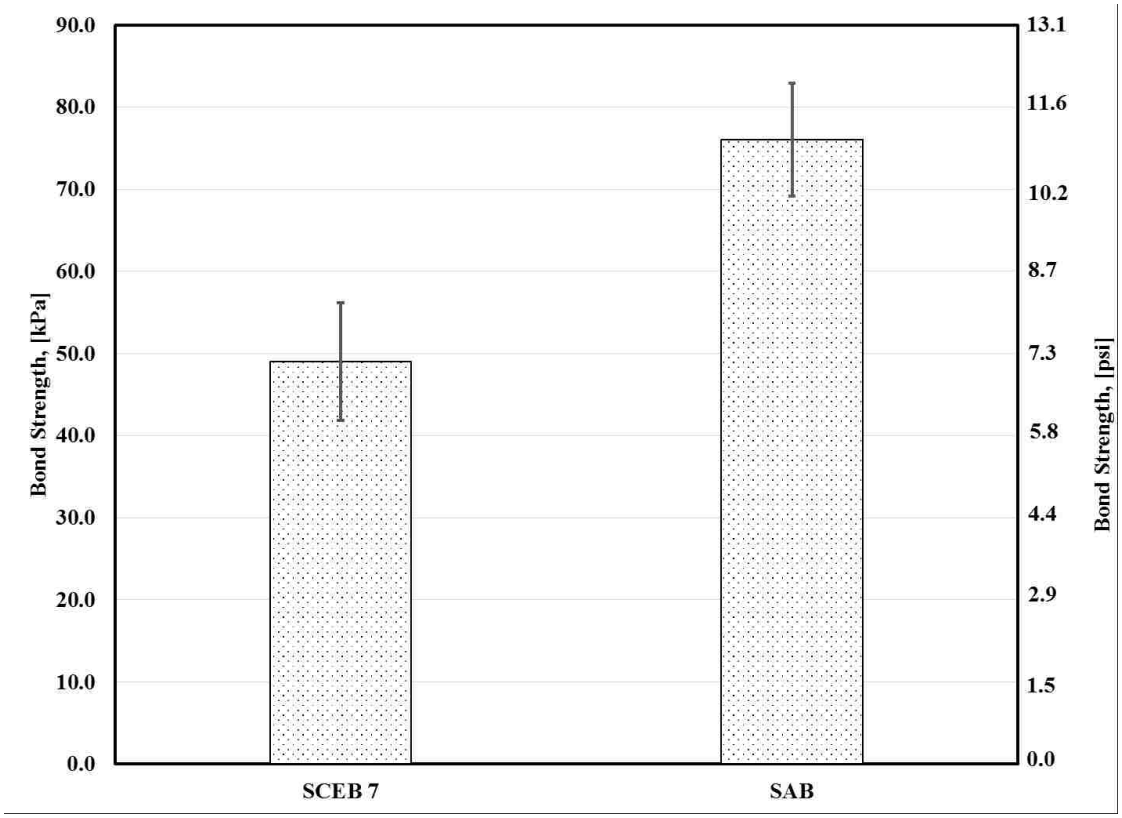

Figure 4. 33. Prism bond strength test results plotted.

4.4.4 Bond Shear Testing

The shear strength of SCEB prisms was determined for SCEB 7 and SAB. The prisms were constructed of 3 blocks and a type S mortar. Five specimens of each SCEBs and adobe prisms were tested. The average bond shear strength was calculated for SCEB 7 and SAB and the results are listed in Table 4.43 and plotted on Figure 4.34. SCEB 7 obtained a bond shear strength of 257.8 kPa (37.4 psi) which is 8% higher than the shear strength of SAB with a value of 242.4 kPa (35.2 psi).

Table 4. 43. Shear Bond Strength results and coefficeint of variation.

Prism Specimen ID	Average Pre-Compressive Strength, MPa [psi]	COV (%)	Average Shear Strength, kPa [psi]	COV (%)
SCEB 7	0.1 [10.1]	2.33	257.8 [37.4]	38
SAB	0.1 [9.8]	1.92	242.4 [35.2]	23

The results for the bond shear strength of SCEBs and adobe blocks are compared to published mechanical strength results of earthen materials using data summarized in Table 2.2 of Chapter 2. Soil RSI and NS1 have soil properties similar to Soil 2 and each were stabilized with 8% Portland cement. Therefore, Soil RS1 and NS1 can be compared to SCEB 7. Soil RS1 (Reddy et al. 2007) had a bond shear strength of 0.04 MPa (5.8 psi) and Soil NS1 (Reddy et al. 2007) had a shear bond strength of 0.13 MPa (18.9 psi). SCEB 7 obtained a shear bond strength 147% higher than Soil RS1 and 67% higher than Soil NS1.

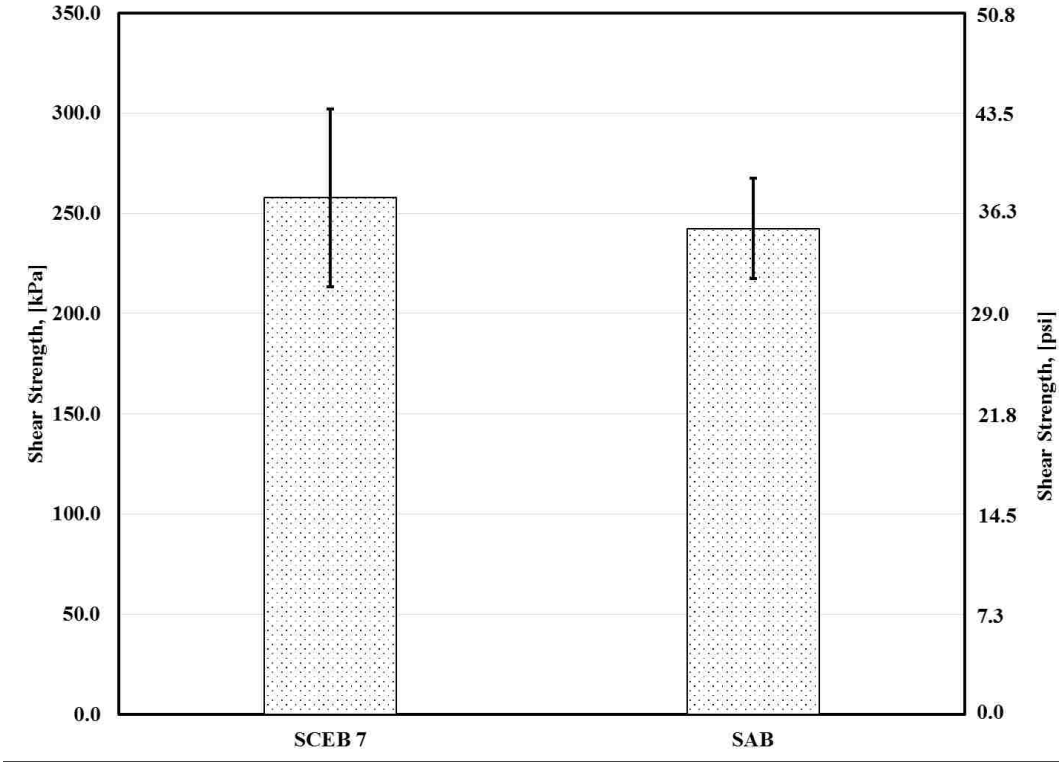

Figure 4. 34. Prism bond shear strength test results plotted.

4.4.5 Creep Testing

Two prisms each comprised of two SCEB 7 blocks with a Type S mortar joint were tested to determine the effect of creep on a SCEB prism. The prisms were loaded to a constant load of 13.3 kN (3000 lbs), which is 20% of its compressive strength capacity. The displacement of the prism over 56 days were measured using three Linear Voltage Displacement Transducers (LVDTs) on each frame. On Frame 1, LVDT 1-A measured the displacement of the bottom block and mortar joint, LVDT 2-A measured the displacement of the bottom block, and LVDT 3-A measured the displacement of the top block. The displacements measured for Frame 1 were plotted on Figure 4.35. On Frame 2, LVDT 1-B measured the displacement of the bottom block and mortar joint, LVDT 2-B measured the displacement of the bottom block, and LVDT 3-B measured the displacement

of the top block. The displacements measured for Frame 2 were plotted on Figure 4.36. The vertical elastic strain was calculated for LVDT 2-A, LVDT 3-A, and LVDT 2-B, and LVDT 3-B and are plotted on Figure 4.37.

As shown in Figure 4.35 and Figure 4.36, the difference in displacement for SCEB 7 top block and bottom block was miniscule. In addition, the displacement of the bottom block and mortar joint of the prism was very similar to the displacement of the bottom block. Therefore, it was determined that there was no creep behavior exhibited by the mortar. This may have been due to the stiffer material properties than the compressed earth block.

The creep coefficient and the creep compliance were the desired parameters from the collected data. In order to determine the creep compliance, the creep strain had to be calculated. The creep strain from SCEB 7 top block and bottom block of Frame 1 are plotted on Figure 4.38. The creep compliance for SCEB top block and bottom block of Frame 1 are plotted on Figure 4.39. The creep coefficients for all SCEBs on Frame 1 and Frame 2 are listed in Table 4.44.

The results for creep coefficient for SCEB 7 blocks are compared to published creep coefficient results of clay fired masonry. In an article published by Shrive et al. (*1997*), the clay brick masonry creep coefficient ranged between 0.7 and 3.33 for dry conditions. The average creep coefficient for SCEB 7 was 2.21 which had a value between 104% higher and 40% lower than the clay brick masonry. It was also found in an article published by Kim et al. (*2012*) that the creep coefficient used for clay brick masonry ranged from 2 to 4. The average creep coefficient for SCEB 7 had a value between 10% higher and 58% lower than the clay brick masonry.

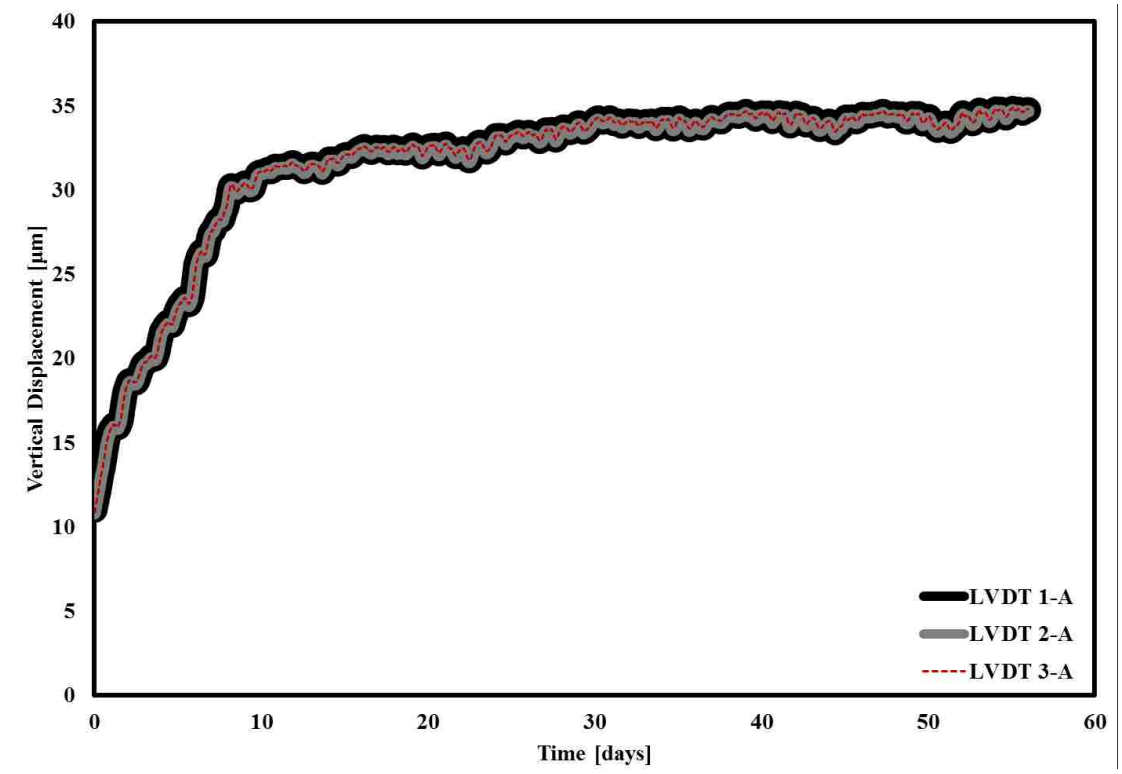

Figure 4. 35. Creep Tests on Frame 1- Displacement.

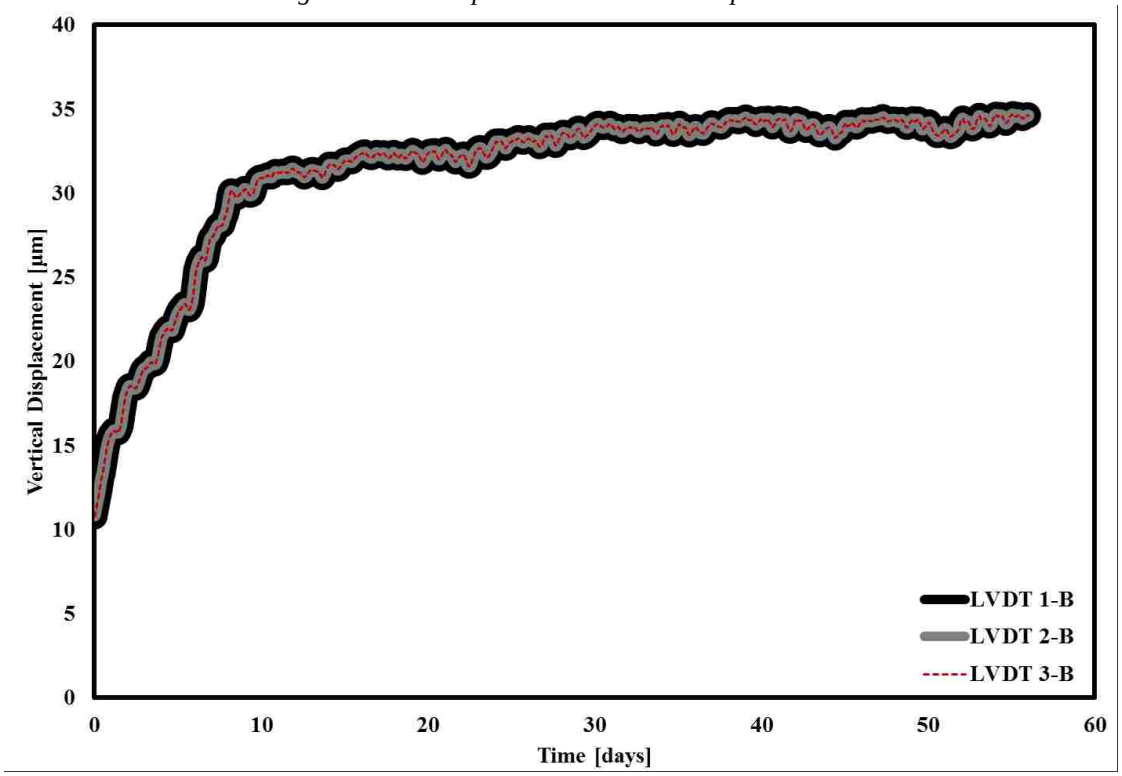

Figure 4. 36. Creep Tests on Frame 2- Displacement.

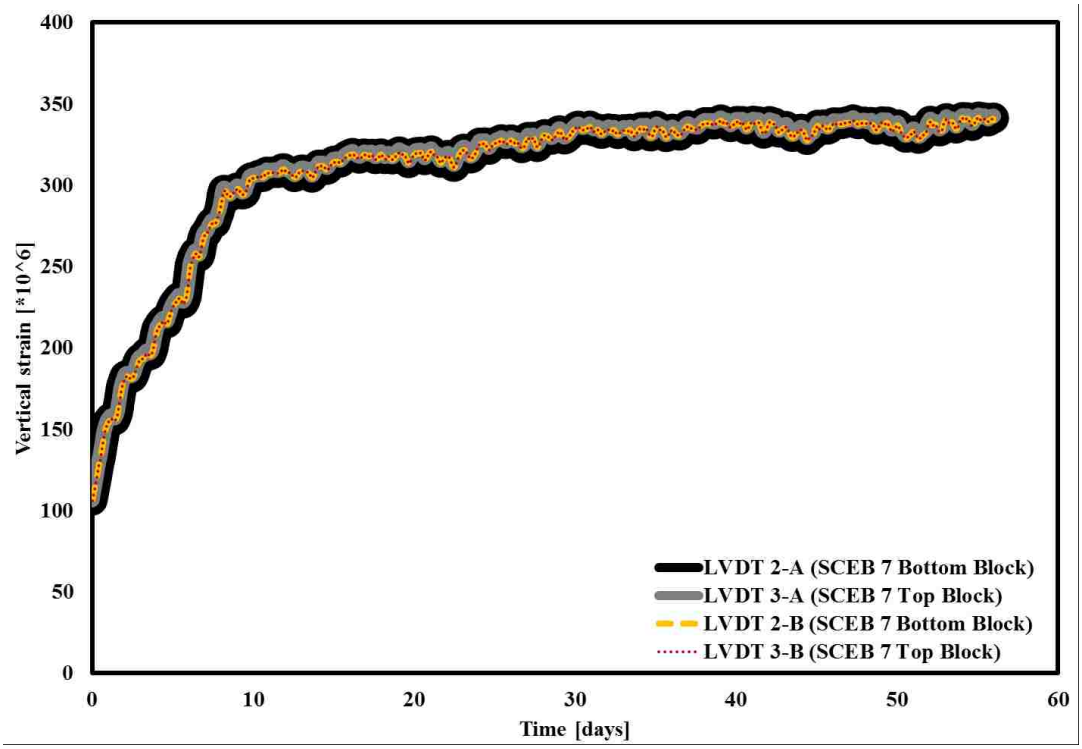

Figure 4. 37.Vertical Elastic Strain for SCEB 7.

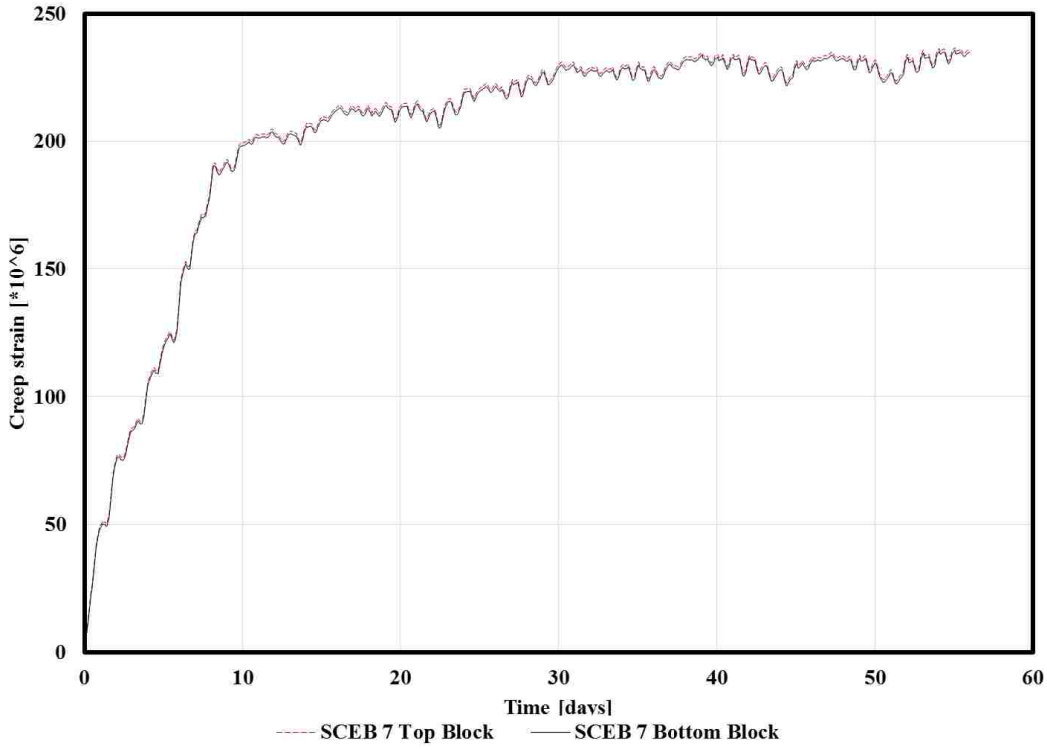

Figure 4. 38. Creep Strain

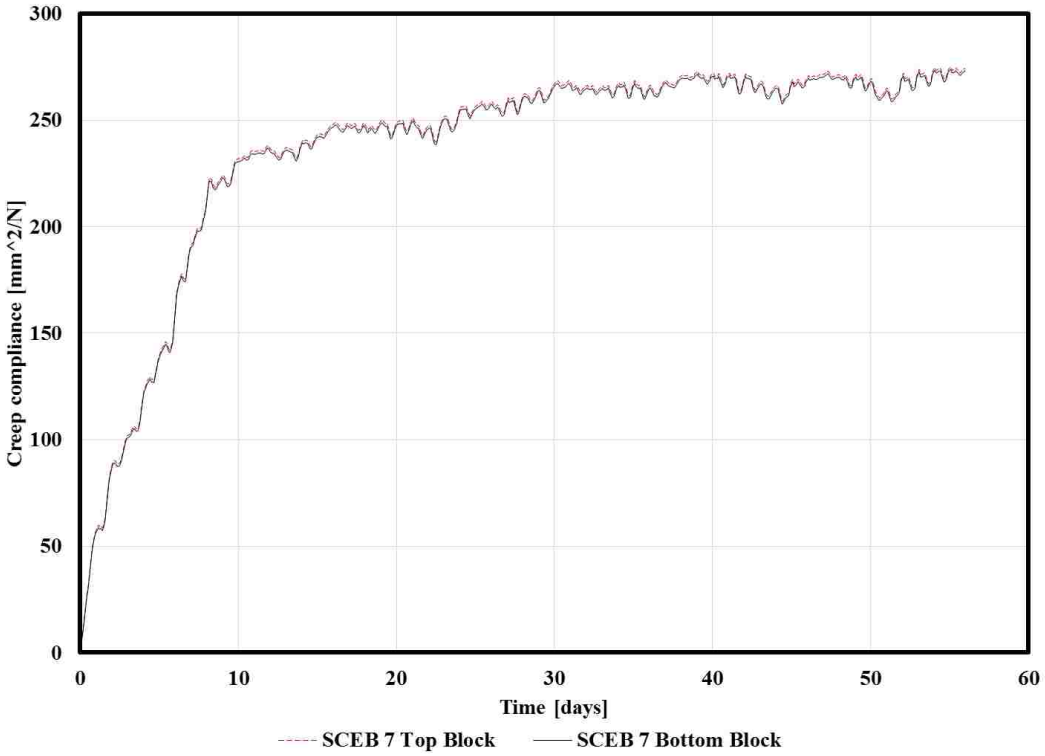

Figure 4. 39. Creep Compliance of Frame 1.

Table 4. 44. Creep Coefficeint

Specimen	Φ
SCEB 7 Frame 1 – Top Block	2.22
SCEB 7 Frame 1 – Bottom Block	2.21
SCEB 7 Frame 2 – Top Block	2.23
SCEB 7 Frame 2 - Bottom Block	2.19
SCEB 7 Average Creep Coefficient	2.21

4.5 Wall Testing

The shear strength of the masonry assemblage was determined by loading the walls in compression along the diagonal. Four approximately 570 x 570 x 127 mm^3 (22 x 22 x 5 $in.^3$) SCEB wall panels made of the SCEB 7 were tested under diagonal compression. SCEB 7 Wall 2 was not a successful test. The diagonal compression testing results of SCEB 7 Wall 1, 3, and 4 are listed in Table 4.45. SCEB 7 Wall 4 obtained the highest shear stress of 0.15 MPa as highlighted in Table 4.45. The vertical and horizontal

displacements were measured on SCEB 7 Wall 4 in order to calculate the shearing strain and determine the modulus of rigidity. The values are listed in Table 4.46. The force versus displacement plots of SCEB 7 Wall 1, 3, and 4 are shown in Figure 4.40. Figure 4.41 shows the crack patterns on both faced of the SCEB 7 Wall 1, 3, and 4 under diagonal compression. It can be observed that most of the cracks are mortar joint cracks confirming the ability of SCEBs to resist load. The cracking pattern of SCEB walls is very similar to that observed in clay fired masonry brickwork walls.

Table 4. 45. SCEB 7 Wall panel resuls of diagonal compression testing.

Wall Specimen	**Max Force, kN [kip]**	**Max Displacement, mm [in]**	**Shear Stress, Ss, MPa [psi]**
1	14.1 [3.2]	9.09 [0.36]	0.14 [20.8]
3	12.4 [2.8]	10.58 [0.42]	0.06 [8.3]
4	14.7 [3.3]	6.55 [0.26]	0.15 [21.3]
Average	13.7 [3.1]	8.7 [0.3]	0.12 [16.8]
COV	8.7%	23.3%	42.2%

Table 4. 46.SCEB 7 Wall 4 results including shear strain and modulus of rigidity.

Parameter	**SCEB 7 (Wall 4)**
ΔV, mm [in]	3.1 [0.13]
ΔH, mm [in]	5.1 [0.20]
Shear Strain, γ, mm/mm	0.03
Modulus of Rigidity, G, MPa [psi]	4.8 [702.4]

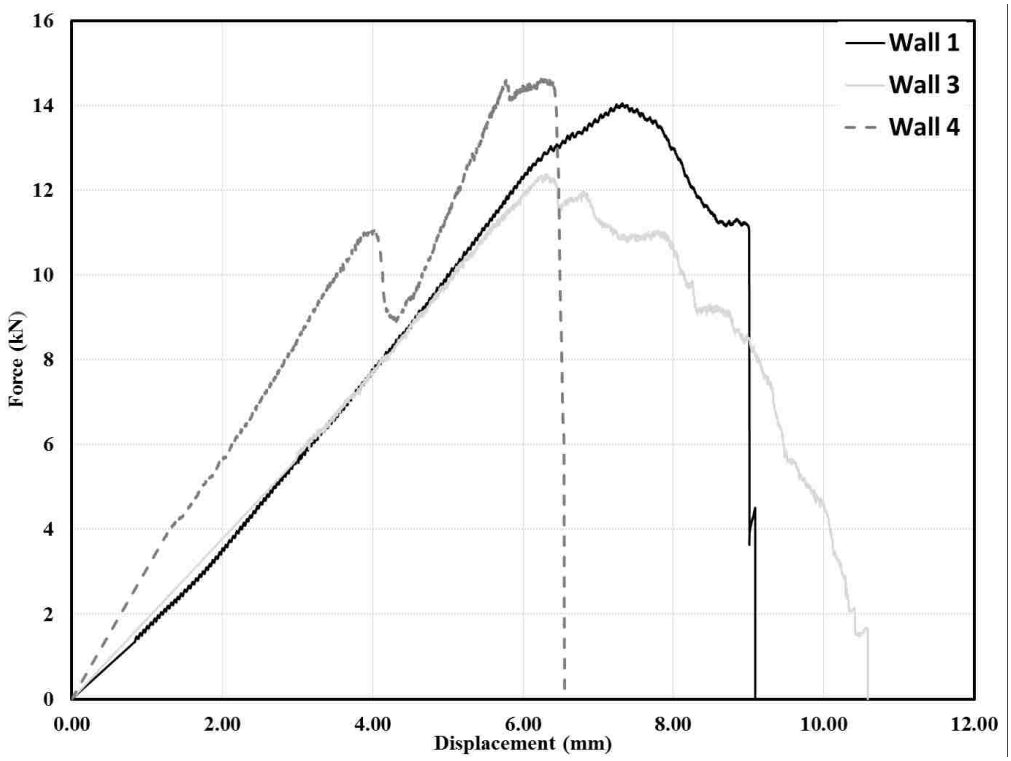

Figure 4. 40. SCEB 7 Wall 1, 2, 3 diagonal compression test results plotted, Force vs. Displacement.

The results for the diagonal compression tests of SCEB wallets are compared to published diagonal compression test results of earthen materials using data from Chapter 2. Miccoli et al. *(2014)* performed diagonal compression tests on a 500 x 500 x 110 mm^3 wall (20 x 20 x 4 $in.^3$). The shear strength of: wetted earth block masonry was 0.34 MPa (49.3 psi), earth block masonry was 0.09 MPa (13.1 psi), rammed earth was 0.71 MPa (102.9 psi), and cob was 0.50 MPa (. SCEB 7 Wall 4 obtained a shear strength 78% lower than wetted earth block masonry and 50% higher than earth block masonry. Rammed earth obtained a shear strength 4.7 times higher than SCEB 7 Wall 4 and cob obtained a strength 3 times greater than SCEB 7 Wall 4. Varum et al. (*2007*) evaluated the shear strength of traditional adobe masonry walls. Thirteen wallets of dimensions, 170 x 170 x 100 mm^3 (

7 x 7 x 4 in.^{3}) obtained results that varied between 0.07 to 0.19 MPa (10.2 psi to 27.6 psi) (*Varum et al. 2007*). SCEB 7 Wall 4 obtained a shear strength between 73% higher and 24% lower than traditional adobe wallets. Silva et al. (*2013*) obtained the shear strength of three geopolmer stabilized rammed earth wallets of 550 x 550 x 200 mm^3 (22 x 22 x 8 in.^{3}). The shear strength obtained for GRSE_2.5 was 0.14 MPa (20.3 psi), GRSE_5.0 was 0.14 MPa (20.3 psi), and GRSE_7.5 was 0.18 MPa (26.1 psi) (*Silva et al. 2013*). SCEB 7 Wall 4 obtained a shear strength 7% higher than GRSE_2.5 and GRSE_5.0. While, GRSE_7.5 had a shear strength 18% higher than SCEB 7 Wall 4. The shear testing of SCEB wall assemblies confirms that walls built using SCEB blocks will have a satisfactory structural performance. The shear strength and ductility of SCEB are very comparable to those published in literature and are also comparable to structural masonry walls.

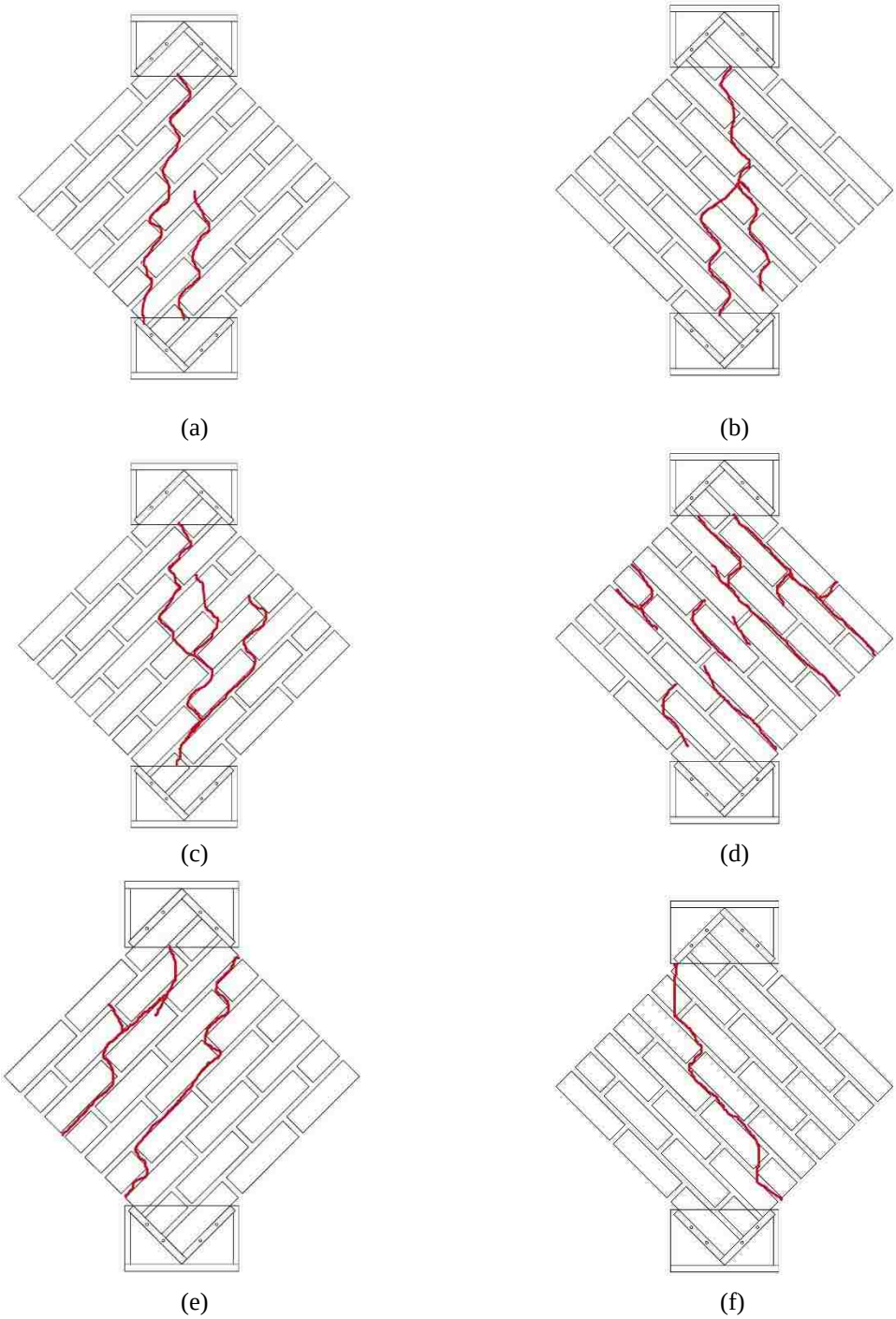

Figure 4. 41. SCEB 7 Wall specimens under diagonal compression. Crack patterns are marked in red lines (a) Wall # 1 front. (b) Wall # 1 back. (c) Wall #3 front. (d) Wall #3 back. (e) Wall #4 front. (f) Wall #4 back.

CHAPTER 5: CONCLUSIONS AND RECOMMENDATIONS

5.1 Conclusions

SCEBs can provide a sustainable building material that meets strength criteria from the New Mexico Earthen Building Materials Code. This investigation demonstrated that the SCEBs composed of native soils and stabilized with 10% Portland cement are suitable by the NM Earthen Building Materials Code for use in residential construction for the Jemez Pueblo in New Mexico. The optimum block for use in this investigation was specimen SCEB 7.

The three main objectives of this investigation were accomplished. The first objective aimed at understanding the effect of the clay to sand ratios on two locally sourced, yet suitable clay (ey) soils for the SCEBs on block compressive and flexural strength. Nine SCEB mix designs were tested to determine the mechanical properties of the block and the results were evaluated using the New Mexico Earthen Building Materials Code (NM-EBMC). Out of the nine SCEBs tested, two specimens satisfied the NM-EBMC requirements. These blocks were SCEB 4 and SCEB 7. Additionally, the mechanical properties of SCEB 7 indicated it as the optimum mix. It was evident that the particle size distribution and plasticity of the soils have significant effects on the SCEBs mechanical properties. The clay(ey) soil with more than 50% passing #200 sieve and obtaining a plasticity classification of CL or ML produced suitable soils for use in SCEB production. In addition, the swelling potential of the soil as defined by the expansion index (EI) indicated which soils would not expand greatly when exposed to water. It was determined that an EI less than 90 produced a sufficient soil for use in SCEBs. Lastly, there was also indication that mineralogy contributed an important role on the performance of SCEBs

than originally expected. The predominant clay mineral found in the two clay(ey) soils obtained from the sourced soils for SCEB production was Kaolinite. Kaolinite is a nonexpandable clay mineral, meaning they will only expand slightly in the presence of water. In determining the swelling potential of the clay(ey) soils, Clay 1 had a "very low" expansion index while Clay 2 had a "very high" expansion index. This means that there is a presence of another mineral in the Clay 2 soil which will expand when exposed to water.

The secondary objective was to compare the performance of SCEB to traditional commercially available Adobe bricks. To satisfy the second objective, this investigation showed that suitable SCEBs have higher compressive and flexural strengths than commercial stabilized adobe. The investigation also showed that SCEB 7 had a wet compressive strength twice that of the stabilized adobe brick (SAB) and a wet modulus of rupture five times that of SAB. SCEB 7 had an amount of water absorption 5.7 times greater than SAB and SCEB 7 had an initial rate of absorption (IRA) 8.9 times greater than SAB. Therefore, the saturated compressive and flexural strength of SCEB 7 was greater than SAB, but the amount of water absorption for SAB was lower than SCEB 7 because asphalt absorbs water at a slower rate than cement. The mechanical properties of SCEB compared well to results published in literature. SCEB 7 has a saturated compressive strength 26% higher than Earth Block determined by Walker (1999).. This demonstrated that the SCEBs constructed in this research project obtained results in the range of results for earthen materials published in the literature.

In order to fulfill the third objective (i.e. evaluation of the SCEB assemblies using Type S standard mortar), it was demonstrated that a prism made of SCEB 7 had similar material property values as compared to the literature. These values include: prism

compressive strength, shear bond strength, bond flexural strength and creep coefficient of SCEB prisms and the shear strength of SCEB wall panels. The average prism compressive strength value of SCEB 7 was 4.2 times greater than SAB. SCEB 7 obtained a bond flexural strength 46% lower than SAB. While results published in literature had similar results to SCEB 7, Soil IV had a bond flexural strength which was the equivalent value obtained for SCEB 7. SCEB 7 obtained a bond shear strength which was 8% higher than the shear strength of SAB. SCEB 7 obtained a shear bond strength 147% higher than Soil RS1 and 67% higher than Soil NS1 found in previous investigations. The average creep coefficient for SCEB 7 had a value between 104% higher and 40% lower than the clay brick masonry. Therefore, the prism compressive strength of SCEB 7, bond strength of SCEB 7 and Type S mortar and shear strength of SCEB 7 and Type S mortar had sufficient performance as compared with SAB and other earthen materials and masonry prisms in the literature.

Masonry structures are often subjected to lateral loads (eg. wind loads or seismic loads), therefore the structural performance is dependent on the shear strength of the wall to resist lateral movement. SCEB 7 Wall 4 obtained a shear strength 50% higher than earth block masonry. Rammed earth obtained a shear strength 4.7 times higher than SCEB 7 Wall 4 and cob obtained a strength 3 times greater than SCEB 7 Wall 4. SCEB 7 Wall 4 obtained a shear strength 7% higher than geopolymer stabilized rammed earth wallets stabilized with 2.5% and 5.0% fly ash content. The shear testing of SCEB wall assemblies confirmed that SCEB walls will have a suitable structural performance. The shear strength and ductility of SCEB walls are comparable or improved than other earthen materials and are comparable to traditional clay fired masonry.

To conclude, we determined that the mechanical properties of specimen SCEB 7 indicated it as the optimum soil mixture, potentially leading to a better structural performance than traditional adobe. In addition, it met New Mexico Earthen Building Materials Code. It also had a suitable interaction of block and Type S mortar. We also successfully used this combination of SCEB 7 and Type S mortar to build wall assemblies with favorable structural performance. In our opinion, it will be a suitable stabilized compressed earth block to be used in residential earthen construction on the Jemez Pueblo in New Mexico.

5.2 Recommendations for Future Research

- It was apparent that approaches and criteria for the soil selection were varied and not sufficiently strict enough. In the literature, particle size distribution is the property found with more recommendations, due to its high influence on the soil behavior. Other factors for using the particle size distribution is due to ease of testing causing it to be an inexpensive test. Maximum particle size should be limited to a certain value for all the earthen material production techniques. It should be noted and understood by professionals, the harmful influence of clay "lumps" in a soil mix. These should be grinded to have similar maximum particle size as the sand. In addition to specified grain size distribution for SCEBs, there should be limitations and understanding of the clay content on a mix. This should be specified in earthen building codes. It was determined that mineralogy also contributed to the suitability of a soil to be used in SCEB production. This should be further investigated to understand how the clay minerals react with Portland cement and how that impacts the strength of SCEBs.

- The linear shrinkage and plasticity index are the best indicators of soil suitability for SCEB production. As humid soils dry, they reduce their volume. During this shrinkage, the appearance of cracks were common, especially if the water is lost quickly and in the presence of clay minerals. Therefore, it is important to measure the linear shrinkage of a soil. The Australian Standards AS1289.C4.1 may be a suitable method to be used to determine the linear shrinkage of a soil.
- In order to complete a material test on a SCEB, the durability testing should include freeze thaw and erosion testing. Testing should be done to determine the effect of freeze-thaw cycles on SCEB units. Non-destructive testing should be used to determine the modulus of elasticity of SCEBs before and after freeze-thaw. In addition, compressive and flexural strength testing of the SCEB units after exposure to a specified duration of standard freeze-thaw cycles should be conducted to determine its strength due to weathering. In addition, erosion testing of CEB units should be performed, which includes several wetting and drying cycles of SCEBs. Cycles of wetting and drying should be followed by ultrasonic measurements to determine its modulus of elasticity. Also, the unconfined compressive strength to determine its strength should be determined following erosion cycles.
- The results for the measurement of rate of water absorption (sorptivity) testing were inconclusive since the specimen started losing material in addition to gaining water. From the literature review, it appears that this was the first investigation testing the sorptivity of earthen materials. Therefore, the test should be modified and further investigated in order to be used to accurately measure the rate of absorption of SCEBs.

- There are no specified curing requirements for SCEBs. Therefore, testing should include the comparison of curing in an exterior environment as opposed to in a lab at 23°C and a Relative humidity of 20%. The curing conditions should be specified in the building code. According to the New Zealand building code, curing shall be carried out by air drying for a minimum of 28 days in an exterior environment which is protected from strong winds and rain. For SCEBs using Portland cement, there shall be a minimum of one week of damp curing before air drying is commenced in an exterior environment.
- Mortar is of major importance in the overall performance of earth walls. If the composition of the mortar is similar to that of the brick, the mortar bond may be improved and differential weathering avoided. Therefore, it may be valuable to investigate the performance of different standard mortar mixes as well as soil mortar mixes. It would be valuable to test the compression, shear, bond and creep behavior of SCEB prisms and the shear strength of SCEB wall panels using various mortar mixes.
- Currently, the most utilized stabilizers for SCEBs are lime and Portland cement. In order to reduce the CO_2 emissions and produce an even more sustainable earthen material, alternative stabilizers are being investigated. Synthetic materials like geopolymers are one solution as an alternative binder, as they are made by alkaline activation of solid particles rich in silica and alumina. These materials also allow the complete elimination of cement in SCEBs without compromising the strength and durability of SCEBs.

- Finally, in order to provide structures resistant to seismic loads, methods such as interlocking compressed earth blocks should be further investigated.

APPENDIX A

A.1 Supplemental Results – Soils Data

A.1.1 Moisture Content

Phase 1 Soil Testing	
Specimen ID	**Water Content, %**
UNM 1	4.2
UNM 2	17.3
UNM 3	10.6
UNM 4	5.7
UNM 5	2.5
UNM 6	9.9
UNM 7	4.9
UNM 8	2.6
UNM 9	4.4
UNM 10	8.6
UNM 11	9.6
UNM 12	5.9
UNM 13	6.1

Phase 2 Soil Testing	
Specimen ID	**Water Content, %**
UNM 11-1A	2.4
UNM 11-1B	3.6
UNM 11-1C	3.3
UNM 11-1D	4.0
UNM 11-2A	2.1
UNM 11-2B	2.1
UNM 11-3A	9.4
UNM 11-3B	8.5
UNM 11-4A	28.4
UNM 11-4B	25.0
UNM 11-4C	17.8
UNM 12-1-1A	6.3
UNM 12-1-2B	29.1
UNM 12-2-1A	4.5
UNM 12-2-2B	4.6
UNM 12-3-1A	18.2
UNM 12-3-2B	12.5
UNM 12-4-1A	15.7
UNM 12-4-2B	8.5
UNM 12-5-1A	9.9
UNM 12-5-2B	27.8

Phase 3 Soil Testing	
Specimen ID	**Water Content, %**
UNM 11 1A	25.9
UNM 11 1B	22.9
UNM 11 2A	13.7
UNM 11 2B	19.9
UNM 11 4A	24.8
UNM 11 4B	27.2
UNM 12 1A	10.0
UNM 12 1B	5.7
UNM 12 2	25.4
UNM 12 3A	26.2
UNM 12 3B	28.4
UNM 12 4A	26.6
UNM 12 4B	21.2

Phase 4 Soil Testing	
Specimen ID	**Water Content, %**
Clay 1	15.7
Clay 2	14.9
Sand 1	5.0
Sand 2	1.1
Soil 1	-
Soil 2	-
Adobe Soil	5.1
SCEB 7	12.3
SCEB 8	11.4
SCEB 9	13.1

A.1.2 Specific Gravity

Phase 1 Soil Testing	
Specimen ID	**Specific Gravity, G_s**
UNM 1	2.63
UNM 2	2.63
UNM 3	2.71
UNM 4	2.64
UNM 5	2.67
UNM 6	2.66
UNM 7	2.64
UNM 8	2.64
UNM 9	2.60
UNM 10	2.66
UNM 11	2.71
UNM 12	2.67
UNM 13	2.65

The specific gravity for the soil samples in Phase 2 were not determined.

Phase 3 Soil Testing	
Specimen ID	**Specific Gravity, G_s**
UNM 11 1A	2.66
UNM 11 1B	2.65
UNM 11 2A	2.60
UNM 11 2B	2.62
UNM 11 4A	2.61
UNM 11 4B	2.60
UNM 12 1A	2.70
UNM 12 1B	2.61
UNM 12 2	2.64
UNM 12 3A	2.65
UNM 12 3B	2.62
UNM 12 4A	2.67
UNM 12 4B	2.62

Phase 4 Soil Testing	
Specimen ID	**Specific Gravity, G_s**
Clay 1	2.62
Clay 2	2.60
Sand 1	2.64
Sand 2	2.64
Soil 1	2.68
Soil 2	2.68
Adobe Soil	2.63
SCEB 7	2.64
SCEB 8	2.67
SCEB 9	2.67

A.2 Data Sheets developed for use in the research project.

UNM

ASTM D422 Particle Size Analysis (PSA), Wet Sieve

Moisture (%)	0	Tech	CJR	Total initial mass (g):	500.0
Balance ID	173477	Project	Jemez Phase 2C		
Oven ID	266414	Sample	SCEB Soil 2		

Sieve Data (+10 Sieve)

Test Date:	5/22/2016	Tare wt (g):	13.6	
Date in oven:	5/20/2016	Dry + tare wt (g):	264.4	
from oven:	5/22/2016	Dry wt (g):	250.8	

	Total Dry wt. of Mass Retained (g)	Dry wt. of Mass Ret. (g)	% Passing	% Retained		
3/8 inch	0	0.0	100.0%	0.0%		
No. 4	29.9	29.9	94.0%	6.0%	% retained #4 =	5.98%
No. 10	122.3	92.4	75.5%	24.5%	% passing #4 =	94.02%
No. 20	167.3	45.0	66.5%	33.5%		
No. 40	189.3	22.0	62.1%	37.9%	% retained #10 =	24.46%
No. 60	211.9	22.6	57.6%	42.4%	% passing #10 =	75.54%
No. 140	243.6	31.7	51.3%	48.7%		
No. 200	250.2	6.6	50.0%	50.0%	% retained #200 =	50.04%
Pan	250.8	0.6			% passing #200 =	49.96%
Total dry recovery wt.		250.8				

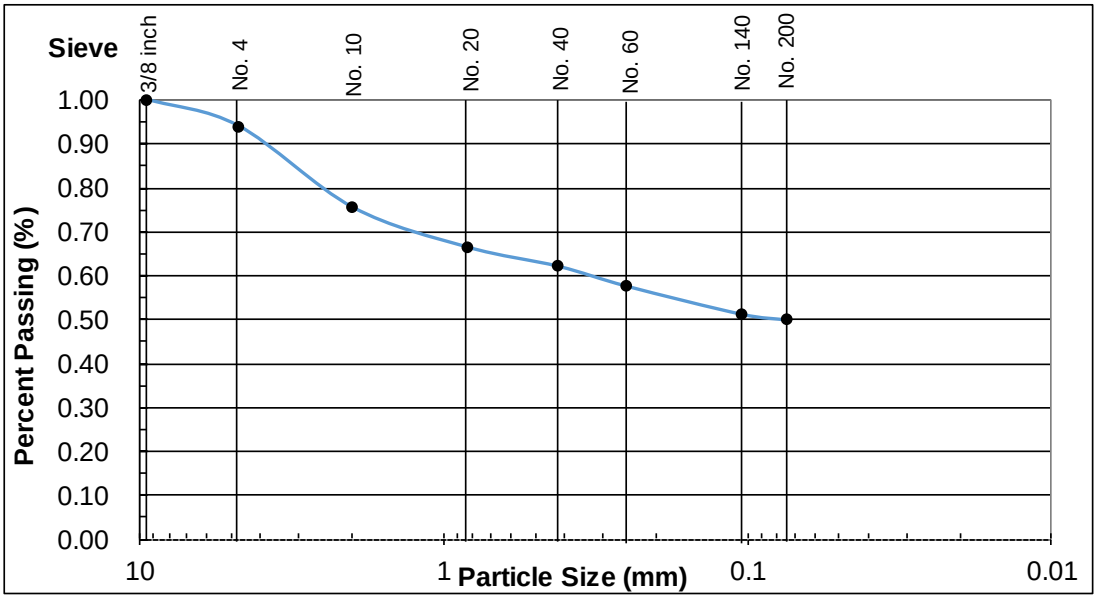

ASTM D854 SPECIFIC GRAVITY

Tech: MH
Project: Jemez Phase 2C
Scale: 173477

Sample No.	Date	Flask Mass (g)	Mpw, Mass of Flask + Water (g)	Mw, Mass of Water (g)	Temp (°C)
Calibr. 1	3/11/16	104.3	353.3	249	21.0
Calibr. 2	3/21/16	97.4	345.9	248.5	20.0
Calibr. 3	4/6/16	107	356.5	249.5	21.0
Calibr. 4	5/16/16	108.2	356.4	248.2	22.0
Calibr. 5	5/25/16	75.8	344.9	269.1	21.0

Sample No.	Date	Volume of Flask (mL)	Ms, Mass of dry soil (g)	Mpws, Mass Flask + Water + Soil (g)	Temp (°C)	Mpw, Mass of Flask + Water (g)	Mw, Mass of Water (g)	Temp Corr	Specific Gravity, Gs
SCEB 7	3/21/16	250	65.40	386.50	22.0	345.90	24.80	0.99957	2.636
Clay 2	3/21/16	250	65.00	385.90	21.0	345.90	25.00	0.99979	2.599
Sand 2	3/21/16	250	65.20	386.40	22.0	345.90	24.70	0.99957	2.639
Adobe Soil	3/21/16	250	65.20	386.30	23.0	345.90	24.80	0.99933	2.627
Clay 1	3/11/16	250	65.00	393.50	22.0	353.30	24.80	0.99957	2.620
SCEB 9	4/6/16	250	65.20	397.30	22.0	356.50	24.40	0.99957	2.671
SCEB 8	4/6/16	250	65.20	397.30	22.0	356.50	24.40	0.99957	2.671
SCEB Soil 1	4/6/16	250	65.30	397.40	22.0	356.50	24.40	0.99957	2.675
SCEB Soil 2	5/16/16	250	66.80	398.30	23.0	356.40	24.90	0.99933	2.681
Sand 1	5/25/16	250	65.10	385.30	21.0	344.90	24.70	0.99979	2.635

ASTM D422 HYDROMETER ANALYSIS

Sample Wt.	50.0	g	Date	5/20/2016
Moisture (%)	0		Tech	CJR
Specific Grav.	2.68		Project	Jemez Phase 2
			Sample	SCEB Soil 2

Meniscus Correction, 22°C	(m)	3	Hydrometer type:	152H
Gs Correction Factor	(a)	0.9938		
Suspension Constant	(k)	0.01320	% Passing #10:	75.54%
Corrected Sample Wt.	(Ws)	50.0	Calculated Hydrometer Sieve Weight (W) (g):	66.190098
Time Begun:	11:29 AM			

T	H	Ra		L	L	D	P
Elapsed Time	Hydrometer Reading	Hydrometer Reading with (m)	Temperature	Effective Depth	Effective Depth (corrected)	Particle Diameter	% Ret. In Suspension
Min.			℃	cm	cm	mm	%
0.25	39	36	22	10.4	10.3357	0.085	54.39%
0.5	37	34	22	10.7	10.6338	0.061	51.37%
1	37	34	22	10.7	10.6338	0.043	51.37%
2	37	34	22	10.7	10.6338	0.030	51.37%
5	36	33	22	10.9	10.8326	0.019	49.86%
10	36	33	22	10.9	10.8326	0.014	49.86%
15	35	32	22	11.1	11.0313	0.011	48.35%
20	35	32	22	11.1	11.0313	0.010	48.35%
30	34	31	22	11.2	11.1307	0.008	46.83%
60	33	30	22	11.4	11.3295	0.006	45.32%
250	30	27	22	11.9	11.8264	0.003	40.79%
1440	25	22	22	12.7	12.6214	0.001	33.24%

ASTM D422 Particle Size Analysis (PSA), Wet Sieve

Sieve Data

Moisture (%)	0	Tech	CJR
Balance ID	173477	Project	Jemez Phase 2
Oven ID	266414	Sample	SCEB Soil 2

Hydrometer Sieve Data (-10/+200)

Test Date:	5/20/2016	Tare wt (g):	13.2
Date in oven:	5/19/2016	Dry + tare wt (g):	28.6
from oven:	5/20/2016	Total Initial Mass (g):	15.4

Dry wt. of -10 Sieve Mass Retained (g)		Weight Retained	Weight Passing	% Passing	% Retained		
No. 20	4.9	21.09	45.10	68.1%	31.9%	% retained #10 =	24.46%
No. 40	3.5	24.59	41.60	62.8%	37.2%	% passing #10 =	75.54%
No. 60	2.7	27.29	38.90	58.8%	41.2%		
No. 140	3.4	30.69	35.50	53.6%	46.4%	Calculated Hydrometer	
No. 200	0.9	31.59	34.60	52.3%	47.7%	Sieve Weight (W) (g):	66.1901
Pan	0.0					Calculated +10 mass (g):	16.19
Total dry recovery wt.	15.4					Total -200 mass (g):	34.60

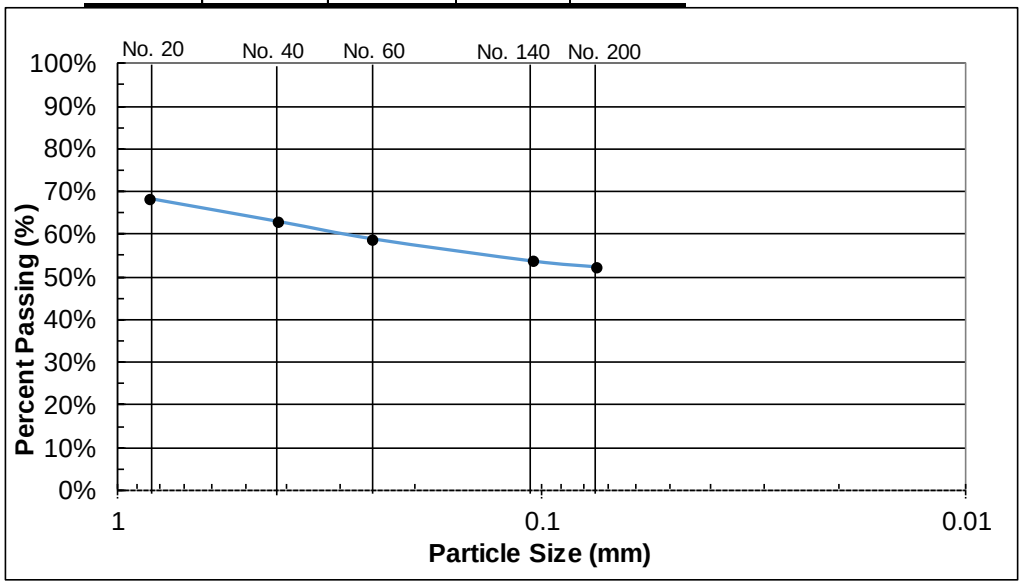

ASTM D4318 ATTERBERG LIMITS DETERMINATION

Date 5/20/2016
Tech CJR
Project Jemez Phase 2C
Sample SCEB Soil 2

Prep Method: Dry
Liquid Limit
Test Method: One point

Nonplastic:

Liquid Limit Determination	1	2
Tare wt. (g)	7.24	6.98
Wet soil + tare wt. (g)	17.76	14.29
Dry soil + tare wt. (g)	14.12	11.78
Wet soil (g)	10.52	7.31
Dry soil (g)	6.88	4.80
Water content, w (%)	52.9	52.3
No. of blows (N)	28	29
Liquid limit=w(N/25)^0.121	54	53
Avg. Liquid Limit	53	

Plastic Limit Determination	1	2
Tare wt. (g)	6.96	6.98
Wet soil + tare wt. (g)	14.24	14.05
Dry soil + tare wt. (g)	12.96	12.48
Wet soil (g)	7.28	7.07
Dry soil (g)	6.00	5.50
Water content, (%)	21.3	28.5
Plastic limit	21	29
Avg. Water content, %	25	

Plasticity Index

Plasticity Index, Ip	28
Plasticity Chart Classification	CH

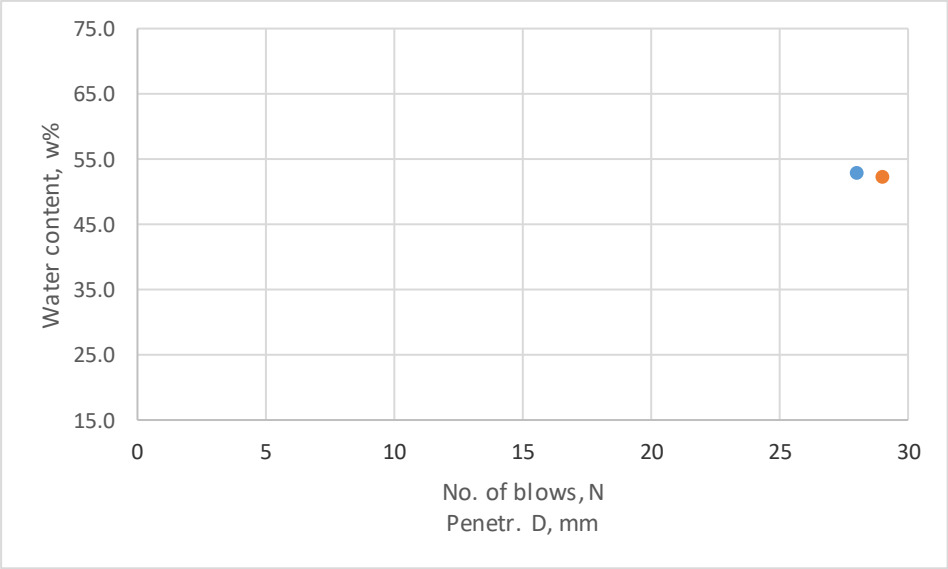

ASTM D4829 EXPANSION INDEX

Date	5/19/2016	Soil Sample:	SCEB Soil 2
Tech	CJR	Visual Description:	-
Project	Jemez Phase 2C	Scale:	173477

Processing

Percent Passing #4 Sieve	
Wt. Passing #4 Sieve:	769.4
Retained on #4 Sieve:	62.8
% Retained:	7.5%
% Passing :	92.5%

Moisture Calculations

	Initial	Final
Tare Wt. (g)	47.8	47.2
Wet Wt. (g)	88.1	148.2
Dry Wt. (g)	77.8	117.9
Weight of water (g)	10.3	30.3
% Water, w	0.1	0.3

Sample Dimensions

Height (in): 1.003 Diameter (in): 4.003

Volume (cm^3): 206.8526

$$\rho_m = k \times \frac{(M_t - M_{md})}{V}, \left[\frac{g}{cm^3}\right]$$

$$k = 1 \; for \; g/cm^3$$

Two lifts, 15 blows/lift @ slightly below optimum moisture content

	Initial	Final	
Ring & Sample, Mt:	749.8	790.3	g
Ring, Mmd:	380.0	380.0	g
Remolded Wet Wt.:	369.8	410.3	g
Wet Density, ρm:	111.6053	123.8282	pcf
Dry Density, ρd:	98.5913	98.5187	pcf
% Saturated =	50.5	98.1	**50 +/- 1 %**

$$\rho_d = \frac{\rho_m}{1 + \frac{w}{100}}, \left[\frac{g}{cm^3}\right]$$

$$1\frac{g}{cm^3} = 62.4279606 \; \frac{lb}{ft^3}$$

$$\% \; sat = \frac{2.7 \times w \times \rho_d}{2.7 * (62.3) - \rho_d}$$

Expansion Test

Date	Time	Dial	Delta h, %	Remarks:
5/19/16	3:58 PM	0.06980	0.0%	
	4:00 PM	0.07040	0.1%	
	4:10 PM	0.07210	0.2%	
	4:20 PM	0.07300	0.3%	
	4:37 PM	0.07360	0.4%	
	4:58 PM	0.0738	0.4%	
5/20/16	8:50AM	0.0894	2.0%	
	11:10 AM	0.0899	2.0%	
	1:48 PM	0.0906	2.1%	
	3:58 PM	0.0912	2.1%	
		Total Dial	2.1%	

Results

Expansion Index

Uncorrected EI: 21

$$EI = \frac{\Delta H}{H_1} \times 1000$$

ASTM D1557 Standard Test Methods for Laboratory Compaction Characteristics of Soil Using Modified Effort

Date 5/16/2016
Tech CJR
Project Jemez Phase 2
Sample SCEB Soil 2

Proctor Type A

	Moisture content					Soil Weight and volume				Compation Test Results				
Point	Pan tare g	Wet + Pan g	Dry + Pan g	Wet g	Dry g	Mold Tare g	Mold Volume ft^3	Mold + Soil g	Mold + Soil lbs	Weight of Water g	Moisture content %	Wet Density, ρm pcf	Dry Density, ρd pcf	Water content for complete saturation, wsat %
1	13.2	740.6	695	727.4	681.8	1935	0.0333	3690	8.1	45.6	6.7%	116.2	108.9	20.2
2	13.2	930.4	850.1	917.2	836.9	1935	0.0333	3896.4	8.6	80.3	9.6%	129.9	118.5	15.5
3	13.6	747.6	663	734	649.4	1935	0.0333	4011.3	8.8	84.6	13.0%	137.5	121.6	14.2
4	13.2	786.8	676	773.6	662.8	1935	0.0333	3974	8.8	110.8	16.7%	135.0	115.7	16.8

$$\rho_m = k \times \frac{(M_t - M_{md})}{V}, \left[\frac{g}{cm^3}\right] \qquad k = 1\ for\ g/cm^3 \qquad 1\frac{g}{cm^3} = 62.4279606\ \frac{lb}{ft^3}$$

$$\rho_d = \frac{\rho_m}{1 + \frac{w}{100}}, \left[\frac{g}{cm^3}\right] \qquad w_{sat} = \frac{2.7*(62.3) - \rho_d}{2.7 \times \rho_d} \times 100$$

ASTM D1557 Standard Test Methods for Laboratory Compaction Characteristics of Soil Using Modified Effort

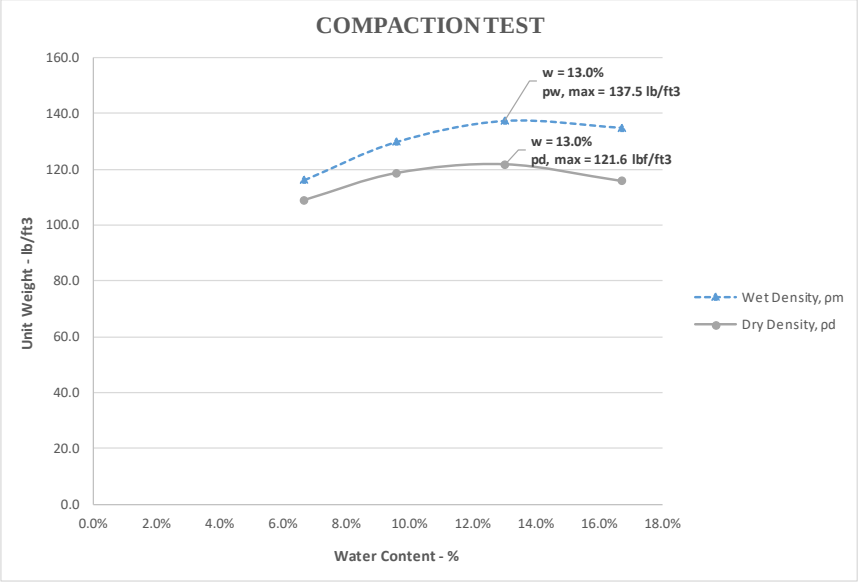

Molded Date:	2/18/2016	Sample No.:	SCEB 7
Tech:	NBT	Sample Description:	-
Project:	Jemez Phase 2C		

ASTM C67: Standard Test Methods for Sampling and Testing Brick and Structural Clay Tile
2009 New Mexico Eaarthen Building Materials Code
14.7.4.23 NMAC - Dry Compression

Oven ID: 266413 Oven Temp.: 110 °C

Drying and Cooling		1	2	3	4	5
Date/Time In Oven:		3/17 12PM	3/17 12PM	3/17 12PM	3/17 12PM	3/17 12PM
2 hour interval	1- Weight of Specimen (g):					
	2- Weight of Specimen (g):					
% Loss in Weight:						
Date/Time Out Oven:		3/18 12PM	3/18 12PM	3/18 12PM	3/18 12PM	3/18 12PM
Cooling time (hr):		> 4 hr	> 4 hr	> 4 hr	> 4 hr	> 4 hr

Test Machine: Tinius Olsen

Dry Compression	1	2	3	4	5
Test Date:	3/19/2016	3/19/2016	3/19/2016	3/19/2016	3/19/2016
Length of specimen (in.)	14 1/32	14 1/8	14 1/8	14 1/8	14 1/8
Width of specimen (in.)	4 7/8	4 5/8	5	5 1/16	4 15/16
Maximum Load (lbf):	97410	84671	85592	85886	88414
Unconfined compressive strength (psi):	1424.1	1296.1	1211.9	1201.1	1267.7
Average Unconf. compressive strength	1280.2				
Coefficeint of Variation:	7%				

Molded Date:	2/18/2016	Sample No.:	SCEB 7
Tech:	NBT	Sample Description:	-
Project:	Jemez Phase 2C	Scale ID:	Explorer Pro OHAUS

ASTM C67: Standard Test Methods for Sampling and Testing Brick and Structural Clay Tile
Absorption

Oven ID: 266413 Oven Temp.: 110 °C

Drying and Cooling		1	2	3	4	5
Date/Time In Oven:		3/20 10:30am	3/20 10:30am	3/20 10:30am	3/20 10:30am	3/20 10:30am
2 hour interval	1- Weight of Specimen (g):					
	2- Weight of Specimen (g):					
% Loss in Weight:						
Date/Time Out Oven:		3/21 12pm	3/21 12pm	3/21 12pm	3/21 12pm	3/21 12pm
Cooling time (hr):		> 4hr	> 4hr	> 4hr	> 4hr	> 4hr

Absorption

24 Hour Cold Water Submersion	1	2	3	4	5
Start Date/Time:	3/22 1:25pm	3/22 1:26pm	3/22 1:27pm	3/22 1:28pm	3/22 1:29pm
End Date/Time:	3/23 1:30pm	3/23 1:30pm	3/23 1:30pm	3/23 1:30pm	3/23 1:30pm
24 Hour Submersion - Dry weight (Wd, g)	9162.8	8791.6	8937.9	9367.8	8757.1
24 Hour Submersion - Wet weight (Ws, g)	9887.2	9675.0	9439.4	10069.1	9765.2
24 Hour Submersion in Cold Water (%)	7.91%	10.05%	5.61%	7.49%	11.51%

ASTM C67: Standard Test Methods for Sampling and Testing Brick and Structural Clay Tile
2009 New Mexico Earthen Building Materials Code
14.7.4.23 NMAC - Wet Compression

Test Machine: Tinius Olsen

Wet Compression	1	2	3	4	5
Test Date:	3/30	3/30	3/30	3/30	3/30
Length of specimen (in.)	13 7/8	14	14 1/8	14	14
Width of specimen (in.)	5	4 3/4	4 7/8	5	4
Thickness of Specimen (in.)	4 1/8	4	4 1/8	4	4 1/16
Maximum Load (lbf):	76749	83535	71779	84139	43447
Unconfined compressive strength (psi):	1106	1256	1042	1202	776

Molded Date:	2/18/2016	Sample No.:	SCEB 7
Tech:	NBT	Sample Description:	-
Project:	Jemez Phase 2C	Scale ID:	Explorer Pro OHAUS

ASTM C67: Standard Test Methods for Sampling and Testing Brick and Structural Clay Tile
Initial Rate of Absorption (Suction) (Laboratory Test)

Oven ID: 266413 Oven Temp.: 110 °C

Drying and Cooling		1	2	3	4	5
Date/Time In Oven:		3/20 10:30AM	3/20 10:30AM	3/20 10:30AM	3/20 10:30AM	3/20 10:30AM
2 hour interval	1- Weight of Specimen (g):	-	-	-	-	-
	2- Weight of Specimen (g):	-	-	-	-	-
% Loss in Weight:		-	-	-	-	-
Date/Time Out Oven:		3/21 12PM	3/21 12PM	3/21 12PM	3/21 12PM	3/21 12PM
Cooling time (hr):		> 4 hr	> 4 hr	> 4 hr	> 4 hr	> 4 hr

IRA (Oven Dried Method)	1	2	3	4	5
Test Date:	3/22/16	3/22/16	3/22/16	3/22/16	3/22/16
Start Time:	1:17 PM	1:37 PM	2:45 PM	2:53 PM	2:58 PM
End Time:	1:18 PM	1:38 PM	2:46 PM	2:54 PM	2:59 PM
Length of specimen (in.)	14 1/16	14 1/16	14 1/16	14 1/16	14 1/16
Width of specimen (in.)	9 7/8	10	10 1/8	10	9 7/8
Initial Dry Weight of specimen (g)	18321.2	18259.6	18522.0	18631.4	18363.8
Wet Weight of specimen (g)	18508.2	18421.8	18746.2	18808.8	18574.2
Gain in Weight Corrected to 30 in2 (g)	40.4	34.6	47.2	37.8	45.5

2009 New Mexico Earthen Building Materials Code
14.7.4.23 NMAC - Modulus of Rupture

Modulus of Rupture	1	2	3	4	5
Test Date:	3/29/16	3/29/16	3/29/16	3/29/16	3/29/16
Maximum Load (lbf):	1017	310	1067	215	134
Distance between supports (in.):	10	10	10	10	10
Net width at plane of failure (in.):	9 7/8	10	10 1/8	10	9 7/8
Depth at plane of failure (in.):	4	4 1/16	4 1/16	4 1/16	4
*Distance from mid to the failure (in.):	0.50	0.25	0.50	0.50	0.50
Modulus of Rupture (psi):	96.6	28.2	95.8	19.5	12.7

Note: *Average distance from the midspan of the specimen to the plane of failure measured in the direction of the span along the centerline of the bed surface subjected to tension.

Molded Date:	2/18/2016	Sample No.:	SCEB 7
Tech:	NBT	Sample Description:	-
Project:	Jemez Phase 2C	Scale ID:	Explorer Pro OHAUS

ASTM C67: Standard Test Methods for Sampling and Testing Brick and Structural Clay Tile

Absorption

Oven ID: 266413 Oven Temp.: 111 °C

Drying and Cooling		1	2	3	4	5
Date/Time In Oven:		3/20 10:30am	3/20 10:30am	3/20 10:30am	3/20 10:30am	3/20 10:30am
2 hour interval	1- Weight of Specimen (g):					
	2- Weight of Specimen (g):					
% Loss in Weight:						
Date/Time Out Oven:		3/21 12pm	3/21 12pm	3/21 12pm	3/21 12pm	3/21 12pm
Cooling time (hr):		>4 hr	>4 hr	>4 hr	>4 hr	>4 hr

Absorption

24 Hour Cold Water Submersion	1	2	3	4	5
Start Date/Time:	3/22 1:20PM	3/22 1:21PM	3/22 1:22PM	3/22 1:23PM	3/22 1:24PM
End Date/Time:	3/22 2:59PM	3/22 2:59PM	3/22 2:59PM	3/22 2:59PM	3/22 2:59PM
24 Hour Submersion - Dry weight (Wd, g)	18548.7	18842.6	18567.0	17977.0	18394.5
24 Hour Submersion - Wet weight (Ws, g)	20111.6	20216.5	20008.0	19342.5	19682.3
24 Hour Submersion in Cold Water (%)	8.4%	7.3%	7.8%	7.6%	7.0%

ASTM C67: Standard Test Methods for Sampling and Testing Brick and Structural Clay Tile

2009 New Mexico Earthen Building Materials Code

14.7.4.23 NMAC - Saturated Modulus of Rupture

Modulus of Rupture	1	2	3	4	5
Test Date:	3/29	3/29	3/29	3/29	3/29
Maximum Load (lbf):	698.0	748.0	671.0	391.0	623.0
Distance between supports (in.):	10	10	10	10	10
Net width at plane of failure (in.):	9 7/8	9 15/16	9 7/8	9 3/4	9 7/8
Depth at plane of failure (in.):	4 1/16	4 1/16	4 1/8	4 1/8	4 1/16
*Distance from mid to the failure (in.):	0.25	0.88	0.00	1.00	0.25
Modulus of Rupture (psi):	64.2	68.4	59.9	35.4	57.3

Note: *Average distance from the midspan of the specimen to the plane of failure measured in the direction of the span along the centerline of the bed surface subjected to tension.

Tech: NBT
Project: Jemez Phase 3 **Equipement ID:** Tinius Olsen

ASTM C1314: Standard Test Method for Compressive Strength of Masonry Prisms

Prism Identification: SCEB 7

Prism Details

Number of Mortar Bed Joints:	1
Number of Masonry Units Used:	2
Date Constructed:	2/18/2016
Date Grouted:	N/A
Date Received from Site:	3/10/2016
Date Delivered to Lab:	3/10/2016
Date Tested:	3/31/16
Prisms Constructed By:	NBT
Max/Min Temperature (1st 48hr)	-

Masonry Unit Information:

Unit Supplier:	HPA
Type of Unit:	Solid Unit

Mortar Information

Mortar Preparer:	NBT
Mortar Type:	Type S
Date Mortar Mixed:	3/17/16

Test Machine Information

Diameter of Spherical Seat (in):	10
Required Upper Bearing Plate Thickness(in):	-
Provided Upper Bearing Plate Thickness(in):	0.761
Required Lower Bearing Plate Thickness(in)	-
Provided Lower Bearing Plate Thickness(in)	1.09

Tested Prism Properties

Prism No.	Age at Test (days)	Avg. Width (in.)	Avg. Length (in.)	Avg. Height (in.)	Max Load	h/t CF*	Corrected Net Strength (psi)	Mode of Failure**
1	14	4.893	5.0925	8.5000	14770	0.93	549	3, 7
2	14	4.9065	5.1100	8.7500	16933	0.94	634	3, 7
3	14	4.925	5.1335	8.6875	15757	0.93	582	1, 7
4	14	5.1	5.0020	8.6875	15260	0.93	554	1, 7
5	14	4.8435	4.9970	8.6250	17807	0.94	691	3, 7

* Height to thickness correction factor from Table 1 of ASTM C1314.

** Refer to ASTM C1314 Figure 4 and report number of corresponding mode failure.

Average Compressive Strength (psi)	**602**
COV (%)	**10%**

Tech: NBT/CJR
Project: Jemez Project Phase 4

ASTM C1072 - Standard Test Methods for Measurement of Masonry Flextural Bond Strength

Specimen Id: SCEB 7
Date Tested: 5/17 & 5/18

Test Machine Information

Equipement ID: Enerpac RC-106
Diameter of Spherical Seat (in): 1.50

Prism Details

Number of Mortar Bed Joints:	2
Number of Masonry Units Used:	3
Date Constructed:	2/18/2016
Date Delivered to Lab:	3/10/2016
Prisms Constructed By:	NBT/CJR/MH
Block Curing- Age at Test Date:	>28 days
Block Curing- Temperature (°F):	23
Block Curing- Humidity (%):	20

Masonry Unit Information:

Unit Supplier:	HPA
Type of Unit:	Solid Unit

Masonry Unit Information:

Mortar Preparer:	NBT/CJR/MH
Mortar Type:	Type S
Date Mortar Mixed:	4/13/2016

Tested Prism Properties

Prism No.	Test Date	Mortar Joint No.	Avg. Width (in.)	Avg. Height (in.)	Avg. Length (in.)	Total Weight (lb)	Max Pressure (psi)	Description of Failure*
1	5/17	1	4.7775	4.1900	5.0910	10550.2	14	bottom of mortar joint
		1/2	4.8455	4.2705	4.9900			
	5/18	2	4.9550	4.1900	4.9030		-	fail prematurely
				13.5000				
2	5/17	1	4.7970	4.1190	4.9785	10572.8	12	bottom of mortar joint
		1/2	5.0575	4.4720	4.9445			
	5/18	2	4.8995	4.2700	5.0620		-	fail prematurely
				13.3750				
3	5/17	1	5.0735	4.0845	4.8815	10655.4	28	top of mortar joint
		1/2	4.9935	4.0455	4.9800			
	5/18	2	5.0530	4.0155	4.7665		14	top of mortar joint
				13.0000				
4	5/17	1	4.9270	4.1860	6.1110	10698.6	66	bottom of mortar joint
		1/2	4.0600	3.8865	5.0050			
	5/18	2	4.9625	4.0970	5.3135		10	top of mortar joint
				13.0000				
5	5/17	1	4.7965	4.3295	4.9355	10781.7	-	fail prematurely
		1/2	5.0305	4.5385	4.9255			
	5/18	2	5.0395	4.1740	5.0760		16	top of mortar joint
				13.3750				

* Indicate whether failure occurred at top or bottom of the mortar joint or both. Or if joint broke prematurely.

Tech: NBT
Project: Jemez Phase 4
Equipement ID: Tinius Olsen

BS EN 1052-3:2002 Methods of test for masonry - Part 3: Determination of initial shear strength

Test Procedure Used:	A
Specimen Id:	SCEB 7
Date Tested:	5/12/2016

Test Machine Information

Equipement ID:	Enerpac RCS-302
Diameter of Spherical Seat (in.):	2.62

Prism Details

Number of Mortar Bed Joints:	2
Number of Masonry Units Used:	3
Date Constructed:	2/18/2016
Date Delivered to Lab:	3/10/2016
Prisms Constructed By:	NBT
Block Curing- Age at Test Date:	> 28 days
Block Curing- Temperature (°F):	73
Block Curing- Humidity (%):	20

Masonry Unit Information:

Unit Supplier:	HPA
Type of Unit:	Solid Unit

Masonry Unit Information:

Mortar Preparer:	NBT
Mortar Type:	Type S
Date Mortar Mixed:	3/28/2016

Tested Prism Properties

Prism No.	Test Date		Avg. Width (in.)	Avg. Length (in.)	Avg. Height (in.)	Pre-compression Pressure (psi)	Max Load (lbf)	Mode of Failure	Shear Strength (psi)
1	5/12	T	4.8155	4.9030	3 7/8	44	1319	A1	27.59
		M	4.8085	5.0280	3 7/8				
		B	4.7935	4.9350	3 7/8				
		Tot			13				
2	5/12	T	4.7965	4.8025	3 7/8	44	792	A1	17.34
		M	4.8175	4.8335	3 7/8				
		B	4.6545	4.6670	3 7/8				
		Tot			13				
3	5/12	T	4.7955	5.0575	4	44	2715	A1	57.26
		M	4.6595	4.9460	4				
		B	4.9285	4.9695	4				
		Tot			13 1/8				
4	5/12	T	4.8380	4.9680	4	44	1546	A1	31.82
		M	4.9470	4.9535	4 1/8				
		B	4.9915	4.8345	4				
		Tot			13 1/8				
5	5/12	T	4.9545	4.8560	4	44	2227	A1	47.32
		M	4.6085	4.9900	4				
		B	4.8780	4.9360	4 1/8				
		Tot			13				

Mechanical Properties of Block

Mean compressive strength of units (psi):	1280.2
Coefficeint of Variation (%):	7

Mechanical Properties of Mortar

28 day - Mean compressive strength (psi):	4813.2
Coefficeint of Variation (%):	4.8

Types of Failure (BS EN 1052-3:2002 Methods of test for masonry - Part 3: Determination of initial shear strength)

Annex A

(informative)

Types of failure

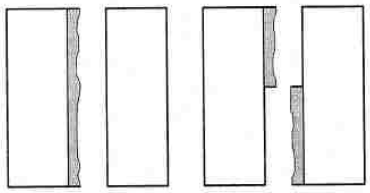

Figure A.1 - Shear failure in the unit/mortar bond area either on one or divided between two unit faces

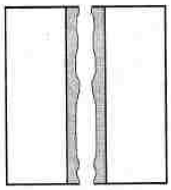

Figure A.2 - Shear failure only in the mortar

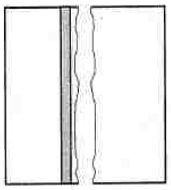

Figure A.3 - Shear failure in the unit

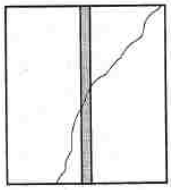

Figure A.4 - Crushing and or splitting failure in the units

Tech: NBT
Project: Jemez Phase 3 Scale ID: Toledo

ASTM C109: Standard Test Method for Compressive Strength of Hydraulic Cement Mortars (Using 2-in. Cube Specimens)

Mortar Mix and Curing Data

Date Mixed	Specimen	Sand Wt (lb)	Lime Type-S Wt (lb)	Portland Cement Wt (lb)	Water Wt (lb)	Date In Curing Room	Date Out of Curing Room (7 day)	Date Out of Curing Room (28 day)
3/28/2016	**#1)** Wall (1) and (2)	63.0	3.5	16.5	12.0	3/29	4/4	4/25
	#2) Wall (1), (2), (3), and (4)	65.0	3.6	17.0	13.0	3/29	4/4	4/25
	#3) Wall (3) and (4) (5)	62.5	3.4	21.5	13.0	3/29	4/4	4/25

Mortar Compressive Strength

Date	Specimen	Time of Loading (Sec)	Length (in)	Width (in)	Total Load (lbf)	Cross-sectional Area of Specimen (in2)	Specimen Strength (psi)
4/4/2016	7day (#3)	80	2.0590	2.0090	15814	4.14	3823.01
4/4/2016	7day (#3)	80	2.0375	2.0050	15932	4.09	3899.94
4/4/2016	7day (#3)	83	2.0400	2.0095	16395	4.10	3999.39
4/25/2016	28day (#3)	102	2.0140	2.0050	20372	4.04	5044.98
4/25/2016	28day (#3)	92	2.0150	1.9900	18368	4.01	4580.72
4/25/2016	28day (#3)	97	2.0055	2.0030	19337	4.02	4813.77

ASTM C1437: Standard Test Method for Flow of Hydraulic Cement Mortar

Mortar Flow

Date	Using caliper specified in Spec C230/C230M?	Reading 1:	Reading 2:	Reading 3:	Reading 4:	Sum of all readings, Total Reading	Flow
3/17/2016	Yes (Mix #1)	24	24	25	25	98	98%
3/17/2016	Yes (Mix #2)	25	25	26	25	101	101%
3/17/2016	Yes (Mix #3)	24	26	25	26	101	101%

Tech: NBT **Project:** Jemez Phase V

ASTM E519: Standard Test Method for Diagonal Tension (Shear) in Masonry Assemblages

Specimen Id: SCEB 7 Wall #4
Date Tested: 5/6/2016

Test Machine Information

Equipement ID:	Instron
LVDT ID:	LVDT 3-1
LVDT ID:	LVDT 4-1

Prism Details

Bond Type:	Running
Number of Masonry Units Used:	8 full blocks
Date Block Constructed:	2/18/2016
Date Blocks Delivered to Lab:	3/10/2016
Walls Constructed By:	HPA Team
Block Curing- Age at Test Date:	>28 days
Block Curing- Temperature (°F):	76
Block Curing- Humidity (%):	20

Masonry Unit Information:

Unit Supplier:	HPA
Type of Unit:	Solid Unit

Masonry Unit Information:

Mortar Preparer:	HPA Team / NBT
Mortar Type:	Type S
Date Mortar Mixed:	3/28/2016

Tested Wall Properties

Test Date	Width (in)	Height (in)	Diagonal Length (in)	Thickness (in)	1) Gage Length (in)	2) Gage Length (in)	Max Load (lbf)
5/6/16	22.9	22.6	32.0	4.8	10	11	3301.7

Mechanical Properties of Block

Mean compressive strength of units (psi):	1280.2
Coefficeint of Variation (%):	7

Mechanical Properties of Mortar

28 day - Mean compressive strength (psi):	4813.2
Coefficeint of Variation (%):	4.8

ASTM E519: Standard Test Method for Diagonal Tension (Shear) in Masonry Assemblages

FRONT ELEVATION

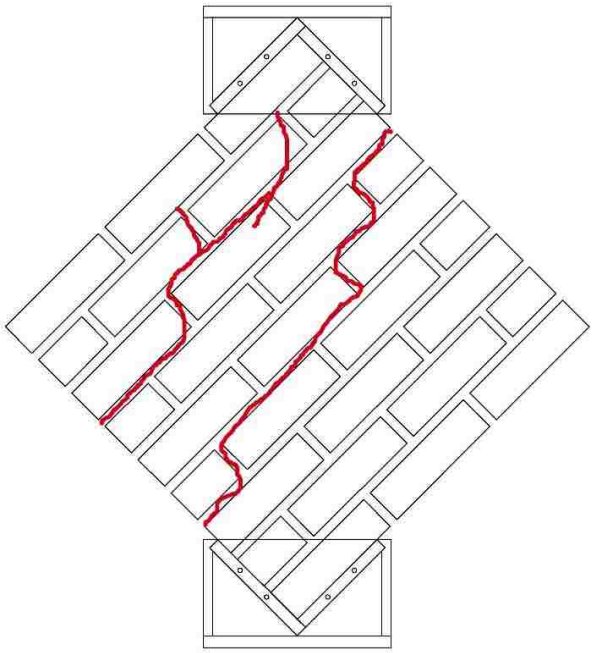

BACK ELEVATION

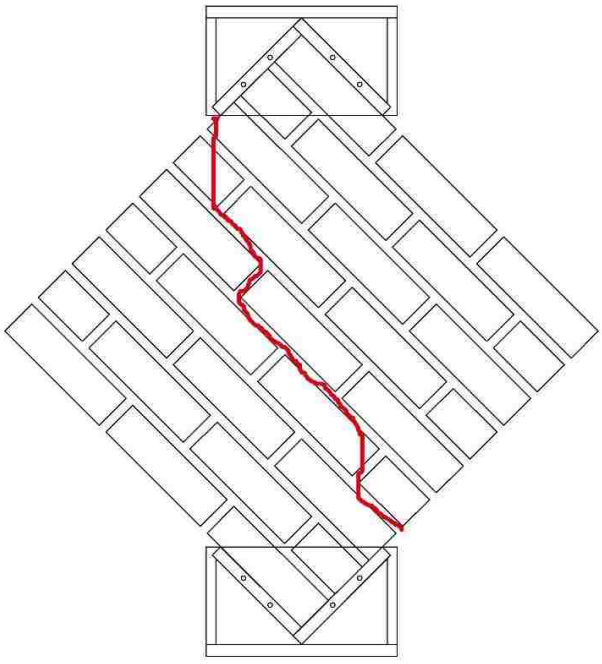

REFERENCES

Allen, G.T.R. (2012). Strength Properties of Stabilized Compressed Earth Blocks with Varying Soil Compositions (Master's thesis).

Anzani, A., Garavaglia, E., & Binda, L. (2009). Long-term damage of historic masonry: A probabilistic model. *Construction and Building Materials*, 23(2), 713-724.

ASTM C67-12. (2012). Standard Test Methods for Sampling and Testing Brick and Structural Clay Tile. West Conshohocken, PA: ASTM International.

ASTM C109/C109M-13. (2013). Standard Test Method for Compressive Strength of Hydraulic Cement Mortars (Using 2-in. or [50-mm] Cube Specimens). West Conshohocken, PA: ASTM International.

ASTM C270-14. (2014). Standard Specification for Mortar for Unit Masonry. West Conshohocken, PA: ASTM International.

ASTM C702/C702M-11. Standard Practice for Reducing Samples of Aggregate to Testing Size. West Conshohocken, PA: ASTM International.

ASTM C1072-13. (2013). Standard Test Methods for Measurement of Masonry Flexural Bond Strength. West Conshohocken, PA: ASTM International.

ASTM C1202-12. (2012). Standard Test Method for Electrical Indication of Concrete's Ability to Resist Chloride Ion Penetration. West Conshohocken, PA: ASTM International.

ASTM C1314-14. (2014). Standard Test Method for Compressive Strength of Masonry Prisms. West Conshohocken, PA: ASTM International.

ASTM C1437-13. (2013). Standard Test Method for Flow of Hydraulic Cement Mortar. West Conshohocken, PA: ASTM International.

ASTM C1585-13. (2013). Standard Test Method for Measurement of Rate of Absorption of Water by Hydraulic-Cement Concretes. West Conshohocken, PA: ASTM International.

ASTM D422-63. (2007). Standard Test Method for Particle-Size Analysis of Soils. West Conshohocken, PA: ASTM International.

ASTM D854-14. (2014). Standard Test Methods for Specific Gravity of Soil Solids by Water Pycnometer. West Conshohocken, PA: ASTM International.

ASTM D1557-12. (2012). Standard Test Methods for Laboratory Compaction Characteristics of Soil Using Modified Effort (56,000 ft-lbf/ft^3 (2,700 kN-m/m^3). West Conshohocken, PA: ASTM International.

ASTM D2216-10. (2010). Standard Test Methods for Laboratory Determination of Water (Moisture) Content of Soil and Rock by Mass. West Conshohocken, PA: ASTM International.

ASTM D2487-11. (2011). Standard Practice for Classification of Soils for Engineering Purposes (Unified Soil Classification System). West Conshohocken, PA: ASTM International.

ASTM D4318-10. (2010). *Standard Test Methods for Liquid Limit, Plastic Limit, and Plasticity Index of Soils*. West Conshohocken, PA: ASTM International.

ASTM D4829-11. (2011). Standard Test Method for Expansion Index of Soils. West Conshohocken, PA: ASTM International.

ASTM E519/E519M-10. (2010). Standard Test Method for Diagonal Tension (Shear) in Masonry Assemblages. West Conshohocken, PA: ASTM International.

ASTM E2392/E2393M-10. (2010). Standard Guide for Design of Earthen Wall

Building Systems. West Conshohocken, PA: ASTM International.

Australian Standards AS1289.C4.1. (1995). Methods of testing soil for engineering purposes, part C - soil classification tests. Sydney, Australia. Standards Association of Australia.

Bei, G. & Papayianni, I. (2003). Compressive strength of compressed earth block masonry. *Structural studies, repairs, and maintenance of heritage architecture VIII*, 367-375.

Bharath, B., Reddy, M. Pathan, J. & Patel, R. (2014). Studies on Stabilised Adobe Blocks. International Journal of Research in Engineering and Technology, 3(6), 259-264.

Binda, L. Gatti, G., Mangano, G., Poggi, C. & Sacchi, L. (1992). The collapse of the Civic Tower of Pavia: a survey of the materials and structure. *Masonry International*, 6(1), 11-20.

Binda, L., Schueremans, L., Verstrynge, S., Ignoul, S., Oliveira, D., Lourenco, P., & Modena, C. (2008). Long term compressive testing of masonry - test procedure and practical experience. *SAHC08–6th International Conference on Structural Analysis of Historical Constructions*, 1345-1355.

BS EN 1052-3. (2002). Methods of Test for Masonry: Part 3: Determination of Initial Shear Strength. London: British Standards Institution.

Burroughs, S. (2008). Soil Property Criteria for Rammed Earth Stabilization. *Journal of Materials in Civil Engineering*, 20(3), 264-273.

Fahmy, A. (2007). Adobe Architecture: New Appropriate Methods Of Construction,

Proceedings Fourth International Adobe Conference of the Adobe Association of the Southwest AdobeUSA, El Rito, NM, 2007. NM: NNMC and Adobe Association of the Southwest.

Houben, H. & Guillaud, H. (1994). *Earth construction: a comprehensive guide*, London: Intermediate Technology Publications.

Jayasinghe C., & Mallawaarachchi, S. (2009). Flexural of Compressed Stabilized Earth Masonry Materials. *Materials and Design*, 30: 3859-3868.

Jenkins Swan, A. Rteil, G. & Lovegrove, G. (2012). *Wood-frame vs. Compressed Earth Block Construction: Which Alternative is better?*. Proceedings, Annual Conference - Canadian Society for Civil Engineering, 3, 2547-2556.

Jimenez Delgado, M. & Canas Guerrero, I. (2007). The selection of soils for unstabilised earth building: A normative review. *Construction and Building Materials*, 21, 237-251.

Kim, J. Fan T. Reda Taha, M. & Shrive, N. (2012). The effect of damage and creep interaction on the behavior of masonry columns including interface debonding and cracking. Materials and Structures, 45(1-2), 15-29.

Klein, C. & Dutrow, B. (2007). *The 23rd Edition of the Manual of Mineral Science*. New York: John Wiley & Sons.

Lawson, W., Kancharla, C., & Jayawickrama, P. (2011). Engineering Properties of Unstabilized Compressed Earth Blocks. *Geo-Frontiers*, 2679-2688.

Low, P.F. (1985). The clay-water interface. *Proceedings of the international clay conference*. 247-256.

Marques Timoteo de Sousa, S., Maviael de Carvalho, C., Marden Torres, S., Perazzo

Barbosa, N., Gomes, K., & Ghavami, K. (2012). Mechanical Properties and Durability of Geopolymer Stabilized Earth Blocks. *ENARC*, Maceió, Brazil, 2012.

Maskell, D., Heath, A. & Walker, P. (2014). Inorganic stabilization methods for extruded earth masonry units. *Construction and Building Materials*, 71, 602-609.

Miccoli, L. Muller, U. & Fontanta, P. (2014). Mechanical behavior of earthen materials: A comparison between earth block masonry, rammed earth and cob. *Construction and Building Materials*, 61, 327-339.

Moore, D.M. & Reynolds, R.C. (1997). *X-Ray Diffraction and the Identification and Analysis of Clay Minerals*. Oxford: Oxford University Press.

Morel, J. Mesbah, A. Oggero, M. & Walker, P. (2001). An example of houses built with local materials to reduce the environmental impact of construction. *Building and Environment*, 36, 1119-1126.

NZS 4298:1998. (2000). New Zealand Standard Materials and Workmanship for Earth Buildings Including Amendment#1. Wellington: Standards New Zealand.

Niroumand, H. Zain, M. & Jamil, M. (2013). Various Types of Earth Buildings. *Procedia - Social and Behavioral Sciences*, 89, 226-230.

NMAC. (2009). New Mexico Earthen Building Materials Code. Title 14. Chapter 7. Part 4. Section 23.

Pacheco-Torgal, F. & Jalali S. (2012). Earth construction: Lessons from the past for future eco-efficient construction. *Construction and Building Materials*, 29, 512-519.

Prost, B., Koutit, T., Benchara, A., and Huard, E. (1998). State and location of water absorbed on clay minerals: consequences of the hydration and swelling-skrinage

phenomena. *Clays and clay minerals*, 46(2), 117-131.

Qu, B. Stirling, B. Jansen, D. Bland, D. & Laursen P. (2015). Testing of flexure-dominated interlocking compressed earth block walls. *Construction and Building Materials*, 83, 34-43.

Reda, M. & Shrive, N. (2000). Enhancing Masonry Bond Using Fly Ash. *Masonry International*, 14(1), 9-17.

Reddy, B.V., Lal, R., & Rao, K. (2007). Enhancing Bond Strength and Characteristics of Soil-Cement Block Masonry. Journal of Materials in Civil Engineering, 19(2), 164-172.

Reddy, B.V., Lal, R., & Rao, K. (2007). Optimum Soil Grading for the Soil-Cement Blocks. *Journal of Materials in Civil Engineering*, 19(2), 139-148.

Shrive, N., Sayed-Ahmed, E., & Tilleman, D. (1997). Creep analysis of clay masonry assemblages. Canadian Journal of Civil Engineering, 24(3), 367-379.

Silva, R., Oliveira, D. Miranda, T. Cristelo, N. Escobar, M., & Soares, E. (2013). Rammed earth construction with granitic residual soils: The case study of northern Portugal. *Construction and Building Materials*, 47, 181-191.

Skempton, A. W. (1953). The Colloidal “Activity" of Clays :*Proceedings of the Third International Conference on Soil Mechanics and Foundation Engineering*. Zurich. v. 1. , 57-61.

Smith, E.W. & Austin, G. S. (1996). *Adobe, pressed-earth, and rammed-earth industries in New Mexico (revised edition)*. Socorro, New Mexico: New Mexico Bureau of Mines and Mineral Resources.

Sturm, T., Ramos, L., Lourenco, P. (2015). Characterization of dry-stacking interlocking

compressed earth blocks. *Materials and Structures*, 48, 3059-3074.

Terzaghi, K. & Peck, R.B. (1948). *Soil Mechanics in Engineering Practice*. New York: John Wiley and Sons, Inc.

Thomas, K. (1996). *Masonry walls: specification and design*. Boston: Butterworth-Heinemann.

Varum, H., Costa, A., Silveira, D., Pereira, H., Almeida, J., & Martins, T. (2007). Structural Behaviour Assessment and Material Characterization of Traditional Adobe Constructions, AdobeUSA, El Rito, NM, 2007. NM: NNMC and Adobe Association of the Southwest.

Venugopal, K., Raju, R., & Dar, M. (2015). Properties and Application of Geopolymer Masonry Units. *SSRG International Journal of Civil Engineering*, 117-119.

Venkatarama Reddy, B. & Uday Vyas, C. (2008). Influence of shear bond strength on compressive strength and stress-strain characteristics of masonry. *Materials and Structures*, 41(10), 1697-1712.

Walker, P. (1999). Bond Characteristics of Earth Block Masonry. *Journal of Materials in Civil Engineering*, 11(3), 249-256.

Walker, P. (2004). Strength and erosion characteristics of earth blocks and earth block masonry. *Journal of Materials in Civil Engineering*, 16(5), 497-506.

Wolfskill, L., Dunlap, W., & Gallaway, B. (1980). *Handbook for Building Homes of Earth*. College Station, Texas: Texas Transportation Institute Bulletin.